PHYTOPLANKTON DYNAMICS IN THE NORTHERN GULF OF MEXICO (NGOM): FIELD AND LABORTORY EXPERIMENTS

A Dissertation

by

YAN ZHAO

Submitted to the Office of Graduate and Professional Studies of
Texas A&M University
in partial fulfillment of the requirements for the degree of

DOCTOR OF PHILOSOPHY

Chair of Committee,	Antonietta S. Quigg
Co-Chair of Committee,	You Wang
Committee Members,	Daniel C.O. Thornton
	Steven F. DiMarco
Head of Department,	Debbie Thomas

December 2014

Major Subject: Oceanography

ABSTRACT

The freshwater inflow of the Mississippi-Atchafalaya River system and the local circulation patterns result in nutrient enriched waters in the Northern Gulf of Mexico (NGOM) in spring, which fuels phytoplankton blooms, increases the vertical transportation of organic matters and initiates the bottom hypoxia. In 2012, we conducted two research cruises in the NGOM in April and August, in order to investigate phytoplankton diel cycles and nutrient limitations. Our results indicated that the diel rhythms of phytoplankton photosynthetic physiology and carbon fixation were regulated by light penetration, the mixed layer depth and phytoplankton community structure. Further, phytoplankton in the NGOM responded to light stress by means of fast (secs-mins) and long-term (days-weeks) photoacclimation. At our research stations, nitrogen (N) limitation was diagnosed by nutrient enrichment bioassays. The supplement of N not only stimulated phytoplankton biomass and restored the photosynthesis but also changed the community structure with a shift mainly from the large cells to small cells. This part of study provided new empirical data on the phytoplankton dynamics in the NGOM, filled some former studies' gaps including the diel changes of photosynthesis and community structure shift under nutrient pulses. Based on the results of field studies, a series of laboratory experiments were performed to test the effect of nutrient fluctuations on the diatom *Phaeodactylum tricornutum* and the coccolithiophore *Emiliana huxleyi*. The results indicated that *E. huxleyi* was more competitive than *P. tricornutum* under N and P starvation. For both species, cell growth was more limited by

P starvation, while photosynthetic apparatus and cellular constituents were more impaired by N starvation. The photosynthetic functions were less impaired and the photoprotective effects were more active in *E. huxleyi* than *P. tricornutum*. Also, photosynthetic functions and cellular constituents of N starved cells in both species showed recovery within 24 hours after supplementing nitrate (N). *P. tricornutum* prioritized recovery of photosynthesis and cell divisions over cell constituents, giving this species a competitive advantage for N-pulses. The performance of the two species was consistent with the findings in field studies.

DEDICATION

To my parents Gangyi Zhao and Chunrong Ren

ACKNOWLEDGEMENTS

I would like to show my highest appreciation to my committee chair, Dr. Antonietta S. Quigg. She advised my PHD research project with her profound academic knowledge and patient guidance. I thank her for offering the opportunities to attend multiple research cruises and international conferences, as well as the valued suggestions in the lab experiments designing and data interpretations.

I would like to thank my committee members, Dr. Daniel C.O. Thornton, Dr. Steven F. DiMarco, and Dr. You Wang, for their guidance and support throughout the course of this research.

Thanks also go to colleagues in the Phytoplankton Dynamics Lab who assisted me for the sample measurements. I also want to extend my gratitude to the National Oceanic and Atmospheric Administration and Chinese Scholarship Council, who provided me the funding for research and living expense, respectively.

Finally, I want to thank my mother and father for their unconditional love and encouragements.

TABLE OF CONTENTS

Page

LIST OF FIGURES

Page

Page

LIST OF TABLES

Page

CHAPTER I

INTRODUCTION

1.1 The introduction of marine phytoplankton

Phytoplankton are free-floating organisms of the sea that are capable of photosynthesis, which incorporate inorganic carbon into organic carbon via photosynthesis, acting as food source to the high trophic leveled organisms (eg. zooplankton) and initiating the complicated marine food web as well (Miller, 2003; Falkowski and Raven, 2007). The incorporated carbon is known in ecological parlance as primary productivity. Marine phytoplankton contribute up to 50% of total carbon assimilation annually, plays an important roles in the global carbon cycles (Behrenfeld et al., 2001). The study of primary productivity is of importance in terms of the evolution of fishery production, the interactions to global climate change (eg. ocean acidification, global warming) and the influence of eutrophication (eg. the harmful algal blooms), etc. Primary productivity could be measured by the traditional light-dark bottle method, the ^{14}C labeling method and/or the new technology based on chl *a* fluorescence (Miller, 2003; Thornton, 2012).

Marine primary productivity is mainly controlled by two factors: light and nutrient availability. Phytoplankton can only use the light in the spectrum from 400nm - 700nm, which is known as photosynthetic active radiation (PAR) (Kirk, 1983). In marine ecosystems, the amount of PAR that phytoplankton cells use not only depends on the natural fluctuations of solar light (seasonal changes and instant cloud cover), but also

relies on the hydrographic conditions of the water column, such as the depth of euphotic zone, light attenuation, vertical mixing and stratification (Kirk, 1983). For example, the time scale of water movements can vary from minutes to hundreds of hours, and the vertical mixing in the water column leads to the vertical movement of phytoplankton cells, thus changing the light they experiencing all the time (Kirk, 1983). Sverdrup (1953 and after) established the "critical depth theory" to interpret the relationship among light, phytoplankton blooms and the mixed layer. Critical depth is where the net primary production equals zero (photosynthetic production = phytoplankton respiration). In this theory, Sverdrup suggested the phytoplankton blooms could happen only if the critical depth was lower than the mixed layer depth. In general, mixing is maximal but irradiance is minimal in winter. In spring, the critical depth is deepened by increasing irradiance, while the mixed layer becomes shallower due to the formation of thermocline, thus the spring blooms may occur (Miller, 2003).

Along with light, nutrients are also pivotal for phytoplankton growth requirements. Phytoplankton structures and biological functions mainly involve the assimilation of carbon (C), nitrogen (N) and phosphorus (P) (Sterner and Elser, 2002). In marine ecosystems, nitrogen (N), phosphorus (P) and silicon (Si, for diatoms) are considered as the major limited marco-nutrients for phytoplankton (Redfield et al., 1963; Hecky and Kilham, 1988), while iron can be a limiting micro-nutrient (Martin and Fitzwater, 1988; Moore et al., 2013). Generally speaking, N limitation is more significant in coastal areas, while iron limitation is more frequent in the upwelling regions in open ocean (Moore et al., 2013). Anthropogenic activities have significantly increased the input of nutrient (N and P)

to the marine ecosystems via atmospheric deposition (e.g., elevated N deposition) and fluvial fluxes (Moore et al., 2013). Compared to open ocean, nutrients are more abundant and fluctuated in coastal areas due to the introduction of fluvial nutrients. The primary production in coastal areas can be as high as 4000 gC m^{-2} yr^{-1}, whereas in the open ocean, values can be as low as 1 gC m^{-2} yr^{-1} (Huston and Wolerton, 2009).

1.2 Northern Gulf of Mexico (NGOM)

The Northern Gulf of Mexico (NGOM), which includes the Texas-Louisiana shelf from Rio Grande east to the Mississippi Delta (Fig. 1.1), has the world's fifth largest river, the Mississippi River, flowing in (Rabalais et al., 2007). The drainage basin of Mississippi-Atchafalaya River system covers 41% of the continental United States, including regions with intensive population density, industry and agriculture. Depending on the time of year and river flow, the mean annual dissolved inorganic nitrogen (DIN) flux was between about 40 and 150 μM (<200 μM for total nitrogen), and the orthophosphate flux was about 1 to 3 μM (<5-6 μM for total P), and the silicate flux was from 50 to 130 μM (Turner et al., 2007; Bianchi et al., 2010).

Due to the seasonal variations of river discharge, N and P loading show significantly temporal variations in the NGOM. On average, river discharge is the largest in spring, while the discharge in fall is only 30% of spring discharge (Turner et al., 2007). Spatial nutrient variations are mainly determined by the transportation of fresh water, and the transportation of fresh water is correlated with the local circulation patterns and wind patterns (Dagg and Breed, 2003). The circulation pattern on the

Texas-Louisiana Shelf was explained by Cochrane et al. (1986) and supported by the following research results: Cho et al. (1998), Nowlin et al. (2005), Walker et al. (2005), using both observational data and models. In general, a cyclonic gyre prevails over shelf most of the time except during summer (July and August). In the summer time, an anti-cyclonic gyre forms from June to late August or September. The shift of circulation patterns results from the corresponding shift of wind patterns from westward in spring to eastward in summer (Cochrane et al., 1986; DiMarco et al., 2010).

One worldwide ecological phenomenon in the NGOM is the largest hypoxic area in the western Atlantic Ocean (and the second largest worldwide) which develops in summer (Rabalais et al., 2002). Hypoxia is defined as that dissolved oxygen (DO) which is lower than 2.0 mg L^{-1} (1.4 mL L^{-1}) in the water column, which happens most frequently in coastal waters (Diaz and Rosenberg, 2008). Nutrient enhanced productivity and strong local stratification are the two key factors required for the development hypoxia in the NGOM (Bianchi et al., 2010; Dale et al., 2010; DiMarco et al., 2010). The decomposition of sinking organic matters results in the consumption of oxygen on the bottom. Combined with stratification, the oxygen produced from the upper-pycnocline water cannot be transported to the subpycnocline water, leading to the occurrence of bottom hypoxia (Hetland and DiMarco, 2008; Bianchi et al., 2010). It is demonstrated that the sinking phytoplankton cells and zooplankton fecal pellets from spring bloom provide the major source of benthic respiration in the NGOM (Rabalais et al., 2002; Bianchi et al., 2010).

1.3 Nutrient dynamics in the NGOM

The average nutrient ratio, in terms of particulate and dissolved forms, is constant in the worldwide ocean system, which was concluded by Redfield in 1930s. The Redfield Ratio refers to the ratio of C, N and P equaling to 106:16:1 (mol/mol), which also fits the average nutrient ratios that phytoplankton assimilate under balanced growth with ample nutrients (Redfield et al., 1963). As a boundary line provided by Redfield Ratio, people usually consider N: P > 30 and N: P < 5 could result in potential P and N limitation, respectively (Darley, 1982). In the NGOM, DIN (dissolved inorganic N: nitrate + nitrite+ ammonium): Pi (inorganic P) is most frequently used to indicate nutrient limitation. The ratios and concentrations of N and P limitation in NGOM refer to DIN: Pi < 10 with DIN $\leq$ 1 μmol L^{-1} and DIN: Pi > 30 with Pi $\leq$ 0.2 μmol L^{-1}, respectively (Quigg et al., 2011).

N is considered as the most limiting nutrient in the NGOM, while recent reports showed the role of P limitation has become more important due to the 50 fold increase of nitrogen loading since 1950s (Bianchi et al., 2010). The average ratio of NOx to PO_4 in the freshwater inflow has changed from 20 in 1960s to 70 in 1990s (Lohrenz et al., 1999). It is now understood that both N and P are controlling factors to the primary productivity in the NGOM as well as the development of hypoxia (Turner et al., 2006; Bianchi et al., 2010).

In the NGOM, the nutrient variability is highly related to the freshwater inflow from the Mississippi River systems. In spring, although large amounts of N and P are inflowed into the NGOM, the fast consumption of N as the occurrence of diatom blooms

increases the requirements of P thus leads to P deficiency nearby the Mississippi River plume (Quigg et al., 2011; Fennel et al., 2011; Laurent et al., 2012). N limitation occurs further west on the shelf as the consumption of nutrients from diatoms, leading to potential Si limitation (Laurent et al., 2012). In summer, N limitation usually dominates the whole shelf area with the development of stratification (Dagg et al., 2007). N limitation also could occur in fall due to the small amount of freshwater input. In winter, the stratification is broken down and the bottom nutrients are brought up to surface, while the phytoplankton growth is mainly limited by light. The shift of nutrient limitation causes the shift of phytoplankton communities, such as the shift from diatoms to non-diatom phytoplankton due to Si limitation, and the shift from diatoms to small-celled phytoplankton due to N limitation (Dortch and Whitledge, 1992; Zhao and Quigg, 2014).

There have been considerable amount of studies focusing on the limiting nutrients and the interactions with phytoplankton productivity and physiology in the NGOM (Lorenz et al., 1997; Sylvan et al., 2006, 2007; Quigg et al., 2011; Turner and Rabalais, 2013; Zhao and Quigg, 2014). Multiple parameters such as biomass increase, community shifts, intracellular compounds (free amino acids/particulate protein ratios for N deficiency, alkaline phosphatase for P deficiency), and chl *a* fluorescence parameters have been found to respond to the N or P deficiency or nutrient enrichment bioassays (Dortch and Whitledge, 1992; Sylvan et al., 2006, 2007; Quigg et al., 2011; Turner and Rabalais, 2013; Zhao and Quigg, 2014). The response time of these

parameters to nutrient enrichments was very short (within 24 hours), providing us fast and efficient diagnostic tools for nutrient limitation in field research.

1.4 The performance of phytoplankton under nutrients variability

Liebig's law of minimum first claimed that plant growth is not determined by the total amount of resource, but limited by the scarcest resource (Danger et al., 2008). Tilman's resource competition theory set up the basic principle to describe and predict the outcome of inter-species competition in steady states. The essence of his theory includes: (1) the outcome of inter-species resource competition is determined by the ambient nutrient ratios, other than the amount of nutrient; (2) phytoplankton with smaller size are more favored by nutrient limitation; (3) non-nutrient environmental factors, such as light and temperature, can also affect the inter-species resource competition (Tilman 1982). Tilman's theory has been applied widely in aquatic ecosystems (Sterner and Elser, 2002). There is however no consideration of intracellular resource storage in Tilman's theory. In fact, it is necessary to consider the intracellular nutrient storage especially in the environments with frequent nutrient pulses. Grover (1990, 1991) established the variable-internal-stores (VIS) model to offset the drawback of the applicability of Tilman's theory in non-steady states (eg. periodic or non-periodic nutrient pulses), and Sommer (1995) further demonstrated that periods of nutrient pulses could also influence the competitive abilities of different phytoplankton groups.

Different phytoplankton species perform different under the nutrient variability, and this could be attributed to their specific nutrient requirements and assimilation

abilities. For single species, nutrient deficiency in culture medium leads to nutrient stress of the phytoplankton cells. Moore et al. (2013) defined the "nutrient stress" of phytoplankton cells as "a physiological response to a nutrient shortage". The physiological response to nutrient stress is related to the elements loss in cellular constituents, for example, N stress inhibits physiological functions on the translational level (from RNA to proteins) and the enzymes level, while P stress inhibits physiological functions on the transcriptional level (from DNA to RNA) (Latasa and Berdalet, 1994; Leonardos and Geider, 2004). Specifically to photosynthesis, the physiological response to nutrient stress was similar to the light stress in terms of the degradation of pigments, the damage of light reaction centers and the inhibition of carbon fixation, which have been studied in multiple culture modes (batch, semi-continuous and continuous) under different kinds of nutrient stress (N, P, Si, iron) (Geider et al., 1993, 1998; Greene et al., 1992; Sterner and Elser, 2002; Young et al., 2003; etc). As the development of new technology for probing cells continues, the comparison of different species and their response in small time scales (secs-mins), and the interactions between nutrient stress and other environmental forcing are currently major topics of investigation.

1.5 Study background

This dissertation includes two major parts with the first part (Chapter II and III) focused on field studies and the second part (Chapter IV and V) involved laboratory experiments. The first component of the thesis reports on work which was part of the project "Mechanism Controlling Hypoxia" conducted in the NGOM from 2010-2012. In

April and August each year, processes cruises were conducted in order to understand the major biological and chemical changes taking place over a 24 hour period in four locations on the shelf (Fig. 1.1). This information is to be used to develop an understanding of the mechanisms which may lead to hypoxia as well as in model development. As part of this larger effort, a sub-project was to investigate phytoplankton photosynthesis dynamics in diel cycles under different nutrient conditions and depths at the four locations.

There are considerable amount of studies of phytoplankton photosynthesis and primary productivity in the NGOM which started by focusing on Mississippi River plume in the 1960s (Thomas and Simmons, 1960; Lorenz et al., 1990, 1994, 1997), and more recently have moved further west to include the Atchafalaya River (e.g., Sylvan et al., 2006, 2007; Lehrter et al., 2009; Quigg et al., 2010). All of their studies demonstrated primary productivity in the NGOM was controlled by the local chemical and physical properties, which was the consequence of Mississippi-Atchafalaya River discharge. Light attenuation is typically applied to calculate the primary productivity with depth, but very few studies talked about how natural light cycles (diel cycles) regulate photosynthesis, which actually is very dynamical in different ecosystems and could influence the calculation of primary productivity to a large degree (Harding et al., 1980, 1981; Erga and Skjoldal, 1990; Doblin et al., 2011). The diel changes of photosynthesis in the NGOM have been poorly studied with Lorenz et al. (1994) and John et al. (2012)'s studies only and these only focusing to surface waters. We aimed at studying the influence of hydrographic conditions (depth, mixing, light attenuation) on

the diel cycles of photosynthetic physiology and carbon fixation in the NGOM, which was done for the first time in this region (Chapter II). The diel changes of phytoplankton were measured at station AB5, 10B and 08C shown in Fig. 1.1.

All the nutrient enrichment bioassays conducted in the NGOM only measured the response of biomass and chl *a* fluorescence, none of which measured the response of the community structure (Smith and Hitchcock, 1994; Sylvan et al., 2007; Quigg et al., 2010; Turner and Rabalais, 2013). In our study, the shift of community structure was measured in 48-hour nutrient enrichment bioassays in both April and August (Chapter III, Zhao and Quigg, 2014) at stations AB5 and 08C shown in Fig. 1.1.

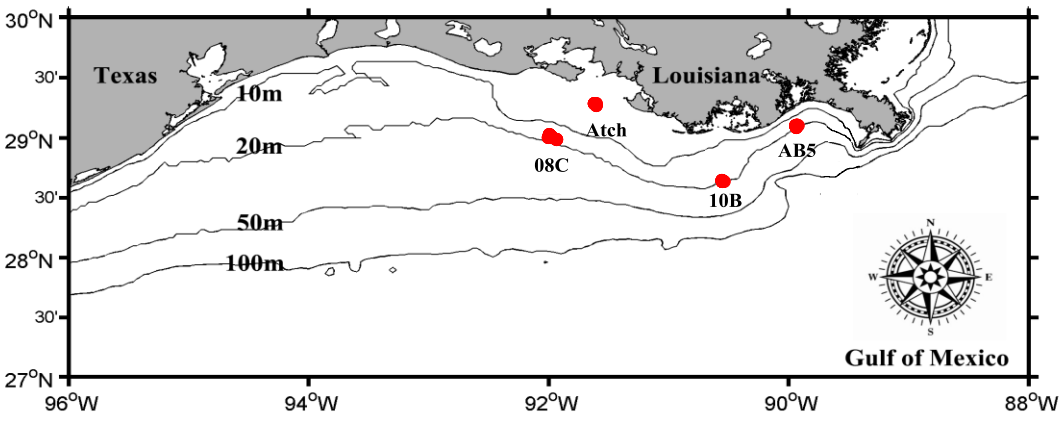

Figure 1.1 Station locations with samples collected from AB5, 10B, 08C and ATCH 2010 to 2012.

Based on the results of Chapter III in which diatoms were found more competitive than coccolithiophores in the nutrient enrichment bioassays, we choose two species from these groups to compare their competition and single species response to different nutrient conditions, including N and P starvation and N re-supplement after N starvation. The diatom *Phaeodactylum tricornutum* and the coccolithiophore *Emiliana huxleyi* were chosen as these are common species found in coastal and offshore respectively. Former studies mostly focused nutrient competition from the point of nutrient assimilation or the effect of nutrient starvation (or limitation) on the physiological functions of a single species (Tilman, 1977; Geider et al., 1993, 1998; Sterner and Elser, 2002; Young and Beardall, 2003; Cermeño et al., 2011; Moore et al., 2013). In Chapter IV, we combined the two aspects together in order to determine the inter-species competition under different nutrient conditions and explained it from the point of physiological responses (mostly photosynthesis) rather than only considering nutrient assimilation kinetics.

Compared to the previous research on nutrient starvation and/or limitation, there have been few studies focused on the short-term (first 24 hours) recovery of phytoplankton cells from nutrient deficiency (Hearly, 1979; Plumley and Schmidt, 1989; Greene et al., 1992; Geider et al., 1993; Young and Beardall, 2003; Dong et al., 2014). Using the same species as in Chapter IV, we measured the photosynthetic functions and cellular constituents in a 24 hour recovery phase after N starvation, in order to provide more species' information for this research direction and compare the results of Chapter IV.

1.6 Study aims

The thesis contains the four chapters which are summarized below:

Chapter 2: Based on ^{14}C uptake assays, in-vivo chlorophyll (chl) *a* fluorescence and HPLC pigment analysis, phytoplankton photosynthetic physiology and productivity in 24-hour cycles were characterized at three stations during April and August 2012 in the Northern Gulf of Mexico (NGOM). The results indicated the sub-pycnocline primary production accounted for 5%-48% of the total integrated primary production, emphasizing the important influence of euphotic zone in shallow coastal areas. In 24-hour diel cycles, chl *a*-specific light-saturated photosynthesis (P^B_{max}) as measured with photosynthesis versus irradiance curves (P-I) and the photoprotective pigment pool (diadinoxanthin /chl *a*) showed acclimation to the effect of mixing and stratification. chl *a* fluorescence and the transformation between photoprotective pigments (diadinoxanthin to diatoxanthin) responses were only observed in surface samples. The dominate phytoplankton groups (diatoms and cyanobacteria in April and August respectively) influenced the photosynthetic parameters we measured. The NGOM is a coastal ecosystem with high variability of mixing, nutrients and light (intensity and attenuation). Our study provided evidence that phytoplankton in this area adapted to the environments by means of fast responses (secs-mins) and long-term (days-weeks) photoacclimation. Understanding the major drivers could help us to improve models involving the calculation of primary productivity, such as those focused towards understanding mechanisms controlling hypoxia.

The findings are under review: Zhao, Y. and Quigg, A. 2014. Study of photosynthetic productivity in Northern Gulf of Mexico: importance of diel cycles and light penetration. Continental Shelf Research.

Chapter 3: Although the Mississippi-Atchafalaya River system exports large amounts of nutrients to the Northern Gulf of Mexico annually, nutrient limitation of primary productivity still occurs offshore, acting as one of the major factors controlling local phytoplankton biomass and community structure. Bioassays were conducted for 48 hrs at two stations adjacent to the river plumes in April and August 2012. High Performance of Liquid Chromatography (HPLC) combined with ChemTax and a Fluorescence Induction and Relaxation (FIRe) system were combined to observe changes in the phytoplankton community structure and photosynthetic activity. Major fluorescence parameters (F_o, F_v/F_m) performed well to reveal the stimulating effect of the treatments with nitrogen (N-nitrate) and with nitrogen plus phosphate ($+NP_i$). HPLC/ChemTax results showed that phytoplankton community structure shifted with nitrate addition: we observed an increase in the proportion of diatoms and prasinophytes and a decrease in cyanobacteria and prymnesiophytes. These findings are consistent with predictions from trait-based analysis which predict that phytoplankton groups with high maximum growth rates (μ_{max}) and high nutrient uptake rates (V_{max}) could most readily take advantage of the addition of limiting nutrients. The shift of phytoplankton community structure, if persistent, could trigger changes of particular organic matter fluxes and alter the micro-food web cycles and bottom oxygen consumption.

The findings have been published: Zhao, Y. and Quigg, A. 2014. Nutrient limitation in Northern Gulf of Mexico (NGOM): phytoplankton communities and photosynthesis respond to nutrient pulse. PLOS ONE. 9(2): e88732.

Chapter 4: In marine ecosystems, diatoms usually dominate in nutrient abundant coastal waters while coccolithiophores usually dominate in offshore areas where nutrients are scarce. In lab-controlled batch culture conditions, mixed-species competition between a diatom *Phaeodactylum tricornutum* and a coccolithiophore *Emiliana huxleyi* and the response of single species were examined under nitrate (N) or phosphate (P) starvation. Based on the logistic growth model and the Lotka-Volterra competition model, *E. huxleyi* showed higher competitive abilities than *P. tricornutum* under N and P starvation. For both species, cell growth was more inhibited by P starvation, while photosynthetic functions (chl *a* fluorescence parameters) and cellular constituents (pigments) were impaired by N starvation. The decline of photosynthetic functions (e.g. decline of F_v/F_m and increase of σ_{PSII} values) occurred later in *E. huxleyi* (day 12) than in *P. tricornutum* (day 9), and the photoprotective effect in terms of the xanthophyll cycle pigment accumulation and the transformation from diadinoxanthin (dd) to diatoxanthin (dt) was more active in *E. huxleyi* than *P. tricornutum* under similar N or P starvation conditions. Although both species responded to N or P starvation, *E. huxleyi* and *P. tricornutum* had different way to allocate resources and energy under nutrient starvation. It appears that *E. huxleyi* had a more economic strategy to adapt the nutrient depleted environment than *P. tricornutum*. These findings are consistent with the patterns observed in nature.

Chapter 5: The response of N (nitrate) starved cells of the diatom *Phaeodactylum tricornutum* and the coccolithiophore *Emiliana huxleyi* were measured after a pulse of N addition. The changes in cell divisions, photosynthetic parameters, pigment compositions, cellular organic carbon, nitrogen and soluble protein contents, cellular malondialdehyde (MDA) and superoxide anion ($O_2^{\bullet-}$) levels were followed in hour-scale over 24 hours. As a control, nutrient replete cultures were followed simultaneously. In *P. tricornutum*, the recovery of F_v/F_m and σ_{PSII} values started within 1 hour, earlier than the other parameters; cellular pigments did not show recovery during the 24 hours but the chl *a*/carotenoids ratios increased to levels measured in the controls; cell divisions were independent of the recovery of chl *a*. In *E. huxleyi*, the recovery of F_v/F_m and σ_{PSII} values started after 1 hour, synchronous with the increase of cellular organic N and chl *a*; the pigments were fully recovered within 14 hours. Therefore, *P. tricornutum* prioritized the recovery of its photosynthetic functions and cell divisions while *E. huxleyi* did not follow this pattern. In *E. huxleyi*, cellular proteins, pigments and photosynthetic functions were all recovered to the levels of the controls before cell divisions started. The different recovery strategies between the two species indicated *P. tricornutum* could be more competitive in N limited waters when N pulses are introduced.

CHAPTER II
STUDY OF PHOTOSYNTHETIC PRODUCTIVITY IN THE NORTHERN GULF OF MEXICO: IMPORTANCE OF DIEL CYCLES AND LIGHT PENETRATION

2.1 Introduction

Phytoplankton dynamics is the outcome of nutrient availability, light conditions and physical mixing. The influence of light in diel rhythms of phytoplankton is seen in many aspects such as cell divisions, photosynthesis, chl *a* fluorescence and gene expressions (Suzuki and Johnson, 2001; Ohi et al., 2005; John et al., 2012). Both laboratory and field studies have shown that the diel rhythms of phytoplankton are predictable (Vaulot and Marie, 1999; Litaker et al., 2002; Bruyant et al., 2005; Brunet et al., 2008; Quigg et al., 2012). Phytoplankton carbon fixation rates usually exhibit peak values in early morning or around noon (Harding et al., 1981; Prézelin, 1992); without consideration of this variability errors in the calculation of total integrated primary production may occur (Harding et al., 1981, 1982). For light reactions, chl *a* fluorescence parameters such as minimum fluorescence (F_o) and the maximum quantum yield of photosystem (PS) II (F_v/F_m) show quenching in the daytime which is typically caused by photoinhibition under excess light stress and recovery at night time (Falkowski and Raven, 2007). Photoprotection involves an enzymatic-controlled epoxidation and de-epoxidation of pigment conversion, in order to dissipate extra energy as nonphotochemical quenching (NPQ) before the damage of light reaction centers (Falkowski and LaRoche, 1991). This process of pigment conversion was named the

xanthophyll cycle (XC) (Long et al., 1994). In chromophyte algae, XC involves the transformation from diadinoxanthin (Dd) to diatoxanthin (Dt) (Lavaud et al., 2004; Falkowski and Raven, 2007). In cyanobacteria, photoprotection involves zeaxanthin and decoupling of phycobilisomes (Falkowski and Raven, 2007).

The diel "bio-clock" in phytoplankton shows variability in terms of frequencies and amplitudes in field studies. Physical mixing causes vertical movement of phytoplankton cells, which changes the irradiance experience at different depths. Claustre et al. (1994) indicated the effect of mixing could diminish the difference in the proportion of Dt between day and night. At a 50m deep coastal site with day-night alternations of thermal induced stratification and mixing, Brunet et al. (2008) found the sinusoidal diel patterns and exponential vertical patterns of Dt/ chl *a*, Dt/ (Dt+Dd) (DES) and $\Delta F/F'_m$ (effective quantum yield of fluorescence). Doblin et al. (2011) found homogenous chl *a* fluorescence and photoprotective pigments within the mixed layer, but a lack of diel rhythm's with carbon fixation rates in the Sub-Antarctic and Polar Front Zones.

As the largest river in the North America, the Mississippi River drains 40% of the area of the United States (Dagg et al., 2007). With the inflow of riverine nutrients in spring, the Northern Gulf of Mexico (NGOM) fuels high phytoplankton biomass and primary productivity (spring blooms), contributing to a large amount of organic matter vertically migrating to the bottom and decomposed by bacteria (Diaz, 2001). In summer, the stability in the water column increases due to thermal heating and freshwater capping, leading to the formation of bottom hypoxia as the consumption of oxygen

(Bianchi et al., 2010; DiMarco et al., 2010). Therefore, nutrients fueled primary productivity is one important component in the models of evaluating and predicting hypoxia in the NGOM, which needs more empirical data to improve the accuracy (Fennel et al., 2011).

In the NGOM, the role of nutrients is frequently investigated, (e.g., Quigg et al., 2011; Laurent et al., 2012; Turner and Rabalais, 2013), but the importance of light is less often examined (e.g., Lohrenz et al., 1994; Lehrter et al., 2009), especially for the diel oscillations. Lohrenz et al. (1994) measured the diel changes of photosynthesis versus irradiance curves (P-I) parameters in the NGOM to find P^B_{max} values were low in early morning and increased during the photoperiod. John et al. (2012) found diel patterns of Rubisco (*rbcL*) mRNA and the chl *a*-specific light-saturated photosynthetic rate (P^B_{max}) in four different size classes of phytoplankton in the Mississippi and Orinoco River plumes on the amplitudes of the diel patterns, but did not consider the influence of hydrographic factors like mixing and depth. Here, we examined diel patterns of primary productivity and photosynthetic physiology at a range of depths above and below the pycnocline, across the shelf at three stations, and during two very different time periods (April and August 2012). Multiple techniques were used in our study, such as the ^{14}C method, Fluorescence Induction and Relaxation (FIRe) System and HPLC pigments analysis, which were also common for the investigations in other field studies (Qian et al., 2003; Suggett et al., 2009a; Sylvan et al., 2011). Collectively this study provides information on the magnitude of productivity across a range of spatial and temporal scales.

2.2 Material and methods

Sample collections and hydrographic conditions

Two research cruises were conducted in April and August 2012 on the R/V Pelican. In each cruise, three 24-hour stations along the 20 m isobath in the NGOM were studied (Fig. 2.1). Station A (29.07 ºN, 89.93 ºW) was in the Mississippi River plume while the other two stations were located further west on the Louisiana shelf area (B: 28.60 ºN, 90.53 ºW and C: 29.00 ºN, 92.00 ºW). A CTD rosette with 12 Niskin bottles and shipboard calibrated sensors was deployed overboard every 2 hours to measure vertical hydrographic profiles such as temperature, salinity, chl *a* fluorescence and photosynthetically active radiation (PAR). Water samples were taken from four depths every 2 or 6 hours and used to measure primary productivity (^{14}C method), chl *a*, pigment compositions and dissolved nutrient (N, P, Si) concentrations. The sampling intervals were dependent on the depth of the pycnocline, with two samples taken above and two below the pycnocline. We will refer to these as surface (sur), middle 1 (mid1), middle 2 (mid 2) and bottom (bot) respectively. The mixed layer depth (MLD) was defined by the depth of maximum Brunt–Väisälä frequency (*N*), calculated using equation 1. The extinction coefficient (k_d) was calculated using equation 2, and the depth of euphotic zone (Z_{eu}) was calculated using equation 3.

Equation 1: $N = \sqrt{-\frac{g}{\rho}\frac{\partial \rho(z)}{\partial z}}$, where ρ is the potential density, g is the local acceleration of gravity, z is the geometric height;

Equation 2: $E_z = E_0 exp^{-k_d z}$, where E_z is the solar irradiance at depth z, E_0 is the solar irradiance on surface;

Equation 3: $Z_{eu} = \ln(0.01) / -k_d$, when the calculated Z_{eu} exceeded the bottom depth, it was considered equal to the bottom depth;

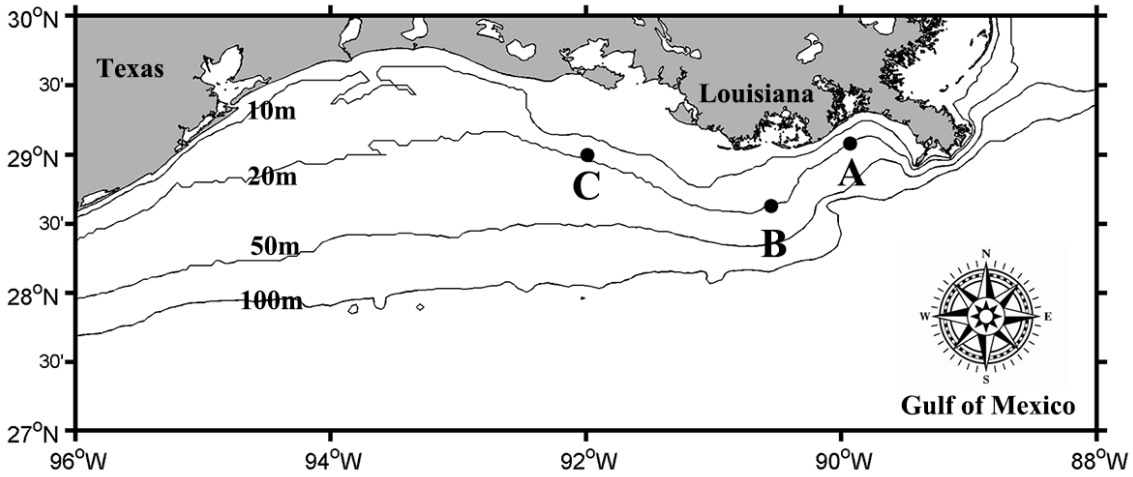

Figure 2.1 Study area and bathymetry on the Texas-Louisiana Shelf in northern Gulf of Mexico. The 10, 20, 50 and 100 m isobaths are shown. Locations of stations A, B and C which were sampled in April and August 2012 are offshore from the Mississippi and Atchafalaya Rivers respectively.

Primary productivity measurements

Photosynthesis versus irradiance (P-I) curves were performed in a photosynthetron attached a water bath to maintain the in situ temperature according to Lewis and Smith (1983). Aliquots (16) of ^{14}C labeled seawater (1 mCi ml^{-1} $H^{14}CO_3^-$) were incubated at a range of PAR from 15 to 1800 μmol m^{-2} s^{-1}. Triplicate samples were

treated with 5 ml Ecolume scintillation cocktail and 50 µl phenethylamine to determine the 'total' amount of ^{14}C added. Before the incubation, triplicate water samples were fixed with buffered formalin for 'background' values. Incubations were terminated with buffered formalin after 60 min in April and 45 min in August. Samples were acidified for 24 hours to purge the unincorporated ^{14}C before counting with a Beckman LS 6500 liquid scintillation counter.

Photosynthetic parameters were calculated by fitting the P-I model of Platt et al. (1980) using equation 4 and the in-situ primary productivity (*PP*) was calculated using equation 5.

Equation 4: $P^B = P^B_{max}\left(1 - e^{-\alpha E/P^B_{max}}\right)e^{-\beta E/P^B_{max}}$, where P^B_{max} is the model estimated maximum production per unit chl a, α is the initial slope of the P-I curve, and E is the light exposure during incubation, β represents photoinhibition;

Equation 5: $PP = P^B_{max} \times Chl\ a \times \tan(\frac{I_z}{I_k})$, where I_z is the solar irradiance in depth, I_k equals to P^B_{max}/α.

Phytoplankton physiology measurements

The Fluorescence Induction and Relaxation (FIRe) System (Satlantic Instruments S/N 2) was used to measure the phytoplankton photo-physiological characteristics. Water samples (3 mL) from each time and depth point were stored in darkness for 30 minutes before being measured. Only information collected from the single turnover (ST) component of the transient, including the minimum and maximum fluorescence (F_o and F_m), F_v/F_m and the functional absorption cross-section for PSII (σ_{PSII}, $Å^2$ $quanta^{-1}$)

were considered (Kolber et al., 1998; Kromkamp and Forster, 2003). Background fluorescence from filtered seawater (0.45 μm) from the corresponding treatments was used to correct F_o and F_m values (Cullen and Davis, 2003). An external light source was applied to measure the photochemistry in PSII under 'light' conditions; we calculated the non-photochemical quenching (NPQ) and photochemical quenching (qP) coefficients according to the equations in Table 2.1.

Pigments analysis

For the chl *a* samples, seawater (400-800 ml) was filtered onto Whatman GF/F glass fiber filters and frozen immediately until analyzed using a calibrated Turner Designs model 10AU fluorometer. The extraction and calculation method used were described in Quigg et al. (2011). In addition, for each sampling point, seawater (500-2000 ml) was filtered and stored at -80^{o}C until HPLC pigments analysis. Using reverse-phase High Performance of Liquid Chromatography (HPLC) method based on Pinckney et al. (1996), with modifications described in Zhao and Quigg (2014). The instrumentations, sample treatments, and procedures were described in Zhao and Quigg (2014). For the purpose of this study, we focused on two pigments which we used to represent the major components of the phytoplankton community: zeaxanthin (Zea, cyanobacteria) and fucoxanthin (Fuco, diatoms). We also measured Dd and Dt to access photoprotective effect in the phytoplankton communities. In an earlier study, a Chemtax analysis of samples used for bioassays during these cruises revealed that diatoms and

cyanobacteria were the dominate members of the communities during the April and August cruises, respectively (Zhao and Quigg; 2014).

Nutrient analysis

Seawater (20 ml) for dissolved nutrient analysis was collected at the same time as samples for pigment analysis and filtered through pre-rinsed 0.45 μm cellulose ester filters (Millipore) into acid-washed polyethylene Nalgene bottles and immediately frozen at -20^{o}C. Samples were analyzed by Geochemical and Environmental Research Group at Texas A&M University (College Station). Dissolved inorganic nitrogen (DIN) was calculated from the sum of nitrate, nitrite and ammonium concentrations.

Data analysis

The statistical analysis in this study was performed using SPSS 16.0. Two-Way ANOVA analysis was applied to time and depth without the consideration of factor interaction. All the data (or after transformation) passed the Leven's test to ensure the homogeneity of variances before performing ANOVAs. The data shown are means ± standard errors.

2.3 Results

Hydrographic conditions

The Mississippi River discharges a large amount of fresh water to the NGOM, with particulates and nutrients, resulting in diverse physical, biological and chemical environments inside and outside of the Mississippi River plume and along the shelf. River discharge data from the Mississippi River at Tarbert Landing (gage 01100) was used to examine the river output preceding the April and August cruises (Fig. 2.2). The April cruise took place after a period of high river flow while August cruise occurred after a prolonged period of low river flows. While the flow rate in April was typical for spring; that in August was low and close to the 1930-2012 low flow average (see http://www2.mvn.usace.army.mil/). The highest recorded spring flow for the Mississippi River was on May 19 2011, some 46,000 m^3 s^{-1}, twice the flow rate than the peak measured in 2012 (Fig. 2.2).

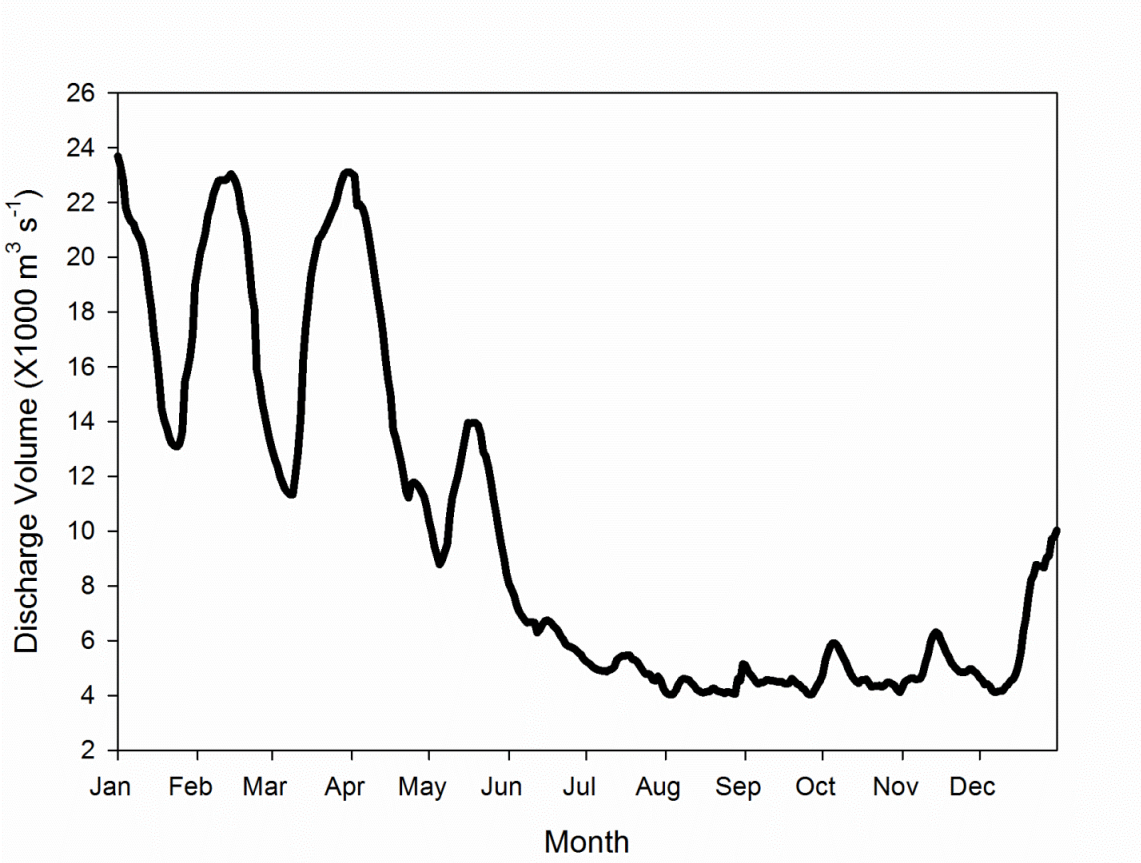

Figure 2.2 River discharge (m^3 s^{-1}) data from the Mississippi River as measured at the Tarbert Landing (gage 01100) for 2012 from the US Army Corps of Engineers (http://www2.mvn.usace.army.mil/cgi-bin/wcmanual.pl?01100).

We summarized the major hydrographic parameters measured and calculated for the water column at the three stations (Table 2.2). Station A, located in the Mississippi River plume, had the lowest surface salinity (25.8±0.38) in August, and the highest phytoplankton biomass (measured as chl *a*; 3.41±0.4 µg l^{-1}), the highest light attenuation coefficient (k_d = 0.29) and the shallowest euphotic zone (Z_{eu}, 15.75m) in April. Stations B and C were less influenced by the Mississippi River with high surface salinities,

phytoplankton biomass, and the euphotic zone which reached down to the bottom of the water column. In April station A and B, August station B, the weather conditions were sunny and cloudless with the highest PAR values recorded at noon. In August station B, the PAR sensor was deployed in the shade before noon due to the location of CTD cast, leading to relatively low 'measured' PAR values before noon. Actually, the peak value at station B should > 2000 μmol m^{-2} s^{-1} at noon based on data from 2010 and 2011 cruises (not shown). The weather was typically rainy and cloudy at station C in April and at station A and C in August (PAR at noon = around 600 μmol m^{-2} s^{-1} in April and 500 μmol m^{-2} s^{-1} in August).

Abbreviation	Full name	Units
P^B_{max}	maximum chl *a*-specific carbon fixation rate	mg C mg chl a^{-1} h^{-1}
PP	In-situ primary productivity	mg C m^{-3} h^{-1}
P-I	photosynthesis versus irradiance curves	
α	the initial slope of P-I curve	mg C mg chl a^{-1} h^{-1}/ μmol m^{-2} s^{-1}
I_k	Index of light saturation=P^B_{max}/α	μmol m^{-2} s^{-1}
chl *a*	Chlorophyll *a*	μg l^{-1}
F_o and F_o'	minimum fluorescence yield in the dark and in the light	relative units
F_m and F_m'	maximum fluorescence yield in the dark and in the light	relative units
F_t	actual fluorescence level at a given time excited by the actinic light	relative units
F_v/F_m	maximum quantum yield of PSII = $(F_m-F_o)/F_m$	relative units
$\Delta F/F'_m$	effective quantum yield of fluorescence	relative units
σ_{PSII}	effective absorption cross section of PSII under dark acclimation	$Å^2$ $quanta^{-1}$
NPQ	Non-photochemical quenching = $(F_m-F_m')/F_m'$	relative units

Table 2.1 The abbreviations, equations and units used in this study.

Abbreviation	Full name	Units
qP	Photochemical quenching=$(F_m'-F_t)/(F_m'-F_o')$	relative units
PSII	photosystem two	
sur, mid1, mid2, bot	four sampling depths from surface to bottom: surface (0-1m), middle1(2.5-11.3m), middle2 (9.2-15.3m) and bottom (17-19.5m).	m
Dd	Diadinoxanthin, photoprotective pigment	$\mu g\ l^{-1}$
Dt	Diatoxanthin, photoprotective pigment	$\mu g\ l^{-1}$
XC	xanthophyll cycle	
DES	Dt/(Dd+Dt)	µg/ µg
Dd pool	Dd/chl *a*	µg/ µg
Fuco	fucoxanthin, representative of diatoms	$\mu g\ l^{-1}$
Zea	zeaxanthin, representative of cyanobacteria	$\mu g\ l^{-1}$
PAR	photosynthetically active radiation	$\mu mol\ m^{-2}\ s^{-1}$
MLD	the mixed layer depth	m
N	the Brunt–Väisälä frequency	relative units

Table 2.1. Continued.

Stations	A	B	C	A	B	C
Month		April			August	
Extinction coefficient (k_d)	0.29	0.11	0.13	0.16	0.14	0.16
Euphotic zone (m)	15.8	20	20	20	20	20
Average chl *a* (µg l^{-1})	3.41±0.4	0.86±0.12	1.21±0.24	1.92±0.14	1.45±0.26	1.34±0.13
chl a_{max}, depth (m)	13	NA	18	NA	13-18	18
N_{max}, depth (m)	0.10, 15	0.14,6	0.12,10	0.19, 4	0.10,8/12	0.14, 10
Surface Midday PAR (µmol m^{-2} s^{-1})	1727	1875	409	352	507	531
Upper-pycnocline						
Temperature (^oC)	22.9±0.10	23.1±0.07	23.2±0.2	31.4±0.08	30.8±0.05	30.7±0.04
Salinity	29.6±0.3	32.1±0.6	31.9±0.5	27.7±1.1	31±0.7	30.9±0.8
DIN (µmo l^{-1})	0.99±0.36	0.52±0.35	0.28±0.13	1.53±0.33	1.24±0.12	0.78±0.16
P_i (µmo l^{-1})	0.17±0.03	0.24±0.04	0.25±0.05	0.72±0.09	0.21±0.02	0.21±0.06
Si (µmo l^{-1})	0.84±0.13	0.79±0.18	1.07±0.27	22.39±4.05	7.41±1.77	4.82±0.58
DIN:Pi:Si	5.8:1:4.9	2.2:1:3.3	1:1:4.3	2.1:1:31	5.9:1:35	3.7:1:23
Sub- pycnocline						
Temperature (^oC)	23.8±0.11	23.9±0.07	23.9±0.06	26.7±0.07	26.4±0.087	27.9±0.14
Salinity	34.1±0.75	35.3±0.29	34.7±0.37	35.5±0.15	35.6±0.26	35.5±0.18
DIN (µmo l^{-1})	6.85±1.15	0.27±0.10	0.78±0.29	9.21±1.62	5.70±1.25	3.43±0.70

Table 2.2 Hydrographic conditions measured during the six diel cycles. When the chl *a* concentration was evenly distributed in the water column, we use NA. Data shown as average value± standard error (S.E.).

Stations	A	B	C	A	B	C
Month		April			August	
P_i (µmo l^{-1})	0.73±0.13	0.51±0.11	0.74±0.17	1.01±0.21	0.56±0.09	0.46±0.05
Si (µmo l^{-1})	14.17±2.43	5.27±1.49	10.19±2.55	26.91±5.07	21.05±3.30	18.75±2.47
DIN:Pi:Si	9.4:1:19	0.5:1:10	1.1:1:14	9.1:1:26	10.1:1:38	7.5:1:41

Table 2.2. Continued.

The MLD was deepest at Station A (15 m) in April and shallowest at Station A (4 m) in August (Table 2.2). The stratification strength (N_{max}) was highest at station A in August (0.19), concurrent with the shallowest mixed layer depth (4 m) (Table 2.2). The MLD was 6 m and 10 m at station B and C, in April, respectively. In August, the MLD was 10 m at station C, while double pycnoclines appeared at station B at around 8 m and 12 m. The average chl *a* concentrations were similar among the three stations (1.34-1.98 $\mu g\ l^{-1}$) during August and generally lower than those measured in April at the same stations (Table 2.2). Surface temperature in August (31.05 ± 0.14°C) was much higher than April (23.11 ± 0.11°C). We also observed a temperature difference with depth (Table 2.2) in August.

The average DIN values above the pycnocline were lower than the values below the pycnocline except at station B in April, and the average DIN below the pycnocline was higher in August (6.11 ± 1.68 $\mu mol\ l^{-1}$) than April (2.62 ± 2.12 $\mu mol\ l^{-1}$) regardless of stations. For dissolved phosphorus (P_i) concentrations, the sub-pycnocline values were also higher than the upper-pycnocline values except station C, August. Despite the variations of nutrients, the DIN:P_i ratio was still much lower than the Redfield ratio of 16 (Table 2.2). Silicate (Si) concentrations were much lower in the upper pycnocline depths at all stations. Si limitation was measured in upper-pycnocline depths in April stations and station C in August (Table 2.2). chl *a* maximum appeared in different depths in different stations except station B in April (Table 2.2).

Diel changes in phytoplankton dynamics on the surface

In August 2012, we collected samples from midnight (time = 0) to late evening (time =18) on a 24 hr clock (time = hrs) to examine fine scale changes in primary productivity and phytoplankton physiology (Fig. 2.3). Given the photoperiod in August, day time samples were collected every 2 hours from 6 to 18 hrs and every 6 hours during night time (18 and 0). Chl *a* was highly variable and did not show a diel pattern at any of the three stations (Fig. 2.3). Chl *a* was generally higher at station A compared to stations B and C during August with values ranging from 1.00 to 2.62 $\mu g\ l^{-1}$. No diel changes were observed in the abundance of diatoms (Fuco/ chl *a*) and cyanobacteria (Zea/ chl *a*), but the average proportions of cyanobacteria were higher at station A (0.61) > B (0.44) > C (0.17), while the opposite pattern was observed in the average proportions of diatoms: station A (0.09) < B (0.17) < C (0.36) (Fig. 2.7).

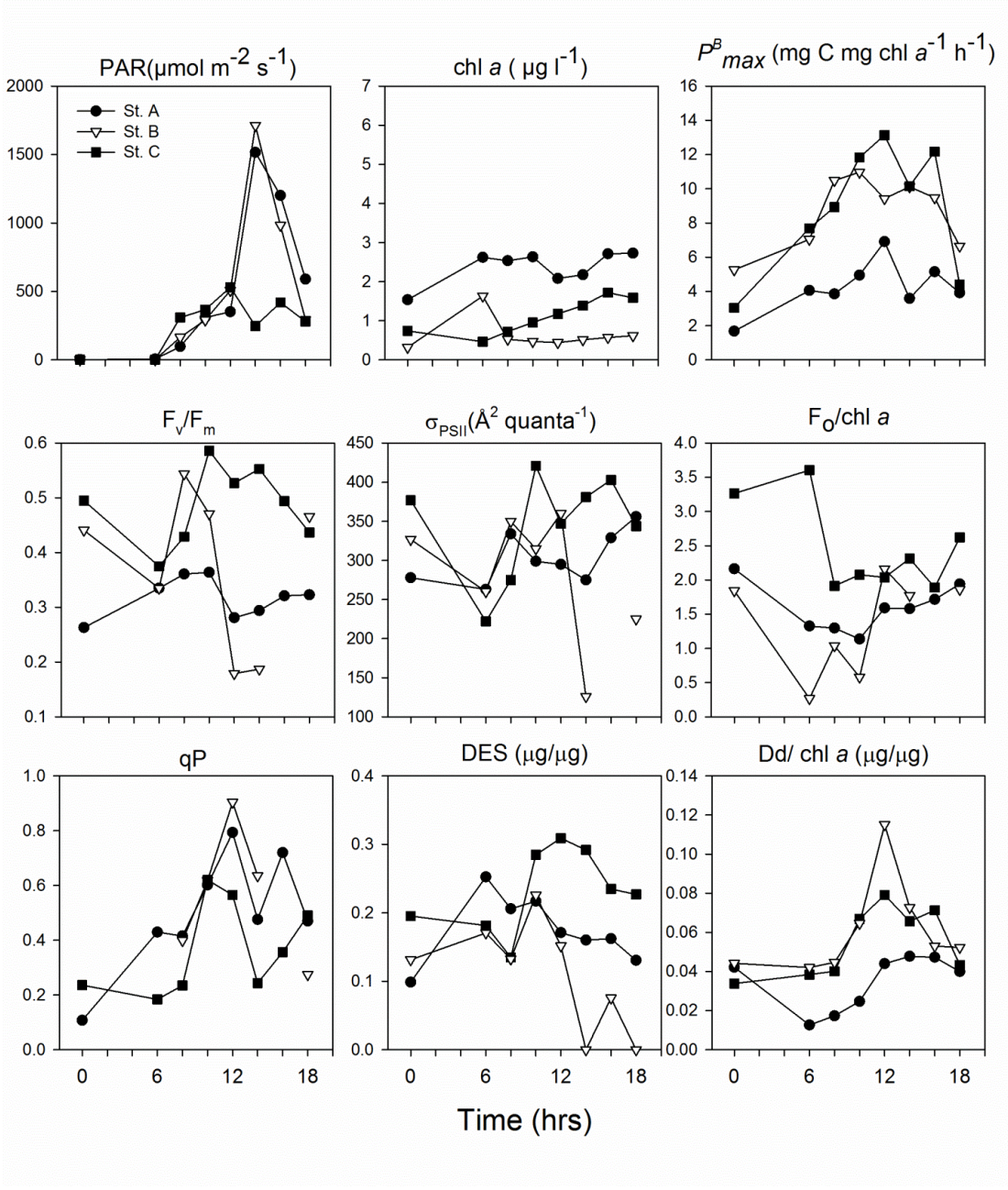

Figure 2.3 During the August 2012 cruise at stations A (●), B (▼) and C (■), measurements were made every two hours from dawn (= 6) or dusk (=18) and one point at midnight (= 0) to examine fine scale changes in primary productivity and phytoplankton physiology in surface waters (top 2 m). We measured PAR (µmol m^{-2} s^{-1}), chl *a* (µg l^{-1}), P^B_{max} (mg C mg chl a^{-1} h^{-1}), F_v/F_m (relative units), σ_{PSII} ($Å^2$ $quanta^{-1}$), F_o/chl *a*, qP (relative units), DES (µg/ µg) and Dd/chl *a* (µg/ µg).

P^B_{max}, the maximum chl *a*-specific carbon fixation rate, measured on the P-I curves from surface samples showed similar diel patterns at the three stations. There was an increase from midnight (0 hr) to peak values around midday (12 hr) or 10 hr (station B) (Fig. 2.3), then followed by a decrease from 12 hr to 18 hr. $P_{max}{}^B$ at station A at midday (6.91 mg C mg chl a^{-1} h^{-1}) was lower than at station B (9.43 mg C mg chl a^{-1} h^{-1}) and C (13.14 mg C mg chl a^{-1} h^{-1}). I_k showed peak values at noon or around noon (Table 2.4), corresponding to the peak values of $P_{max}{}^B$; this was not observed with α values (Table 2.4).

F_v/F_m values at the three stations all showed quenching at midday but to different degrees. Station A had the lowest average F_v/F_m values (0.32 ±0.009) among the three stations, corresponding to the shallowest MLD and cyanobacteria dominance (Table 2.2, Fig. 2.3 and 2.7). F_v/F_m at station B was variable with time of day, with the maximum value measured in the early morning (0.54) and minimum value recorded at midday (0.18), while at station C, F_v/F_m maintained relative high values throughout the diel cycle (0.49 ±0.017) (Fig. 2.3). The ratios of the minimum fluorescence (F_o) to chl *a* was used to indicate if there had been chl *a* fluorescence quenching during the daytime (Fig. 2.3). F_o/chl *a* values were highest at midnight at the three stations, especially at station C. The lowest ratios appeared at 10 hr at station A and B, indicating daytime fluorescence quenching (Fig. 2.3). Calculated qP values supported this finding with highest qP values measured at noon and lowest values closest to midnight (Fig. 2.3).

We calculated the proportion of Dt in the XC pigments pool, which is DES and the Dd pool (Dd/chl *a*) to indicate the effect of XC from minutes scales (DES) to hours

scales (Dd/ chl *a*) (Claustre et al., 1994). Strong photoprotective effects are correlated to the occurrence of NPQ to process heat dispassion (Doblin et al., 2011). Diel changes of Dd/ chl *a* were shown at the three stations, with the consistent increasing pattern during daytime and recovery after noon time (Fig. 2.3). The Dd pool at station A was smaller than at station B and C. Only station B showed obvious diel patterns in DES, and the recovery started around 16 hr, earlier than Dd pool (around 18 hr) (Fig. 2.3). The diel rhythms of DES at station A and C were not consistent with Dd/chl *a* values. DES values did not vary much from 6 hr to 18 hr in station A, and showed a small peak at 10 hr in station C. Station A showed the best correlation between F_v/F_m and Dd/chl *a* and DES among the three stations (R^2=0.52 and 0.52, respectively).

The variations of primary productivity and P-I parameters with depth

Samples were collected at four depths in both April and August 2012 (Figures 2.4-7; Table 2.4), but with a time interval of 6 hours, in order to investigate the changes of phytoplankton diel rhythms with depths in different hydrographic conditions. Multiple factors were measured such as P-I curve parameters (P^B_{max}, I_k, α), F_v/F_m, NPQ, qP, XC pigments and biomarker pigments for different phytoplankton groups.

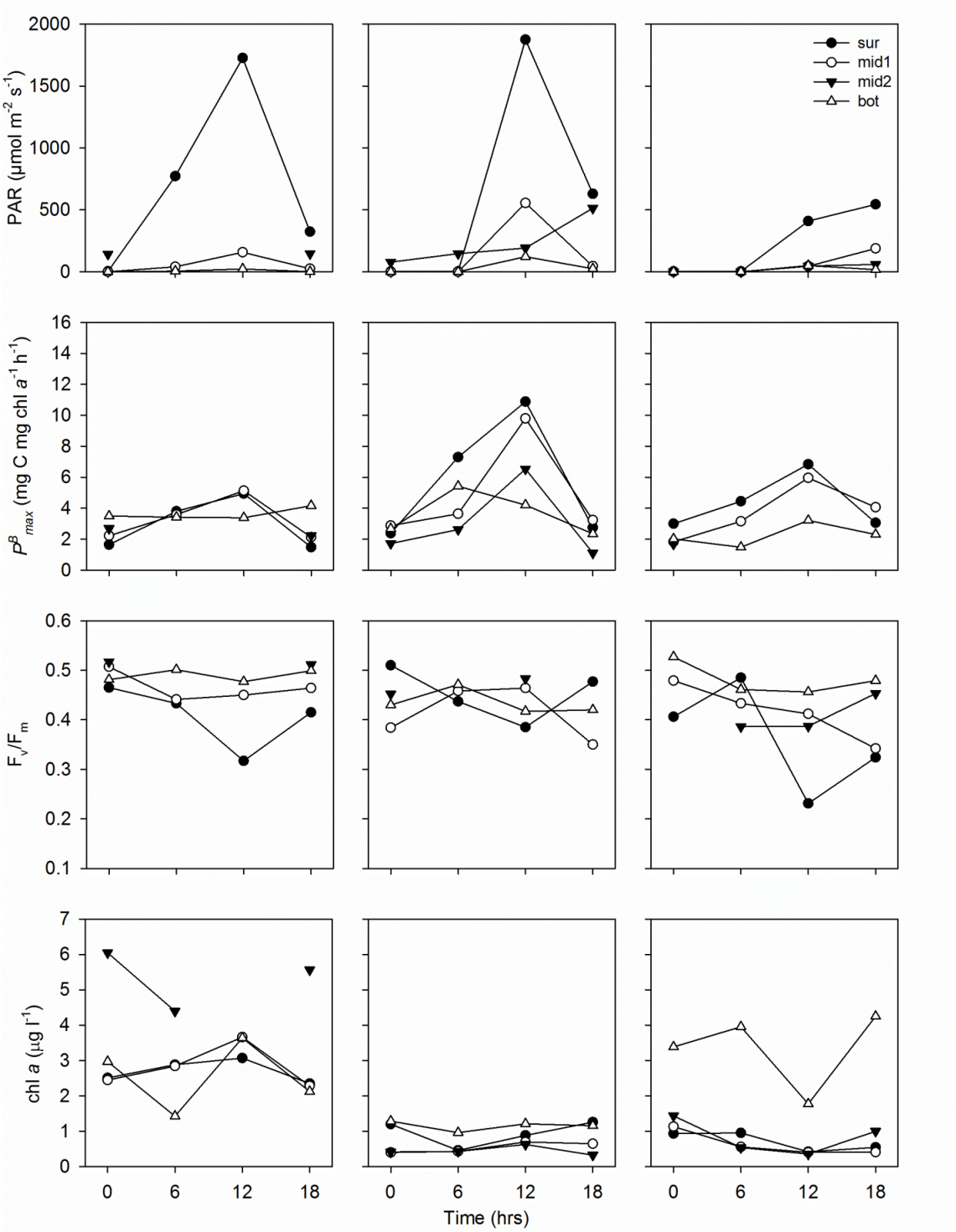

Figure 2.4 During the April 2012 cruise at stations A, B and C, we measured PAR (µmol m^{-2} s^{-1}), P^{B}_{max} (mg C mg chl a^{-1} h^{-1}), F_v/F_m (relative units) and chl *a* (µg l^{-1}) in surface (●), middle 1 (○), middle 2 (▼) and bottom (Δ) waters. This was conducted from midnight (= 0 on x-axis) to late evening (=18 on x-axis) on a 24 hr clock (time = hrs).

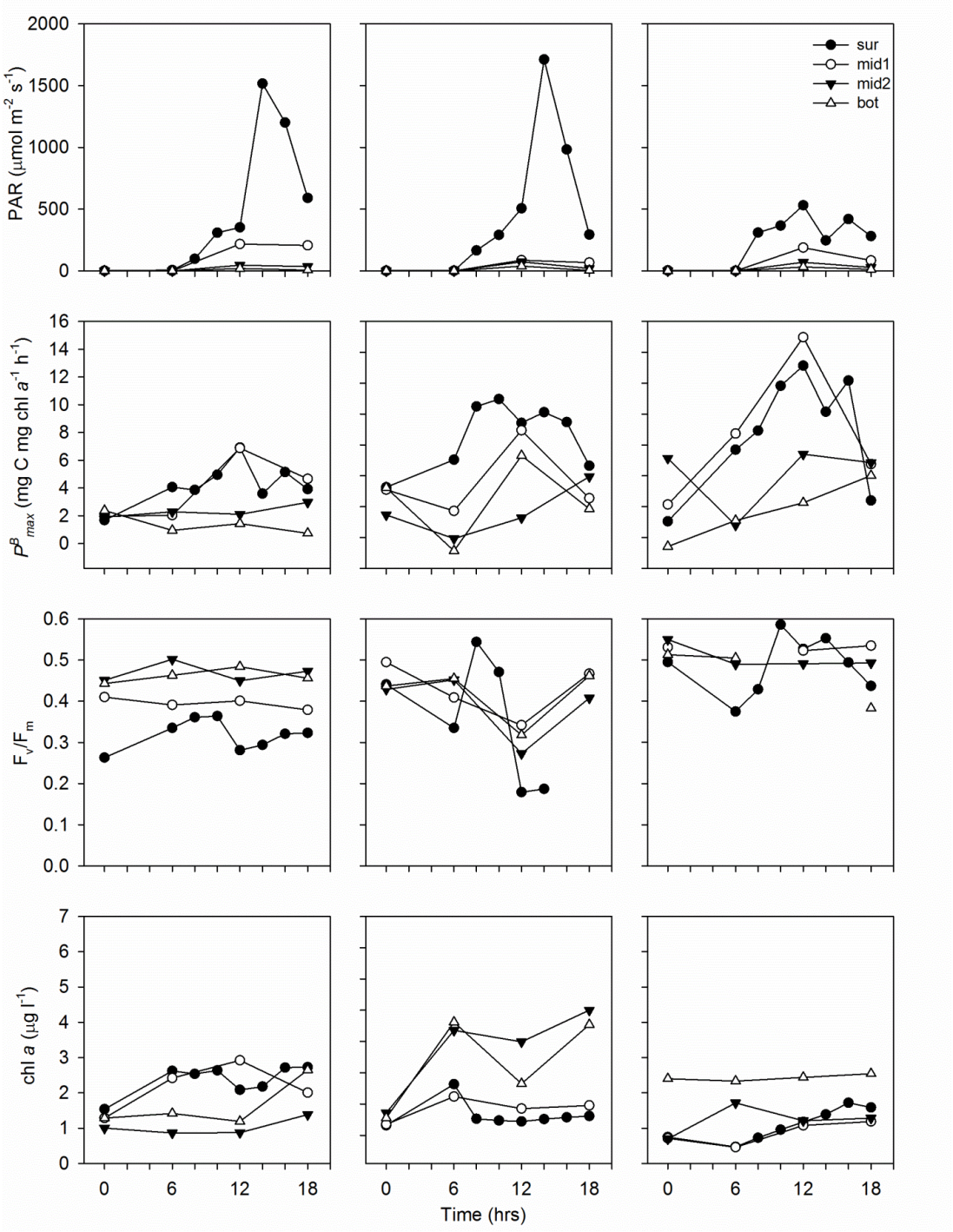

Figure 2.5 During the August 2012 cruise at stations A, B and C, we measured PAR (µmol m^{-2} s^{-1}), P^{B}_{max} (mg C mg chl a^{-1} h^{-1}), F_v/F_m (relative units) and chl *a* (µg l^{-1}) in surface (●), middle 1 (○), middle 2 (▼) and bottom (Δ) waters. This was conducted from midnight (= 0 on x-axis) to late evening (=18 on x-axis) on a 24 hr clock (time = hrs).

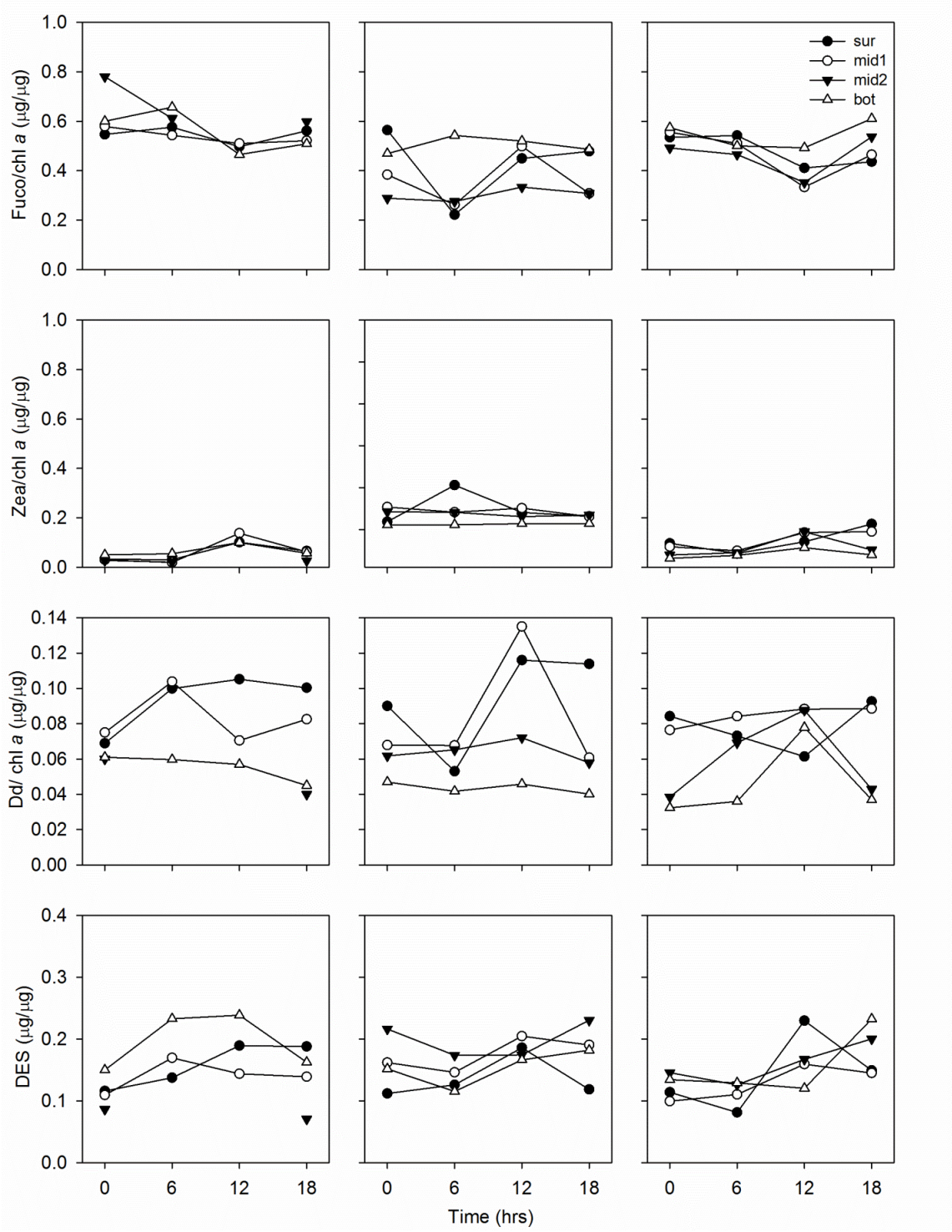

Figure 2.6 During the April 2012 cruise at stations A, B and C, we measured Fuco/chl *a* (µg/ µg), Zea/chl *a* (µg/ µg), Dd/chl *a* (µg/ µg) and DES (µg/ µg) in surface (●), middle 1 (○), middle 2 (▼) and bottom (Δ) waters. This was conducted from midnight (= 0 on x-axis) to late evening (=18 on x-axis) on a 24 hr clock (time = hrs).

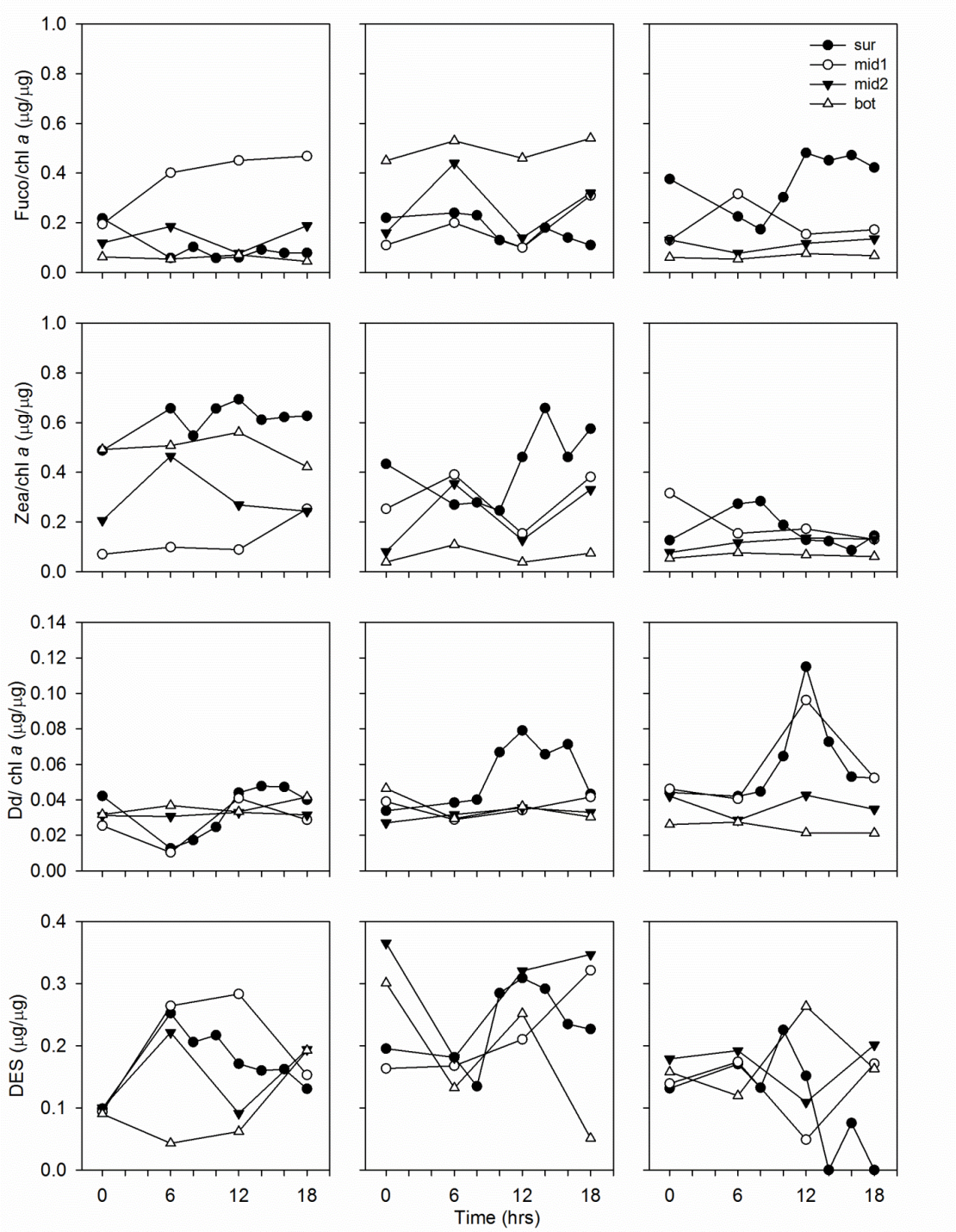

Figure 2.7 During the August 2012 cruise at stations A, B and C, we measured Fuco/chl *a* (µg/ µg), Zea/chl *a* (µg/ µg), Dd/chl *a* (µg/ µg) and DES (µg/ µg) in surface (●), middle 1 (○), middle 2 (▼) and bottom (Δ) waters. This was conducted from midnight (= 0 on x-axis) to late evening (=18 on x-axis) on a 24 hr clock (time = hrs).

The maximum primary productivity (max *PP*), the integrated production (integrated *PP*) and the proportion of sub-pycnocline production relative to the upper pycnocline at each station in April and August are shown in Table 2.3. The highest max *PP* and integrated *PP* in April and August were both measured at station A: 15.16 mgC m^{-3} h^{-1} and 2.14 gC m^{-2} d^{-1} and 13.88 mgC m^{-3} h^{-1} and 2.28 gC m^{-2} d^{-1}, respectively. These parameters at stations B and C were much more variable. For example, max *PP* was 2 fold at station B in April (9.59 mgC m^{-3} h^{-1}) compared to August (5.44 mgC m^{-3} h^{-1}) (Table 2.3). The integrated *PP* was lowest at station C in April (2.03 mgC m^{-3} h^{-1}) in the six diel cycles, and the value in August was 5.7 fold of April (11.65 mgC m^{-3} h^{-1}). The proportion of sub-pycnocline production was higher at station C in April and at station B in August, corresponding to high sub-pycnocline chl *a* concentrations and low k_d (Table 2.2). Low sub-pycnocline production was related to low k_d (station A, April) or a shallow MLD (station A, August) (Table 2.3).

Stations	A	B	C	A	B	C
Month		April			August	
max *PP* (mgC m^{-3} h^{-1})	15.16	9.59	2.03	13.88	5.44	11.65
integrated *PP* (gC m^{-2} d^{-1})	2.14	1.47	0.23	2.28	1.02	1.64
% of sub-pycnocline *PP*	12%	25%	48%	4.5%	38%	23%

Table 2.3 Primary production calculated at the three stations during each cruise

	Station	Station A	Station B	Station C	Station A	Station B	Station C
	Month		April			August	
α	ave S	0.009±0.0038	0.019±0.0035	0.013±0.0027	0.013±0.0014	0.017±0.0014	0.016 ±0.0024
	ave B	0.025±0.0074	0.019±0.0063	0.011±0.0022	0.008±0.0020	0.020±0.0067	0.017±0.0044
	max/T/D	0.026/6/bot	0.023/6/bot	0.015/6/sur	0.021/8/sur	0.033/12/bot	0.024/12/bot
	min/T/D	0.0010/18/sur	0.0021/18/mid2	0.0051/6/bot	0.0051/18/bot	0.0093/12/mid2	0.0059/10/sur
I_k	ave S	277±66	306±93	412±111	509±141	396±62	270±46
	ave B	186±49	238±43	299±45	171±30	167±32	169±5.1
	max/T/D	414/12/sur	568/12/sur	698/18/sur	548/14/sur	727/14/sur	531/12/sur
	min/T/D	93/18/bot	157/6/bot	133/0/bot	103/12/bot	109/0/bot	161/0/bot
NPQ	ave S	0.21±0.10	0.2±0.13	0.22±0.16	0.12±0.01	NA	0.25±0.08
	ave B	NA	0.05±0.01	0.13±0.08	NA	NA	0.07±0.03
	max/T/D	0.47/0/sur	0.57/18/sur	0.56/12/sur	0.24/18/sur	NA	0.41/0/mid2
	min/T/D	0.02/12/sur	0.05/12/sur	0.04/0/bot	NA	NA	NA
qP	ave S	0.42±0.17	0.43±0.12	0.58±0.17	0.53±0.06	NA	0.37±0.06
	ave B	0.38±0.06	NA	0.28±0.06	0.16±0.03	NA	0.16±0.05
	max/T/D	0.78/12/sur	0.67/12/mid1	1.04/12/sur	0.79/12/sur	NA	0.56/12/sur
	min/T/D	0.20/0/mid1	0.17/6/bot	0.22/0/bot	NA	NA	NA
σ_{PSII}	ave S	252±27	272±18	317±25	303±8.2	373±38	346±17
	ave B	222±3.9	293±7.9	268±8.2	280±22.6	280±20.8	352±3.3
	max/T/D	298/0/sur	356/0/mid1	390/12/sur	356/18/sur	452/0/bot	421/10/sur
	min/T/D	174/18/sur	245/18/sur	237/0/mid1	225/18/mid1	126/14/sur	222/6/sur

Table 2.4 Average surface values (ave S) ± standard error, average bottom values (ave B) ± standard error, maximum values/time/depth (max/T/D) and minimum/time/depth (min/T/D) for some parameters in the six diel cycles. NA indicated the values that lower than the instrument detection limits. The units of the parameters were shown in Table 2.1.

In April, the diel patterns of P_{max}^{B} changed with depths varied in different stations, depending on the MLD and the Z_{eu} (Fig. 2.4). Z_{eu} was shallower than the MLD at station A, with sur, mid1 and mid2 showing similar values in all the time points with slight diel changes (4.71 ±2.70 mg C mg chl a^{-1} h^{-1}), while bot samples did not show diel difference (overall F=2.413, p=0.165) (Fig. 2.4, Table 2.2). At this station in August, there was a clear difference between above (sur and mid1) and below (mid 2 and bot) the pycnocline (Fig. 2.5) which we can relate to the water column structure (Table 2.2). Except for station A in April, Z_{eu} reached down to the bottom of the 20 m isobaths at all other stations and particularly during the August cruise (Table 2.2). Station B showed a maximum P^{B}_{max} value of 10.88 mg C mg chl a^{-1} h^{-1} and most obvious diel pattern (F=9.729, p=0.003) among the three stations in April (Fig. 2.4). Station C shared similar MLD with station B, but had lower average PAR values and lower maximum P_{max}^{B}: 6.84 mg C mg chl a^{-1} h^{-1}. Only sur, mid1 and bot waters were sampled at station C in April. A two-way ANOVA indicated diel difference also occurred at this station (F=7.800, p=0.017).

In August, station A showed diel difference in P^{B}_{max} in sur and mid1 samples but not in mid2 and bot samples (Fig. 2.5). P^{B}_{max} at station A was significantly different among different depths (F=4.439, p=0.036), which was the only one among the six diel cycles (Fig. 2.5). Statistically significant diel changes existed in the three stations (p<0.05). Similar with April results, four depths at station A and C were separated to two groups by the mixed layers in which the diel difference was more obvious in sur and mid1 than in mid2 and bot. There was no consistent changing pattern of P^{B}_{max} with depth

at station B, corresponding to the appearance of the double-pycnocline at this station. At station B, sur, mid1 and bot samples showed noon peaks but not in mid2 samples (Fig. 2.5).

In all the diel cycles, average I_k values decreased from surface to bottom and the maximum I_k appeared around noon, with the exception of station C in April (Table 2.4). Stations A in April and C in August had the lowest surface average I_k and max I_k (Table 2.4). The changing patterns of α were not consistent with I_k, except average bottom α at station A in April was much higher than in surface (Table 2.4). The P-I curve regressions in our data did not show any photoinhibition during the incubation.

The variations of chl *a* fluorescence with depth

Although F_o/chl *a* showed diel patterns in August surface waters (Fig. 2.3), the patterns were not observed with depth or in April cruise (data not shown). In general, F_v/F_m of surface phytoplankton showed a decrease in midday and a recovery after that, except at station C in August (Figs. 2.4-2.5). The other three depths did not show consistent diel oscillations with the exception of station B in August (Figs. 2.4-2.5). For the three depths (sur, mid1 and mid2) in station A, April, A and C, August, F_v/F_m shared similar values at different time points, while in the other stations the values were different without showing consistent patterns. Bottom F_v/F_m values were higher than the surface values, especially at stations A and B in August (Fig. 2.4).

There was considerable amount of NPQ and qP, however, not all values could be calculated when phytoplankton biomass was low (FIRe operating close to its sensitivity

limit; signal/noise ratio) (e.g., station B, August), especially in bottom waters during August (Table 2.4). Although NPQ and qP did not show consistent diel patterns, the difference among different time points still indicated their dependence on light (Table 2.4). For example, the minimum NPQ values were measured around noon at station A and B in April, corresponding to highest PAR values and qP (Table 2.4). Highest qP appeared around noon, while minimum qP was calculated at midnight or early morning (6 hr) at all the stations (Table 2.4). Overall, surface average NPQ and qP values were both higher than bottom values at each station (Table 2.4). σ_{PSII} did not show consistent diel and depth difference. σ_{PSII} values in surface were lower or similar with bottom values. Maximum and Minimum σ_{PSII} values appeared in various depths and time points (Table 2.4).

The variations of photoprotective pigments with depth

Dd/chl *a* and DES were used as indictors of photoprotection in our study. The increase during daytime and decrease at night of DES was only observed in surface waters (Figs. 2.3, 2.6-2.7). There was linear regression between DES and F_v/F_m in the surface (R^2=0.70) in April but not in August. Vertical changes of DES were not consistent with each other (Figs. 2.6-2.7). However, the Dd/ chl *a* distributions showed vertical patterns with significant diel rhythms within the mixed layer and no obvious changes below. Two-way ANOVA analysis indicated there was no diel changes in the two depths below (mid2 and bot) the mixed layer (p>0.05). The diel changes within the mixed layer (sur and mid1) were statistically significant in August at station A

(F=22.000, p=0.015) and station C (F=27.105, p=0.011), while the values were not statistically significant in April. Only surface samples showed Dd/ chl *a* diel changes at station B in August, associated with the lack of stratification.

Phytoplankton community structure

At our research stations, the dominate phytoplankton groups were usually diatoms in April (spring) and cyanobacteria in August (summer) (Zhao and Quigg, 2014). In our study, we calculated the biomarker pigments/ chl *a* ratios to represent these two dominant phytoplankton groups. As shown in Fig. 2.6 and 2.7, Fuco/ chl *a* (diatoms) accounted for about 0.2-0.8 of the total in April and about 0.1-0.5 in August, while Zea/ chl *a* (cyanobacteria) accounted for about 0.05-0.3 of the total chl *a* in April and about 0.05-0.7 in August. The other phytoplankton groups, such as dinoflagellates, prymnesiophytes and green algae comprised less than 0.2, 0.2 and 0.15, respectively in April and 0.15, 0.25 and 0.1, respectively in August (Data not shown).

For Fuco/ chl *a* and Zea/ chl *a*, although there was day and night difference in some situations, there was no obviously consistent pattern (p>0.05). In April, diatoms dominated at station A and C in all the depths, and the noon values were lower than at other time points (Fig. 2.6). In contrast, cyanobacteria only accounted for less than 0.2 of the total chl *a*; they had higher values at noon than the other time points (Fig. 2.6). At station B, diatom abundance showed bottom values in early morning (6 hr, about 0.2), but peak values at noon (12hr, about 0.6) in sur, mid1 and mid2 waters (Fig. 2.6). More cyanobacteria were found at this station (>0.2 of total chl *a*), but only surface samples

showed peak values at noon (Fig. 2.6). In August, obvious depth variations were indicated at station A and B with the decrease abundance of cyanobacteria from surface to bottom, while diatoms abundance showed the opposite changing pattern (Fig. 2.7).

2.4 Discussion

While it is well known that primary productivity varies with diel cycles of light, and consequently, with depth, these two factors are rarely examined simultaneously in field situations. This may be partly due to the logistics and expense of such a sampling scheme, but it is also in part due to the challenges associated with interpreting the findings given the range of abiotic and biotic factors which influence the outcomes. As part of determining the mechanisms controlling hypoxia, we were challenged with providing measurements of primary production (surface, integrated, and other) which can be used in models and with these, confidence limits that take into account variability not only associated with the measurements themselves but also the variability along the continental shelf of Louisiana. Diel oscillations of P-I parameters have been reported in both coastal areas and the open ocean (Erga and Skjoldal, 1990; Prézelin, 1992; Doblin et al., 2011), which is considered as an important factor influencing our ability to calculate daily integrated primary production (Harding et al., 1981, 1982). In surface waters, these oscillations in P^{B}_{max} usually but not always exhibit a maximum during the day and minimum at night. Community compositions, its growth rate and nutritional status were found to be important (Haring et al., 1982; Kana et al., 1985). Bruyant et al. (2005) observed significant diel patterns of one *Prochlorococus* strain with P-I

parameters peaked around noon; Erga and Skjoldal (1990) found the P-I parameters usually peaked at 6am in a land-locked fjord station in western Norway; while Doblin et al. (2011) did not observe consistent diel changes of P-I parameters in sub-Antarctic and Polar Front Zones. Consistent with most of the former studies and Lohrenz et al. (1994)'s study in the NGOM, we found surface P^B_{max} peaked at 10 hr or 12 hr in all the diel cycles (Figs. 2.3-2.4). However, we did not find similar significant patterns with α and I_k, which might be influenced by abiotic noise. The lack of correlation between P^B_{max} and α or I_k were also found in other studies in the NGOM (Lohrenz et al., 1994).

Primary productivity and its driving factors

Highest integrated primary production was measured at station A, located in the plume region, with lower values found at stations B and C during both April and August cruises further west. In the spring surface waters, this was driven by diatom communities while in the summer, cyanobacteria were more important (present study; Zhao and Quigg, 2014). Consistent with the shift of phytoplankton community structure between seasons, we found 10-20 times lower Si concentrations in April than in August (Fig. 2.6-2.7). DIN:P_i ratios pointed to nitrogen limitation as reported previously along the Louisiana coastal shelf (Quigg et al., 2011; Turner and Rabalais, 2013; Zhao and Quigg, 2014). Limitation by phosphate has also been shown (e.g., Sylvan et al., 2006, 2007). Differences in the primary limiting nutrient between stations and time are driven by both the magnitude and timing of the Mississippi River flow with low flow years showing mostly nitrogen limitation while high flow years showing more phosphorus limitation

(Sylvan et al., 2006, 2007; Laurent et al., 2012; Quigg et al., 2011; Turner and Rabalais, 2013) .

It is unlikely that nutritional factors alone can explain the patterns we observed. Our results are consistent with earlier studies that found a less obvious diel variation with increasing depth (e.g., McAllister, 1963; Sournia, 1976; Kana et al., 1985; Brunet et al., 2008; Doblin et al., 2011). The depth of light penetration (euphotic zone) and magnitude of the light extinction coefficient (k_d) control particulate light absorption within the water column in the open ocean but less so in coastal shelves. In the NGOM, although k_d was strongly covaried with freshwater discharge from Mississippi-Atchafalaya Rivers, ranging from 0.19-1.01, the euphotic zone extended to the bottom along the 20 m isobaths across much of the Louisiana continental shelf, which emphasized the importance of sub-pycnocline productivity as recently reported in Lehrter et al. (2009). We also found that the proportion of sub-pycnocline production was 5%-48% of the total integrated primary productivity, similar to the 20%-50% in Lehrter et al. (2009). Light is therefore an important driving factor along the Louisiana shelf and needs to be considered in modeling efforts along with nutrients. A few other studies have considered light in addition to nutrients as regulating primary productivity in the NGOM (Lohrenz et al., 1994; Quigg et al., 2011; Turner and Rabalais, 2013).

We found the diel oscillations in P^B_{max} were independent of changes in chl *a*, which were considered as endogenous bio-clock and could be influenced by environmental factors (Kana et al., 1985; Lohrenz et al., 1994). In our study, the carbon fixation ability of phytoplankton cells adjusted to the effect of mixing. P^B_{max}

distributions were divided into two parts of the water column by the pycnocline, except at station B, August where the water column was not well stratified (Table 2.2, Figs. 2.4-2.5). For example, station A and B in April had equal sufficient light conditions and similar community structure at surface, but peak P^B_{max} at station B was 2.2 folds than in station A. Station A had deeper MLD but higher k_d than station B, thus phytoplankton cells in middle depths were under light limitation but within the mixed layer, which decreased the average light availability for each cell, resulted in low but similar P^B_{max} in the three depths. On the contrary, the mixed layer depth at station B was only around mid1 and the observed k_d was low, thus phytoplankton cells in the mixed layer were under more sufficient light conditions.

Photosynthetic physiology

In marine ecosystems, diel changes of chl *a* fluorescence were found in phytoplankton, zooxanthellaes and macroalgae, both in lab and field studies (Vaulot and Marie, 1999; Lavaud et al., 2004; Levy et al., 2004; Quigg et al., 2012). We measured a series of chl *a* fluorescence parameters in our study: the major diel oscillations of these parameters were mainly indicated by high values of qP and low values of F_o/ chl *a*, F_v/F_m and NPQ in daytime. At night time, F_o/ chl *a*, F_v/F_m and NPQ showed recovery patterns. The F_v/F_m values measured in the diel cycles were all lower than the experimental value of 0.65 measured with instruments based on the same principals as the FIRe (Kolber et al., 1998). This finding is consistent with nutrient limitation during unbalanced growth in our research area (Parkhill et al., 2001). The quenching of F_v/F_m in

the daytime was observed in all the six diel cycles but limited to those measurements made in surface waters. The quenching of F_v/F_m is usually associated with the process of photoinhibition which occurs when PSII systems absorb excess solar energy (Long et al., 1994; Kolber et al., 1998). The reaction center is protected by the XC to dissipate the energy by NPQ, which is a process taking from minutes to hours (Demmig-Adams and Adams III, 1992; Long et al., 1994). If the reaction center is further damaged, the repair involves D1 protein synthesis, which needs longer time than XC (Long et al., 1994). The occurrence of photoinhibition in marine phytoplankton has been widely observed (Long et al., 1994; Brunet et al., 2008). In our study, the quenching of F_v/F_m, correlated to the increase of Dt synthesis in surface water (Figs. 2.3-2.7). There was correlation between F_v/F_m and DES in April (R^2=0.70), while this correlation in August was not obvious because the difference of the phytoplankton community structure which is also known to influence the F_v/F_m to a large degree (Suggett et al., 2009b). Further, the dark incubation before measurements may have also relaxed quenching such that we maybe underestimating the real quenching in situ (Chekalyuk et al., 2014).

Compared to F_v/F_m and DES, the diel changes of Dd/ chl *a* were more consistent with the changes of P^B_{max} and influenced by the mixing effect. The transformation from Dd to Dt only needs seconds to minutes to protect the photosynthetic reaction centers. There is a long-term photoprotective mechanism involving the accumulation of the Dd pool, which requires hours to days to accomplish (Claustre et al., 1994). Therefore, the changes of Dd pool are considered as better indictors of physiological photoacclimation and the light history of the phytoplankton cells (Demers et al., 1991; Claustre et al.,

1994). In the NGOM, stratification occurs in the water column starting from April, resulting in high light experiences in the mixed layer (Table 2.2). Station C in April and August both experienced similar low ambient solar light (because of cloudiness), but the Dd/chl *a* diel changes were more obvious in August ($p<0.05$) than in April ($p>0.05$), indicating Dd in August was less influenced by the instant ambient light, which can be taken as evidence of long-term photoacclimation (Figs. 2.6-2.7). Although the euphotic zone reached to the bottom in five of the six diel cycles, the photosynthetic physiological parameters we discussed above did not show obvious diel changes below the pycnocline in most situations. For the sub-pycnocline samples, we only observed slight diel changes at station B and C in April and August in P^B_{max} values. The lack of photoprotection and chl *a* fluorescence quenching indicated insufficient light below the pycnocline.

The influence of phytoplankton communities

The major difference of phytoplankton community structure was the abundance shift from diatoms to cyanobacteria from April to August, which was mainly driven by temperature (seasons) and the nutrient availability (Litchman et al., 2007; Roelke et al., 2013). For the phytoplankton community structure, the lack of consistency in diel cycles in our study area was also found in other studies (Erga and Skjoldal, 1990; Becker et al., 2009). The major vertical change of phytoplankton communities was the decreased abundance of cyanobacteria and increased abundance of diatoms with depth at station A and B in August, which can be explained by the temperature difference with depth at the two stations (Figs. 2.6-2.7, Table 2.2; Zhao and Quigg, 2014).

Chl *a* fluorescence parameters, photoprotective pigments and carbon fixation rates vary with different phytoplankton groups (Geider et al., 1986; Falkowski and Raven, 2007; Suggett et al., 2009b). In our study, the most obvious effect of phytoplankton community structure was indicated by station A in August, which was dominated by cyanobacteria on surface at all the time points. In this station, we observed low average and peak P^{B}_{max}, F_v/F_m values, as well as low XC pigments. Suggett et al. (2009b) illustrated average F_v/F_m values in cyanobacteria assemblages were smaller than in diatoms. Therefore, different phytoplankton community structure could lead to the over- or under-estimation of nutrient limitation; photoinhibition and other environmental forcing that could influence these parameters. Phytoplankton community structure should be considered as an important influence factor when we evaluating the phytoplankton photosynthetic status and light history.

2.5 Conclusion

Our study supported the findings of Lehrter et al. (2009) and others who identified light penetration to the bottom of the euphotic zone as an important driver of primary productivity on the Louisiana shelf along with nutrients and mixing (Lohrenz et al., 1997, 1999; Fennel et al., 2011; Quigg et al., 2011; Laurent et al., 2012; Turner and Rabalais, 2013), and emphasized the importance of sub-pycnocline primary production. Mostly important, we provided evidence of how the characterization of the water column hydrography could affect phytoplankton photosynthesis. The consistent changing patterns of P^{B}_{max} and Dd/ chl *a* within the mixed layer indicated the photoacclimation of

phytoplankton cells in a long-term high light conditions, in order to maintain the high efficiency of light usage. In contrast, the diel rhythms of F_v/F_m and DES were limited to the surface, indicating a fast response for the photoprotection to light changes, emphasized the acclimation of the local phytoplankton communities to the complicated light conditions in this area. Seasonal changes in the phytoplankton community are important in determining both the magnitude of the productivity and photosynthetic physiology. Collectively we have a better understanding of the factors driving phytoplankton productivity and photosynthesis so that modeling efforts, such as those directed towards a better understanding of the mechanisms controlling hypoxia, maybe modified to consider these additional complexities.

CHAPTER III

NUTRIENT LIMITATION IN NORTHERN GULF OF MEXICO (NGOM): PHYTOPLANKTON COMMUNITY COMPOSITION AND PHOTOSYNTHETIC ACTIVITY IN RESPONSE TO NUTRIENT ADDITION*

3.1 Introduction

Liebig' law of minimum first claimed that plant growth is not determined by the total amount of a resource, but instead limited by the scarcest resource (Liebig 1840 in Danger et al., 2008). Microalgal resource competition follows Liebig's law. Tilman et al. (1982) resource ratio theory set up the basis for understanding use/competition for nutrient concentrations or ratios and phytoplankton community structure. Grover (1990) established the variable-internal-stores model to offset the drawback of the applicability of Tilman's theory in non-steady states (eg. periodic or non-periodic nutrient pulses). The intermediate disturbance hypothesis emphasized that periods of nutrient pulse could also control the variability of phytoplankton community structure (Sommer, 1995). All these theories have been tested in laboratory and natural aquatic systems (mostly freshwaters) (eg., Sommer, 1995; Sterner and Elser, 2002; Cermeño et al., 2011). Complex nutrient conditions in coastal environments lead to corresponding variability of phytoplankton community structure. The influence of fluctuating nutrient conditions on production, zooplankton grazing, particulate organic material cycling, and bottom

---

* Reprinted with permission from "Nutrient Limitation in Northern Gulf of Mexico (NGOM): Phytoplankton Communities and Photosynthesis Respond to Nutrient Pulse" by Zhao, Y. and Quigg, A. 2014. PLOS ONE 9(2), e88732. Copyright 2014 Zhao, Quigg.

oxygen consumption, are an important part of research in the Northern Gulf of Mexico (NGOM) (Dagg et al., 2007). It has been suggested that spring phytoplankton blooms are the initial step in the scenario of the development of annually bottom hypoxia (Turner et al., 2006, Dimarco et al., 2010).

Nutrient fluctuations in the NGOM are quite significant due to the large inputs of the Mississippi Atchafalaya River system, one of the ten largest rivers in the world (Dagg and Breed, 2003). In the NGOM, nitrogen (N) limitation and phosphorus (P) limitation can both happen in different locations but during the same time frame (Dagg and Breed, 2003; Quigg et al., 2011; Turner and Rabalais, 2013). As a result of this nutrient loading, dissolved inorganic nitrogen (DIN), inorganic phosphorus (P_i), and silicate (Si) in the Mississippi River have increased to Redfield levels while DIN:P_i ratios in the NGOM exceeds Redfield levels, particularly after high flows (Rabalais et al., 2002; Sylvan et al., 2006). Changing ratios of N: P: Si over the last 50 years imply that the limiting nutrient for primary production may also have changed (Dagg et al., 2007; Bianchi et al., 2010), but this requires investigation. Research on nutrient limitation in this region has been conducted by direct nutrient measurements (e.g., Lohrenz et al., 1999), resource limitation assays (RLAs) (e.g., Sylvan et al., 2007; Quigg et al., 2011; Turner and Rabalais, 2013) and/or measurements of distinctive indicators (like enzymes, amino acids, proteins) (e.g., Dortch and Whitledge, 1992; Sylvan et al., 2011). With the development of fluorescence technology to measure phytoplankton biomass and physiology, this method has also been applied to the studies of nutrient

limitation especially in combination with RLAs, also called nutrient addition assays (e.g., Sylvan et al., 2007).

RLAs have been suggested to be the better diagnostic tool for nutrient limitation than the direct measurement of nutrient concentrations and/or ratios (Turner and Rabalais, 2013). RLAs have been done in NGOM. (e.g. Smith and Hitchcock, 1994; Sylvan et al., 2006, 2007; Quigg et al., 2011; Turner and Rabalais, 2013). However, all these studies focused on evaluating the nutrient status and the changes of phytoplankton biomass (or production) but not the community structure. The study of Lugus et al. (2004) performed in the Baltic Sea showed phytoplankton community shifts occur after the addition of limiting nutrients in RLAs. In fact, there are certain patterns of phytoplankton responding to ambient nutrient stimulations. Litchman et al. (2007) applied trait-based approaches in terrestrial ecology to the research of phytoplankton nutrient competition by means of proposing several nutrient-dependent functional traits which not only are species-specific, but also nutrient-specific. Trait-based ecology in phytoplankton communities has been widely shown in laboratory experiments but seldom in natural environments (Edwards et al., 2011, 2013).

Based on nutrient competition theory and trait-based ecology, phytoplankton community shifts may happen when the nutrient conditions change. The object of this study was to investigate the effect of nutrient pluses on the phytoplankton community structure and physiology in NGOM in April and August 2012. In our research, we focused on the short-term (48 hr) response of the phytoplankton community under ambient conditions to changes only by the addition of nutrients, including nitrogen (as

nitrate), organic and inorganic phosphate as well as a 'bottom' water sample (see below for definition). High Performance Liquid Chromatography (HPLC) combined with ChemTax was used in parallel with a Fluorescence Induction and Relaxation (FIRe) system to examine photosynthetic activities of the changing community, which is the first time this approach has been applied in NGOM studies. While previous studies have investigated the effect of nutrient pluses on phytoplankton biomass in NGOM (Smith and Hitchcock, 1994, Sylven et al., 2007, Quigg et al., 2011, Turner and Rabalais, 2013), the shift in phytoplankton community structure at different times of the year has not been examined.

3.2 Material and methods

Sampling

Four bioassays were conducted during cruises as part of the project 'Mechanisms Controlling Hypoxia' aboard the R/V *Pelican* in April and August 2012. The two sampling stations (A and B, located at 29.07 ºN, 89.93 ºW and 29.00 ºN, 92.00 ºW, respectively) on the Louisiana Shelf are shown in Fig. 3.1. Surface water (0.5-2 m) was collected for in-situ bioassays (BA) using a CTD rosette with twelve 5 L Niskin bottles. Hydrographic parameters (temperature, salinity, PAR, and dissolved oxygen (DO)) were measured using shipboard calibrated sensors attached to the CTD rosette. Water column profiles immediately prior to sample collection are shown in Fig. 3.2. These are representative of the profiles measured ($n \geq 12$) as we remained at each station for no less than 24 hours and measured profiles at least every 2 hours. The four bioassays

referred to as BA1, BA2, BA3 and BA4 correspond to those performed in April at station A and B and then in August at stations A and B respectively.

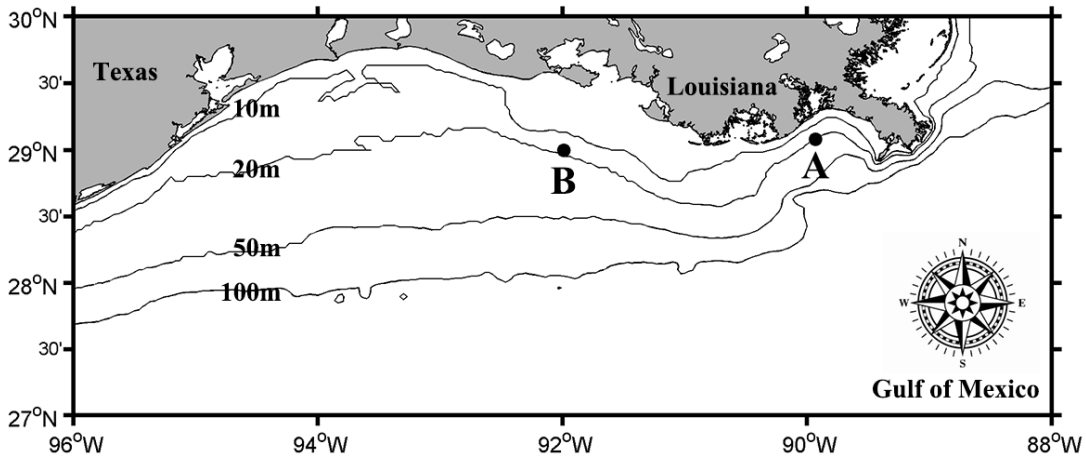

Figure 3.1 Study area and bathymetry for the mechanisms controlling hypoxia program on the Texas-Louisiana Shelf in northern Gulf of Mexico. The 10, 20, 50 and 100 m isobaths are shown. Locations of stations A and B which were sampled in April and August 2012 are offshore from the Mississippi and Atchafalaya Rivers respectively.

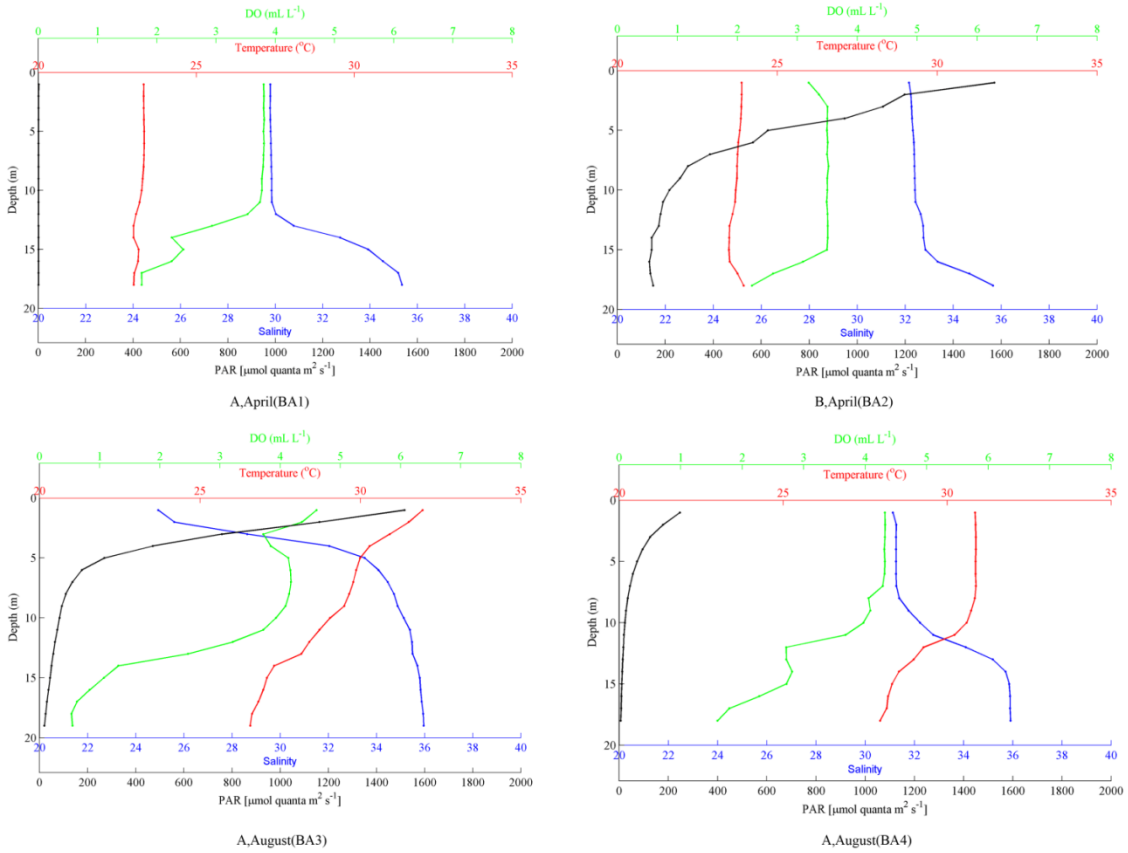

Figure 3.2 Hydrographic features of the water column immediately prior to the start of each bioassay (BA). Water column profiles were measured with calibrated sensors attached to the CTD rosette. At station A and station B in April (BA1 and BA2) and August (BA3 and BA4). The lack of PAR in BA1 was because the bioassay was started at night. The low PAR in BA4 was due to extensive cloud cover.

Bioassays

The bioassays were performed essentially following the procedure of Fisher et al. (1992). In this study, the concentrations of nutrients added to bioassays was based on previous work performed by Sylvan et al. (2007) and Quigg et al. (2011) in NGOM.

Treatments, performed in triplicate 1L bottles included control (no additions), +N (30 μmol L^{-1} NO_3), +P_i (2 μmol L^{-1} PO_4), +organic phosphorus (OP) (2 μmol L^{-1} D Glucose-6-phosphate), +NP_i (30 μmol L^{-1} NO_3, 2 μmol L^{-1} PO_4). We added two treatments to test the effect of grazers (NG) and 'bottom' (SB) water. Grazers were removed by filtering seawater though a 118 μm sieve (Michael Dagg, pers. comm.) before starting the bioassays. No nutrients were added to the grazing treatments.

The 'bottom water' treatment involved collecting waters from between ~15 to 18m along the 20m isobath at the same time as the surface water using the CTD rosette. This was pre-filtered using a 0.2 μm cellulose ester filter (Millipore). The treatment consisted of 90% surface water + 10% pre-filtered bottom water (no nutrients added). The aim of this treatment was to determine if the bottom waters in the NGOM could stimulate the phytoplankton on the surface. Given the water column can be well stratified in the summer, previous observations have shown that nutrients accumulate below the pycnocline. During mixing events (e.g., hurricanes), these will be introduced quickly to the surface and may alleviate nutrient stress. This approach has been applied elsewhere, such as Gulf of Aqaba and Qatar peninsula in Arabian Sea (Suggett et al., 2009; Quigg et al., 2013b).

The above seven treatments were incubated on deck in acid-washed polyethylene bottles for 48 hours in incubators with in-situ surface water continuously flowing through to maintain ambient temperatures. By using shade cloth, samples in the incubator received approximately 50% of ambient light. Samples were exposed to the natural light: dark photoperiod of 12h: 12h in April and 14h: 10h in August. Samples

taken at the end of the incubation period will be referred to by their treatment, for example, control, +N, +P_i etc.

Phytoplankton fluorescence

The Fluorescence Induction and Relaxation (FIRe) System (FIRe fluorometer, Satlantic Instruments S/N 2) was used to measure the photosynthetic parameters of the phytoplankton in the bioassays. Every 24 hours (that is, at 0, 24 and 48 hours), 3ml water samples were taken out and stored in darkness for 30 minutes before measurements. Fluorescence from filtered seawater (0.45μm) collected from the corresponding treatments was subtracted from the F_o and F_m values of samples to correct for the influence of background fluorescence (Cullen and Davis, 2003). In this study, we use only information collected from the single turnover (ST) component of the transient according to Kolber et al. (1998) and Kromkamp and Forster (2003), including the minimum fluorescence (F_o), the photosynthetic efficiency of PS II (F_v/F_m), the functional absorption cross-section for PSII (σ_{PSII}; $Å^2$ $quanta^{-1}$), the minimum turnover time of electron transfer from reaction centers to the acceptor side (τ_{QA}; μs) and the connectivity factor (*p*) for the degree of departure from a simple exponential fluorescence rise ($p = 0$) towards a sigmoidal fluorescence rise during the FIRe trace (*p* approaches 1). The four parameters were sensitive to nutrient or light limitation, which were taken as physiological markers for nutrient limitation in many studies (Parkhill et al., 2001; Sylvan et al., 2007; Moore et al., 2008). The light curves for all the samples were

measured at different gain settings to ensure the signal to noise ratios. Gains were normalized in the calculations to account for these differences.

Nutrients and pigment analysis

Before starting the bioassays, nutrient and chlorophyll (chl) *a* samples were taken to quantify the background nutrient concentrations and phytoplankton biomass. For nutrients, 20mL water samples were filtered thought pre-rinsed 0.45 μm cellulose ester filters (Millipore) into acid-washed polyethylene Nalgene bottles to determine the concentrations of dissolved nitrogen (nitrate, nitrite, ammonium and urea), phosphate and silicate. Samples were frozen at -20^{o}C until analyzed by Geochemical and Environmental Research Group, Texas A&M University. For the chl *a* samples, 400-800 mL seawater was filtered onto GF/F glass fiber filters (Whatman) then frozen immediately until analyzed by a calibrated Turner Designs model 10AU fluorometer. The extraction and calculation method were according to Quigg et al. (2011).

At the beginning and the end of the bioassays, 1L-2L initial background water samples and 900 mL experimental water samples respectively were filtered onto GF/F glass fiber filters (Whatman). Filters were maintained in -80^{o}C until reverse-phase HPLC analysis using the procedures of Pinckney et al. (1996). The HPLC instrument includes a binary gradient pump (Shimadzu dual LC10-ATvp and Controller SCL-10Avp), temperature controlled autosampler (Shimadzu SIL 10-Avp) with a 500 μL injection loop, column oven (Shimadzu CTO-10AS vp), and photodiode array detector (PDA, Shimadzu SPD-M10A vp; 200 to 800 nm). Pigments were extracted in 500-1000

μL cold 100% acetone with 100 μL synthetic carotenoid β-apo-8'-carotenal (internal standard) overnight. Before injection to the HPLC, samples were pre-filtered through a 0.2 μm PTFE (Gelman Acrodisc) filter. 300-400 μL extracted samples mixed with 1.0 mol L^{-1} ammonium acetate (ion-pairing solution) in a ratio of 4 (extracted sample):1(ammonium acetate) were added to the vials then placed in the autosampler rack for HPLC analysis. Pigments peaks were identified based on retention time and pigment spectra shape obtained from liquid standards (DHI, Hørsholm, Denmark).

Major phytoplankton groups were determined from the pigment composition and by using the program CHEMTAX V1.95 (http://gcmd.nasa.gov/records/AADC_CHEMTAX.html). In our study, three different kinds of chlorophylls and 12 kinds of carotenoids were detected by HPLC analysis. The chlorophylls include chlorophyll *c* (chl *c*), chlorophyll *b* (chl *b*) and chlorophyll *a* (chl *a*), and the carotenoids included peridinin (peri), 19'-butfucoxanthin (but), fucoxanthin (fuco), 19'-hexfucoxanthin (hex), neoxanthin (neo), violaxanthin (vio), prasinoxanthin (pras), diadinoxanthin (diad), alloxanthin (allo), diatoxanthin (diat), lutein (lut), and zeaxanthin (zea). Eight groups of phytoplankton were defined from an earlier study in NGOM (Qian et al., 2004), but the pigment/chl *a* in the matrices were derived from multiple studies (Table 3.1). Lewitus et al. (2005) and Schlüter et al. (2000) calculated the pigments ratios for a series lab-cultured costal phytoplankton species in different conditions, providing us good reference to build the initial pigments ratio matrix in Chemtax, which was more suitable for costal studies than the matrix of Macky et al. (1996). Based on the microscopic identification from selected samples we collected

during the 2012 cruises, *Thalassiosira sp.* and *Prorocentrum sp.* were the most dominant species in diatoms and dinoflagellates, thus we applied the pigments ratios of *Thalassiosira minisoula* and *Prorocentrum minimum* in Lewitus et al. (2005) to represent diatoms and dinoflagellates, respectively. The rest of the ratios were all the average values calculated from the pigment summary of Schlüter et al. (2000) for multiple coastal species. For the microscopic identification, samples were preserved in 10% buffered formalin and identified to genus using Tomas (1997).

	chl *c*	peri	but	fuco	hex	neo	vio	pras	diad	allo	diat	lut	zea	chl *b*	chl *a*
Diat	0.289	0	0	0.546	0	0	0	0	0.124	0	0.025	0	0	0	1
Dino	0.099	0.411	0	0	0	0	0	0	0.164	0	0.016	0	0	0	1
Cyan	0	0	0	0	0	0	0	0	0	0	0	0	1.245	0	1
Crypto	0.221	0	0	0	0	0	0	0	0	0.405	0	0	0	0	1
Prymn	0.137	0	0	0.031	0.625	0	0	0	0	0	0	0	0	0	1
Pelago	0.397	0	0.61	0.732	0	0	0	0	0.14	0	0.088	0	0	0	1
Prasino	0	0	0	0	0	0.096	0.069	0.229	0	0	0	0.067	0.051	0.605	1
Chloro	0	0	0	0	0	0.042	0.031	0	0	0	0	0.21	0	0	1

Table 3.1 Initial pigment / chl *a* ratios for the different phytoplankton groups used for ChemTax V1.95. Diat = diatoms, Dino = dinoflagellates, Cyan = cyanobacteria, Crypto = cyptophytes, Prymn = prymnesiophytes, Pelago = pelagophytes , Prasino = prasinophytes , Chloro = chlorophytes. See text (methods) for pigment names.

Data analysis

The statistical analysis was conducted using SPSS 13.0, and the figures were plotted using Matlab 7.11 or Sigmaplot 12.0. All data presented was calculated as means

± standard error (S.E.). One-way analysis of variance (one-way ANOVA) was used to determine the significance among different treatments, in which LSD test was used to group-paired significance test when the variance was homogeneous, and Dunnett's T3 test was applied to the heterogeneity of variance. Correlation test was used to test the correlation relationship between different parameters. $p<0.05$ was considered as significant.

3.3 Results

Hydrographic conditions and nutrients

The water column profiles prior to the start of each bioassay are shown in Figure 3.2, with surface and bottom values given in Table 3.2. Except for BA1, the other bioassays were started around noon. Photosynthetically active radiation (PAR) was highly variable reflecting sunny versus cloud covered days at sea. The low PAR at the start of BA4 may have resulted in light limitation of phytoplankton productivity before incubation. The PAR in BA2 and BA3 represented normal conditions (sunny days) in April and August. PAR decreased with depth, but we still had detectable values in bottom waters in BA2 and BA3 (Fig. 3.2). Surface temperature was higher in August (31 ±1 ^{o}C) than in April (23 ±1 ^{o}C) (Table 3.2). While there was no difference in temperature in the water column in April, bottom waters were 3-5 ^{o}C cooler in August (Fig. 3.2). Station A is closer to the Mississippi River plume which explains the lower surface salinity measured there than at station B which is located west of the Atchafalaya River (Figs. 3.1 and 3.2). Bottom water salinities were around 35 ±1 for all four

bioassays (Table 3.2). In both April and August, DO in station A was higher than in station B (Fig. 3.2), consistent with the higher chl *a* values in station A (Table 3.2). The lowest DO values all appeared in the bottom. In BA3, bottom waters were hypoxic (< 1.4mL L^{-1}; Rabalais et al. 2002).

In NGOM, N, P, Si can all act as limiting nutrients for phytoplankton growth at times (Turner and Rabalais, 1991; Quigg et al., 2011). The Redfield Ratio implies the average optimum nutrient ratio for phytoplankton is N: P: Si = 16: 1: 16. In NGOM, N and P have been defined as DIN:P_i < 10 with DIN < 1 μmol L^{-1} and DIN:P_i > 20 with P_i < 0.2 μmol L^{-1}, respectively (Sylvan et al., 2006; Quigg et al., 2011). In the lower Mississippi River, Si concentration has decreased and its ratio to N changed from 4:1 in 1900s to 1:1 in 1980s (Turner and Rabalais, 1991). Based on this criterion, all our bioassays were conducted in N limited waters (Table 3.2). Si was more sufficient in August bioassays (BA2 and BA4), but BA1 phytoplankton were likely under Si limitation (Table 3.2). In BA1, BA3 and BA4, there were more nutrients (higher concentrations) at the bottom than the surface, indicating a potential nutrient pool for phytoplankton (Table 3.2).

	BA1sur	BA1bot	BA2sur	BA2bot	BA3sur	BA3bot	BA4sur	BA4bot
Nitrate + Nitrite (μmol L^{-1})	0.18	8.41	0.22	0.23	0.58	12.53	1.26	5.26
Ammonia (μmol L^{-1})	0.14	0.66	0.033	0.071	1.04	0.95	1.66	0.69
Phosphate (μmol L^{-1})	0.37	1.76	0.40	0.27	1.56	1.62	0.37	0.51
Silicate (μmol L^{-1})	0.37	18.9	4.24	5.04	31.32	40.36	6.97	26.80
DIN:Pi:Si	1:1:1	5:1:11	1.25:1:10.5	1.7:1:16.7	1.6:1:30	6.5:1:20	7.5:1:17.5	8.5:1:38.5
Chl *a* (μg L^{-1})	2.35	2.12	0.42	1.77	2.08	1.17	1.18	2.44
Temperature (^{o}C)	23.2	23.0	23.1	23.8	31.9	26.6	30.8	28.2
Salinity	29.3	35.5	31.9	35.8	24.9	35.9	31.1	35.9
Incubation start time	8pm	8pm	1pm	1pm	2pm	2pm	2pm	2pm
Surface PAR (μmol quanta m^2 s^{-1})	2.5	0	1875	115	1516	20.2	247	8.9

Table 3.2 Nutrients and hydrographic conditions at the bioassay stations immediately prior to starting the bioassays. (BA1 = station A, April; BA2 = station B, April; BA3 = station A, August; and BA4 = station B, August; sur = water collected in the top 2m; bot = water collected between ~15-18m)

Response of phytoplankton biomass

The change in chl *a* (μg L^{-1}) concentrations in different treatments shared similar patterns in the four bioassays (Fig. 3.3). Only +N and +NP_i treatments showed significant stimulations at the end of incubation (p<0.001, One-Way ANOVA). There was no significant difference among the other five treatments (p>0.05) relative to the T_0 (chl *a* at start of the bioassay) and the control (chl *a* at the end of the bioassay). Compared to the T_0, chl *a* concentration in the control increased in BA4 (p<0.001). In BA1, BA2 and BA3, the chl *a* changes in controls were not statistically significant (Fig. 3.3). In April, chl *a* concentrations were higher in the +NP_i treatments than +N treatment (p=0.012, 0.011, respectively). The situation was opposite in August but there was no statistically difference (p=0.635, 0.221, respectively). The average chl *a*

concentration increased 106% in April after N additions, but increased by 178% in August, indicating higher growth rates of phytoplankton in August than in April after nutrient additions. P additions (P_i and OP) and the removal of grazers did not result in an overall increase in chl *a* concentration in any bioassay compared to the control (Fig. 3.3). Similarly, the addition of 'bottom' waters to surface waters did not stimulate the growth of phytoplankton relative to the control treatments over 48 hours (Fig. 3.3).

F_o is used to an estimate of the initial chl *a* fluorescence measured with the FIRe which can be used to represent chl *a* concentrations (Kolber et al., 1998). Given only small sample's are required and the measurement is relatively fast, it can be used to provide greater temporal information than traditional measures of chl *a*. In our bioassays, F_o was significantly correlated (linear relationships) to chl *a* concentration (correlation analysis, $p<0.001$), regardless of station and cruise (Fig. 3.4). R^2 value in BA3 equation was the lowest among the four bioassays, corresponding to significantly higher cyanobacterial abundance in BA3 compared to the other three bioassays (Fig. 3.6). As with the Fast Repetition Rate florometer (FRRF), the PSII fluorescence yield of cyanobacteria containing phycocyanin instead of phycoerythrin cannot be efficiently harvested at the wave band of the instruments excitation (Raateoja et al. 2004). Although the specific cyanobacterial taxa were not identified in our samples, earlier reports indicated taxa containing phycocyanin (eg. *Aphanizomenon* sp.) are common in our research areas (Schaeffer et al., 2012).

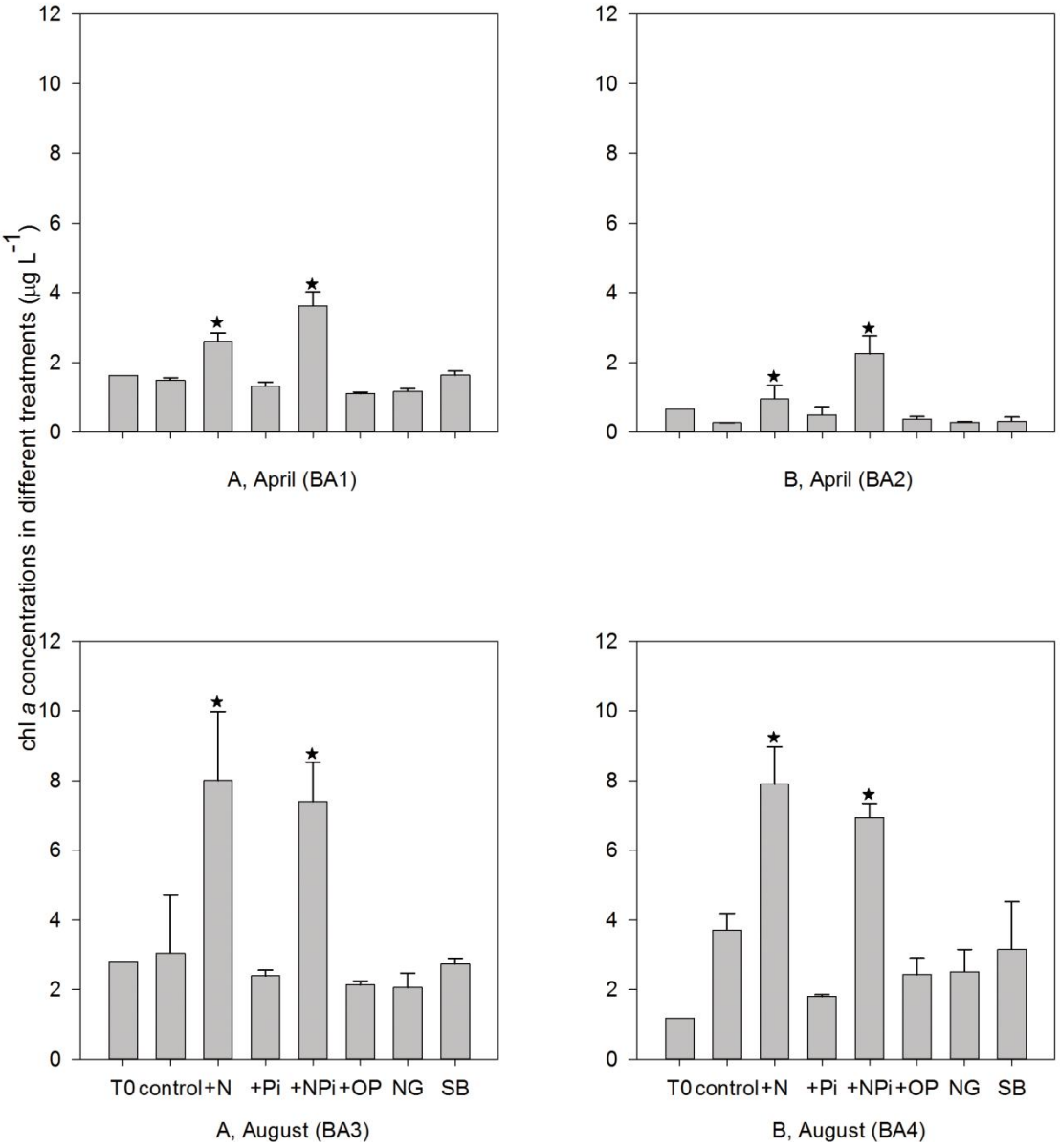

Figure 3.3 Chl *a* (μg L^{-1}) concentrations in the different bioassay treatments (mean ± S.E). ⋆ indicates significant difference compared with the 'control' at the same time point. NG: no grazers, SB: surface+bottom. T_0: chl *a* at start of the bioassay; control: chl *a* at the end of the bioassay (after 48 hours).

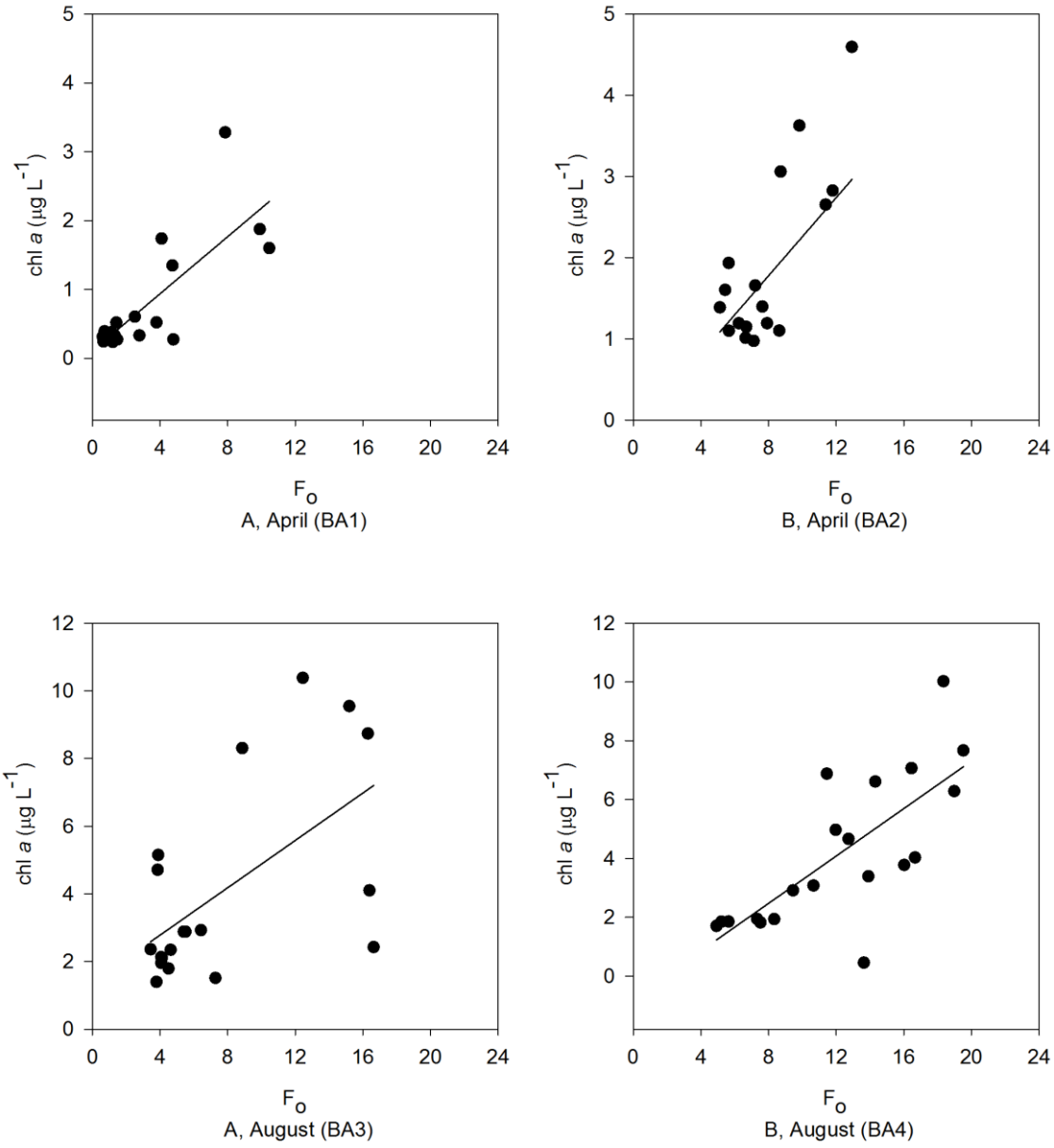

Figure 3.4 Linear relationships between F_o and chl *a* concentration (µg L^{-1}) after 48 hrs incubation in different bioassays in which R^2=0.6212; p<0.001 in BA1, R^2=0.6202, p<0.05 in BA2, R^2=0.3504, p<0.01in BA3 and R^2=0.5488, p<0.05 in BA4.

At t = 48 hours, F_o values in N addition treatments showed the similar patterns with chl *a* changes, which were the significant stimulation effects after N and NP_i additions (p <0.001) (Fig. 3.5). There was significant F_o increase in the NG (no grazers) and SB (surface+bottom) treatments in BA1 and +OP treatments in BA2 (Fig. 3.5) (p=0.036, 0.042, <0.001, respectively). Given we did not see the same pattern in the chl *a* data (Fig. 3.3), this maybe an overestimation of F_o by the FIRe. F_o in +N and +NP_i treatments started to show increases after the first 24 hours incubation in August bioassays (BA3) but not in April bioassays (p=0.03, 0.045, respectively), showing a greater FIRe sensitivity in August (Fig. 3.5). In the first 24 hours, there was significant F_o increase in bottom water treatments in BA3 and BA4 (p=0.003, 0.016, respectively), suggesting the short-term stimulated effects from bottom water, but this could not sustain phytoplankton to the end of incubations (Fig. 3.5).

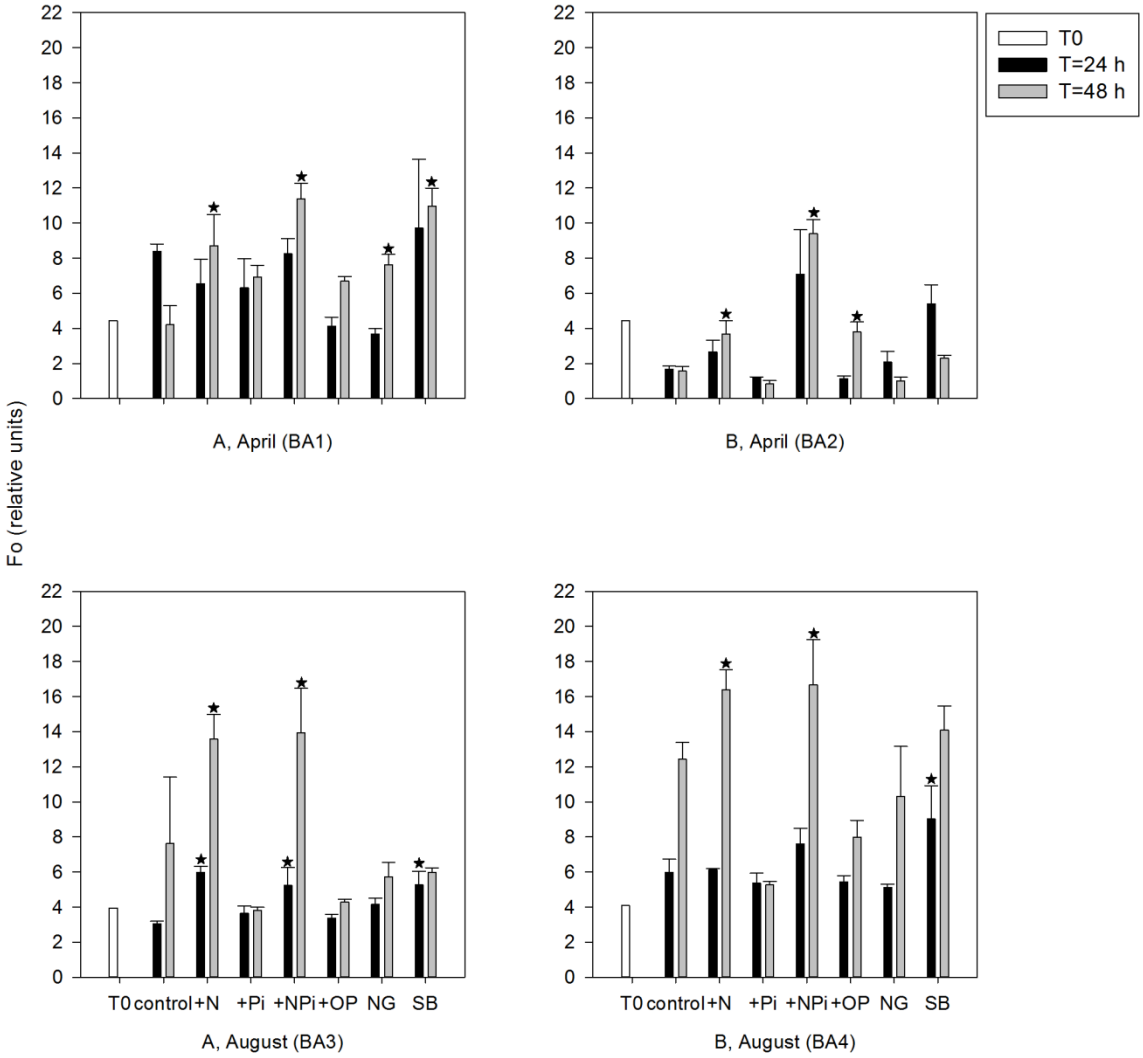

Figure 3.5 Variations in F_o values in measured in the different treatments. Data shown are the means ± S.E.. ★ indicates significant difference compared with the control group at the same time point. NG: no grazers, SB: surface+bottom. Unlike chl *a* which was measured only at the beginning (t=0) and end (t=48 hours), samples for fluorescence parameters were measured at t=0, 24 and 48 hours.

Response of photosynthetic activities

As Table 3.3 shows, F_v/F_m values were not significantly different in the treatments (p>0.05) in April (BA1 and BA2) relative to the controls. In August (BA3 and BA4), F_v/F_m values in the +N and +NP_i treatments were significantly higher than in other treatments (p <0.05), suggesting phytoplankton were recovering photosynthetic efficiency as a result of the alleviation from N limitation. Consistent with the chl *a* results, there were no effects of grazers, the addition of P (OP and P_i) or bottom water on F_v/F_m values in all the bioassays (Table 3.3).

There were three other photosynthetic parameters measured: σ_{PSII} ($Å^2$ $quanta^{-1}$), p (unitless) and τ_{QA}(μs). These three parameters did not change in response to the treatments as was observed for F_o and F_v/F_m, with one exception. In BA4, p in +N and +NP_i treatments was significantly higher than the other groups (p=0.045, 0.018, respectively) at the end of the incubation (Table 3.3). This was not the case in the other three bioassays (Table 3.3). The correlation between p and F_v/F_m in BA4 was significant (correlation analysis, p<0.01). p is the connectivity factor; both N and P limitation could cause the decrease of p values (Sylvan et al. 2007). The response of σ_{PSII} and τ_{QA} to +N and +NP_i was not statistically different from the other treatments (p =0.983, 0.972, respectively) and there was no consistent pattern among the four bioassays (Table 3.3).

F_v/F_m values measured in the four bioassays

Fv/Fm	To	control	+N	$+P_i$	$+NP_i$	+OP	NG	SB
A, April (BA1)	0.507(0)	0.43(0.027)	0.430(0.008)	0.437(0.008)	0.433(0.012)	0.417(0.032)	0.440(0.005)	0.407(0.035)
B, April (BA2)	0.382 (0)	0.546(0.017)	0.557(0.007)	0.530(0.023)	0.531(0.038)	0.610(0.011)	0.543(0.018)	0.575(0.003)
A, August (BA3)	0.294(0)	0.343(0.026)	0.445(0.022)*	0.339(0.045)	0.434(0.004)*	0.327(0.026)	0.324(0.031)	0.296(0.026)
B, August (BA4)	0.521(0)	0.427(0.003)	0.507(0.008)*	0.437(0.008)	0.513(0.013)*	0.450(0.003)	0.490(0.023)	0.443(0.003)

average σ_{PSII} values measured in the four bioassays

σ_{PSII} ($Å^2$ $quanta^{-1}$)	To	control	+N	$+P_i$	$+NP_i$	+OP	NG	SB
average	279(16)	373 (52)	398(48)	393(46)	425(58)	370(31)	378(26)	396(17)

average τ_{QA} values measured in the four bioassays

τ_{QA} (μs)	To	control	+N	$+P_i$	$+NP_i$	+OP	NG	SB
average	977(166)	1007(128)	1251(350)	1096(276)	1276(375)	1274(341)	1143(238)	1127(278)

p values measured in the four bioassays

p	To	control	+N	$+P_i$	$+NP_i$	+OP	NG	SB
A, April (BA1)	0.06(0)	0.077(0.029)	0.11(0.006)	0.07(0.003)	0.135(0.043)	0.155(0.043)	0.07(0.005)	0.113(0.23)
B, April (BA2)	0.09 (0)	0.07(0.003)	0.07(0)	0.07(0.0033)	0.07(0)	0.07(0)	0.07(0)	0.07(0)
A, August (BA3)	0.05(0)	0.10(0.01)	0.14(0.015)	0.085(0.005)	0.10(0.003)	0.16(0.011)	0.11(0.008)	0.077(0.015)
B, August (BA4)	0.06(0)	0.107(0.018)	0.220(0.025)*	0.113(0.029)	0.200(0.04)*	0.120(0.021)	0.140(0.04)	0.130(0.036)

Table 3.3 Variations in photosynthetic parameters derived from FIRe after 48 hrs of incubation. Data shown are the means ± S.E. ⋆ indicate significant difference compared with the control group.

Response of phytoplankton communities

Chl *a*, fuco, hex, zea, chl *b*, and peri were the most abundant pigments in all the samples, indicating the dominant phytoplankton groups were likely to be diatoms, cyanobacteria, dinoflagellates, prymnesiophytes and prasinophytes (Fig. 3.6). These five groups accounted for more than 75% percentage of total phytoplankton biomass in all four bioassays. In all the bioassays, but, vio, allo and lut concentrations were in very low levels, representing low abundance of pelagophytes, cryptophytes and chlorophytes (Fig.

3.6). High chl *b* and pras concentrations in BA3 related to high abundance of green algae (prasinophytes) in only this bioassay.

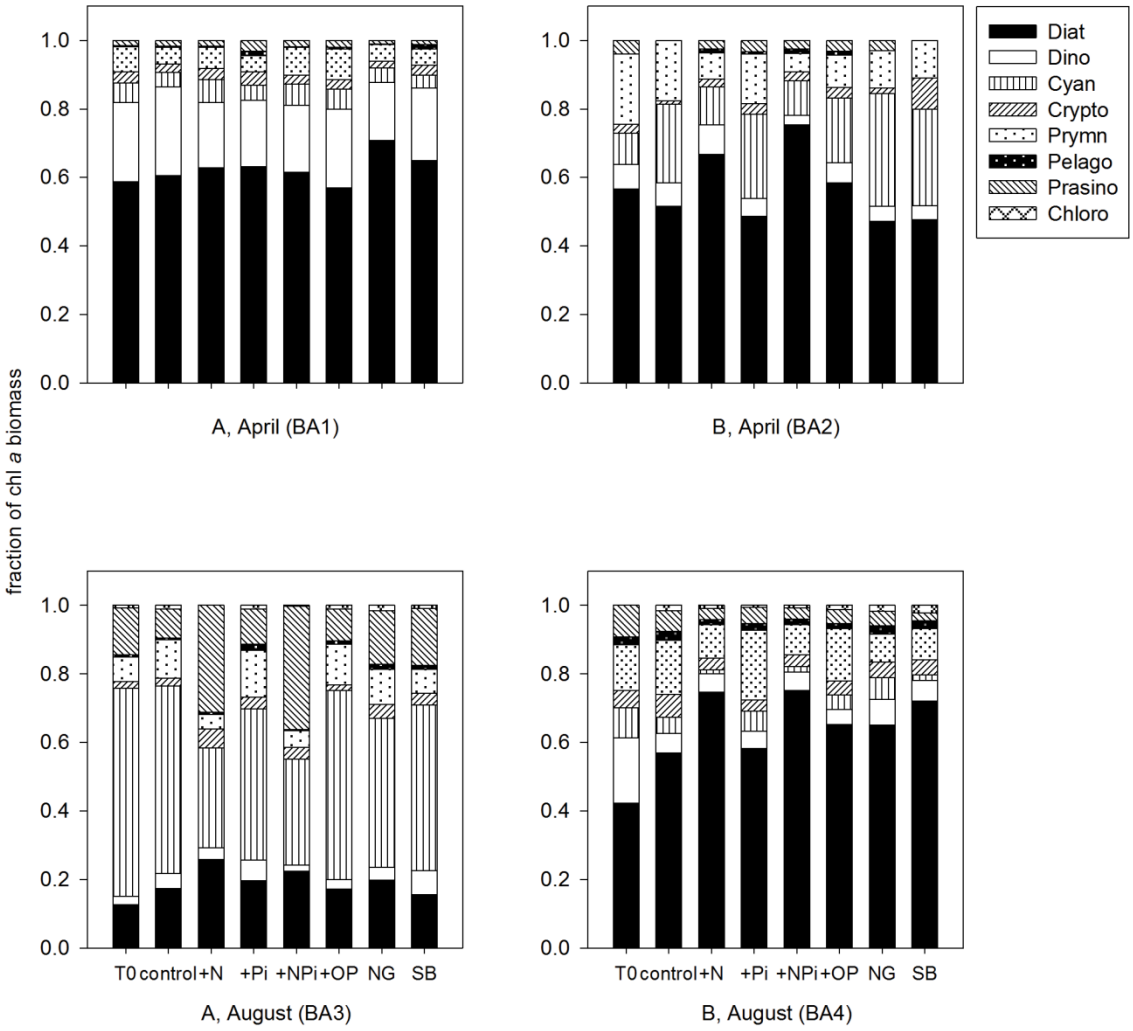

Figure 3.6 Phytoplankton community compositions in the different treatments in the four bioassays determined by ChemTax V 1.95. NG: no grazers, SB: surface+bottom.

Consistent with the chl *a* and F_o results, the most obvious shifts of phytoplankton community also happened in +N and +NP_i treatments (Fig. 3.6). Overall, there was a shift in phytoplankton communities from cyanobacteria and prymnesiophytes to diatoms and prasinophytes in BA2, BA3 and BA4 after N additions, while the community composition did not vary in different treatments in BA1. In BA2 and BA4, diatoms accounted for the highest percentage of the total phytoplankton composition at the start (T_0) and became more dominate after N addition at the end of the incubation. At the T_0, the community compositions in BA3 were very different from the other three bioassays with cyanobacteria dominating and a high proportion of prasinophytes (Fig. 3.6). After N additions, the proportion of cyanobacteria almost equaled to diatoms and prasinophytes after 48 hours in BA3, because diatoms and prasinophytes were more stimulated by N additions than cyanobacteria. In BA1, although dinoflagellates accounted for more than 20% in the community compositions initially, their proportions did not show obvious changes after N additions (Fig. 3.6). For the other treatments, no shift happened to the phytoplankton compositions compared to the control group.

Growth rates

The major groups of phytoplankton were stimulated by N additions to varying degrees. The growth rate (μ) for each group was calculated using 1/t (days)×ln(biomass $_{t=48h}$/biomass $_{t0}$), in which biomass was estimated from "the absolute pigments compositions" calculated by ChemTax (Strom and Strom 1996). In the four bioassays, the average growth rates of the top five groups after N additions (the average values of

+N, and +NP_i treatments) were diatoms > prasinophytes > dinoflagellates > prymnesiophytes > cyanobacteria, and the values were 0.718(±0.404) day^{-1}, 0.565(±0.365) day^{-1}, 0.343(±0.194) day^{-1}, 0.301(±0.363) day^{-1} and 0.255 (±0.243) day^{-1}, respectively. The large error associated with each growth rate reflects (1) seasonal difference (Fig. 3.3) and (2) inherent differences between stations (Fig. 3.1and 3.2).

3.4 Discussion

The significant growth response of phytoplankton (F_o and chl *a*) to +N and +NP_i treatments and the nutrient data indicated the phytoplankton communities were N limited at the two experimental stations in both April and August 2012 in the NGOM. N limitation usually occurs in mid-salinity areas (18-32), where station A and B were located. N limitation has been reported in this area in both spring and summer (Quigg et al. 2011; Laurent et al., 2012), and its effect on biological and chemical cycles in NGOM also has been emphasized in many studies (e.g., Dagg et al., 2007; Turner et al., 2006; Turner and Rabalais, 2013). Reducing nitrogen load is considered as the key factor to reduce the phytoplankton biomass and alleviate the summer bottom hypoxia in NGOM (Rabalais et al., 2007). N limitation of primary productivity has been reported in coastal ecosystems worldwide including the Baltic Sea (Lugus et al., 2004), the Qatar peninsula in the Arabian Sea (Quigg et al., 2013) and many other places as summarized in recent reviews by Howarth and Marino (2006) and Paerl (2009).

Si was plentiful for diatom growth except in BA1, performed in April adjacent to the Mississippi River station. Quigg et al. (2011) also found evidence of Si limitation in

March 2004 in the same area. We did not observe P limitation in all four bioassays, which was different from the former bioassays performed in NGOM (Sylvan et al., 2006, 2007, 2011). P limitation was observed in March, May and July (spring and early summer) of 2004 (Quigg et al., 2011) and with the surface salinity ranging from 10-35 (most happened between 10-20; Turner and Rabalais, 2013). The occurrence of P limitation resulted from the large amount of N loading from river inflow relative to P loading (Sylvan et al., 2011); the river flow in 2012 was relatively low compared to 2010 and 2011 (http://www2.mvn.usace.army.mil/eng/edhd/wcontrol/miss.asp), which may explain the apparent absence of P limitation during our cruises.

The fast response (within 24 hours) of F_v/F_m after the addition of nutrients in some but not all treatments is consistent with former studies (e.g., Sylvan et al., 2007; Suggett et al., 2009a). If phytoplankton communities inhabit an oligotrophic environment for a long period and adapt to it (e.g., the North Atlantic Ocean), F_v/F_m values will not change significantly after the relief of nutrient limitation; this is so called "balanced growth" (Parkhill et al., 2001; Moore et al., 2008). However, when the nutrient fluctuation frequency is high (e.g., NGOM), F_v/F_m could respond more obviously to the additions of limited nutrients (Sylvan et al., 2007). In our study area, the ambient nutrient conditions were more like the second situation although the F_v/F_m changes in April (BA1 and BA2) were not as obvious. More significant phytoplankton response after nutrient additions in summer time was also found by Mahaffey et al. (2012). The incubation effects generally indicated by the biomass decrease in BA2 (not statistically significant) and increase in BA4 ($p<0.001$) in controls could result from the

further nutrient limitation in incubating bottles and initial light limitation in the two bioassays, respectively.

There were higher nutrient concentrations in the bottom waters than the surface waters in BA1, BA3 and BA4 (Table 3.2), which could stimulate phytoplankton communities. Although we did not observe significant bottom nutrient effects in our bioassays (Fig. 3.5), it has been shown in other studies that the bottom water could act as the potential nutrient pool for phytoplankton in euphotic zones (Mahaffey et al., 2012). In NGOM, some extraordinary weather events, like the occurrence of hurricanes, could increase the possibilities of mixing bottom water to surface, adding nutrient pulse to stimulate phytoplankton bloom(s) (Walker et al., 2005). Based on our study, small amounts of bottom water (10%) could not lead to changes in phytoplankton biomass and community structure in 48-hour bioassays (with some stimulation only in first 24 hours).

High abundance of diatoms, cyanobacteria, dinoflagellates, prymnesiophytes and prasinophytes in our samples is consistent with former phytoplankton community studies in GOM (Lambert et al., 1999; Wawrik et al., 2003; Qian et al., 2003; Rabalais et al., 2012). The five phytoplankton groups were stimulated after N additions in the four Bioassays. The shift of phytoplankton communities was the outcome of their different competitive abilities for N (nitrate in this case). According to trait-based approaches, we applied four nutrient- and group-specific functional traits (see Table 3.4): the maximum nutrient uptake rates (V_{max}), the maximum growth rates (μ_{max}), the minimum cell quota (Q_{min}) and the half saturated constant (K_s) to compare the nitrate competition ability

among different phytoplankton groups and explain the community shifts after nitrate additions (Litchman et al., 2007; Litchman and Klausmeier, 2008).

Phytoplankton groups	VmaxN (µmol N µmol C^{-1} day^{-1})	K_N (µmol)	µmax (day^{-1})	QminN (µmol N µmol C^{-1})
Diatoms	0.5-0.8	0.5-1.5	1.1-1.8	0.038-0.065
Green Alage	0.2	0.5-6	1.3-1.6	0.03
Dinoflagellates	~0.0-0.1	2.5-6	0.3-0.7	0.015-0.035
Coccolithophores	0.06-0.08	0.2-0.5	1.1-1.2	0.02

Table 3.4 Different nitrate uptake related parameters in multiple marine species belonging to four eukaryotic phytoplankton groups, modified from Litchman et al. (2007).

In theory, μ_{max} is more cell size related while V_{max} and K_s are more nutrient related (Litchman et al., 2010). V_{max} for a specific kind of nutrients determines the performance of phytoplankton groups when this nutrient is sufficient in their habitats. The higher the V_{max}, the faster the phytoplankton group could take up the nutrient. K_s represents the affinity for nutrients, and high affinity (low K_s) for nutrients giving the phytoplankton group stronger competitive ability for nutrients in scarce environments (Grover, 1991; Edwards et al., 2011). In our case, we focused on the response of different phytoplankton groups to nitrate additions in the N limited background environments, so V_{max} for nitrate and μ_{max} were more important to consider.

Litchman et al. (2007) summarized multiple species values of V_{max}, K_s, μ_{max} and Q_{min} for nitrate competition (subset in Table 3.4). Due to the highest V_{maxN} and μ_{max}

(small celled diatoms) and intracellular nitrate storage vacuoles (high Q_{min}) in large diatoms, this group would show the strongest competitive abilities after nitrate additions (Table 3.4; Litchman et al., 2007; Edwards et al., 2012). Prasinophytes (green algae) have the second highest V_{maxN} and μ_{max}, so they can take advantage in nitrate competition as well (Table 3.4; Litchman et al., 2007). Prymnesiophytes take up nitrate slower than diatoms and prasinophytes, so they potentially are poor at competing for nitrate (Table 3.4; Litchman et al., 2007). There was no information about cyanobacteria in Litchman et al. (2007), but their ability for nitrate uptake should be the lowest among the five groups because of their smallest cell size (Aksnes and Egge, 1991). For dinoflagellates, although their V_{maxN} is higher than in prymnesiophytes and cyanobacteria, given they have a low μ_{max}, they do not show high growth rates after nitrate additions. Based on the characteristics (four functional traits), the average growth rates after N additions should be diatoms> prasinophytes> dinoflagellates>prymnesiophytes >cyanobacteria, which is consistent with the patterns (Fig. 3.6) and the calculated growth rates in our bioassays.

There are also biotic environmental factors that could influence the distribution of phytoplankton communities. For instance, diatoms are more adapted to low light, high turbulent environments, while prymnesiophytes favor sufficient light and calm water (Litchman et al., 2007). Cyanobacteria have the highest optimum growth temperature among the major five groups, which is why cyanobacteria usually dominate in summer (Qian et al., 2003; Litchman et al., 2010). Green algae (prasinophytes, euglenophytes and chlorophytes) distribution is usually associated with low salinity or estuary water (Laza-Martinez et al., 2007). Based on our historical data at the same stations (A, B)

from 2010 to 2012 cruise (Fig. 3.7), the average phytoplankton community composition was diatoms (or dinoflagellates) dominating in spring and cyanobacteria dominating in summer. The seasonal shift from large-celled diatoms (or green algae in freshwater systems) blooms to small-celled cyanobacteria blooms was the typical situation in both marine (Qian et al., 2003; Adolf et al., 2006) and freshwater systems (Habib et al., 1997; Grover and Chrzanowshi, 2006). At station B, August, in 2010 and 2012, diatoms dominated over cyanobacteria, which might be a temporal phenomenon related to windy and rainy weather during the cruise, because coastal diatoms could take more advantages in the fluctuating light conditions (Strzepek and Harrsion, 2004).

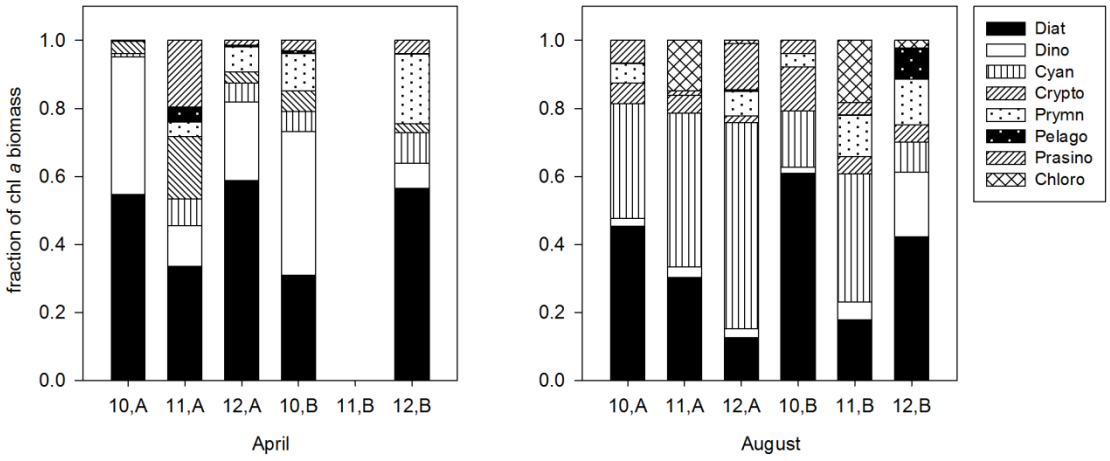

Figure 3.7 Phytoplankton community compositions in April and August 2010-2012, at station A and B. Data from surface samples around noon. Samples for 2011at station B in April were lost.

The responses of phytoplankton communities in the four bioassays demonstrated the applicability of the trait-based ecology to evaluate changes in phytoplankton community structure in field (Litchman et al. 2007; Edwards et al. 2012). Long-term RLAs conducted in other marine ecosystems also supported our short-term results. For example, Lugus et al. (2004) found centric diatoms were the most stimulated phytoplankton group and a big decline of autotrophic picoplankton in 14-day RLAs in N limited northern Baltic Sea. The response of dinoflagellates was highly species-specific in the Baltic study; this supported our finding of variability in the pattern of dinoflagellates responses. Mahaffey et al. (2012) mixed nutrient-enriched bottom water with oligotrophic surface water in the North Pacific Subtropical Gyre and within 5 days, found similar community shifts including a change from small cells to large cells as we hypothesized. We did not find obvious effect of grazers in all the bioassays, consistent with Lugus et al. (2004), thus the response of the phytoplankton communities after N addition was mainly controlled by bottom-up effects, not top-down effects.

Because picoplankton have slow sedimentation rates and grazing effects by microzooplankton, most of them can be recycled in euphotic zone (Kuipers and Witte, 1999). Microzooplankton (<20 um, protozoa) dominated in our research area (mid-salinity 18-32) and peaked in summer (Dagg and Breed, 2003); this is the major grazer for picoplankton. It is hypothesized that increased phytoplankton biomass could induce more severe hypoxia in NGOM, but not many studies examined the outcome of community shifts (Rabalais et al., 2002). In NGOM, the decomposition of diatoms contributed to large proportion of the bottom oxygen consuming, especially in spring

when zooplankton biomass has not peaked (Dagg et al., 2003, Dortch and Whitledge, 1992). Additionally, diatoms are the major food source of zooplankton, and the fecal pellets produced by zooplankton also could sink to the bottom acting as oxygen consuming organic matters (Dagg et al., 2003). For the large contribution of sinking particles, diatoms were considered as an important trigger for the bottom hypoxia when the other involved hydrographic conditions are suitable (Dortch and Whitledge, 1992, Rabalais et al., 2002) Therefore, the increased proportion of diatoms could result in more sinking diatoms, more zooplankton fecal pellets, thus more hypoxia potential. Dortch and Whitledge (1992) proposed another scenario that Si limitation but sufficient N, P could cause the shift from diatom to some noxious flagellates, which was the situation at station A, April. Based on model assimilations, Eldridge and Roelke (2010) also indicated that less edible species dominated in phytoplankton assemblages could enhance the potential of hypoxia, even their growth rates were lower than the edible species. Under this scenario, decreased grazing rates for dinoflagellates will also result in more sinking cells although the growth rates of dinoflagellates are not as high as diatoms.

To conclude, our research results indicated the FIRe could be used for detecting N limitation in NGOM, in which F_o and F_v/F_m performed better than the other fluorescence parameters. The response of phytoplankton communities corresponded to the classic nutrients competition theories, providing evidence for the applicability of trait-based ecology in coastal phytoplankton communities. Furthermore, the dominating phytoplankton group shifted to diatoms (like in BA3) after nitrate addition reflected the

shift trend from small-celled phytoplankton groups to large-celled ones when more ambient nutrients were available. Phytoplankton cells are considered as a major component of particulate flux in empirical and model calculations (Fennel et al., 2013). Therefore, the size shift of sinking phytoplankton cells could lead to a more complex impact on ecosystem in NGOM than merely considering total phytoplankton biomass.

CHAPTER IV

COMPARISON OF POPULATION GROWTH AND PHOTOSYNTHETIC APPARATUS CHANGES IN RESPONSE TO DIFFERENT NUTRIENT STATUS IN A DIATOM AND A COCCOLITHOPHORE

4.1 Introduction

As the major source in the food web of marine ecosystem, phytoplankton are of great importance to impact the carbon biogeochemical cycling, growth dynamics of marine heterotrophic organisms, fisheries, etc. (Miller, 2003). Marine phytoplankton are responsible for around 50% global primary production (Falkowski and Raven, 2007), which is considered to be controlled by environmental factors such as light availability, macro- and micro-nutrients, CO_2, and physical mixing (Miller, 2003). In marine ecosystem, phytoplankton photosynthesis is frequently limited by nitrogen (N), phosphorus (P) and iron (Fe), in which N and P limitation is common in coastal areas (e.g., the Northern Gulf of Mexico), while N and Fe limitations more frequently occur in open ocean (e.g., the North Atlantic Ocean) (Miller, 2003; Dagg et al., 2007; Moore et al., 2013). The fluctuations of N and P availability directly influence phytoplankton biomass, photosynthetic efficiency, carbon fixation capacity, and/or indirectly modify the total primary production by changing the phytoplankton community structure (Gilbert et al., 1988; Greene et al., 1992).

The major pools of organic N in cells are proteins and nucleic acids, while inorganic N is found in large vacuoles to store nitrate, thus the loss of proteins is the

major outcome of N deficiency (Rhee, 1978; Quigg and Beardall, 2003; Flynn et al., 2010). The lack of inorganic N in the culture could impair the structural proteins in photosynthetic reaction centers (RC), and decline the concentrations or activities of the ribulose 1, 5-biphosphate carboxylase (RuBisCO) enzyme, as well as its transcriptional genes (Geider, et al. 1993, 1998; Berges et al., 1996; Liu et al., 2012). As a result of that, the efficiency of both light reaction (PSII photo-physiology) and dark reaction (carbon fixation) could decline (Geider et al., 1993; Kolber et al., 1988; Wykoff et al., 1998; Greene et al., 1992). N also contributes to the structure of chl *a*, *b*, and *c*, thus N deficiency could lead to the reallocation of cellular pigments and/or a reduction in their production (Leonardos and Geider, 2004; Geider et al., 1993; Young and Beardall, 2003; LaRoche et al., 1993). The deficiency of N in cells has been measured in chemostats and N starvation in batch cultures. Phytoplankton cells in N limited chemostats could show acclimation so the photosynthesis decline is not as obvious as cells undergoing N starvation (Cullen et al., 1992; Parkhill et al., 2001; Young and Beardall, 2003; Moore et al., 2006).

P plays an important role in nucleic acids and phospholipids. RNA is the most abundant P-containing macromolecular fraction in cells, followed by phospholipid and DNA (Leonardos and Geider, 2004; Flynn et al., 2010). P is also responsible for the energy carriers in cells, like adenosine triphosphate (ATP) and reduced nicotinamide adenine dinucleotide phosphate (NADPH) (Brooks, 1986; Gauthier and Turpin, 1997). Although P deficiency does not influence protein and pigment synthesis, it could influence the activities of RuBisCO by means of reducing the supply of ATP or down

regulating the transcriptional mRNA (Geider et al., 1993; Liu et al., 2012). Due to the limitation of RNA and ATP synthesis by P deficiency, cell growth rates could be more suppressed than under N deficiency (Raven, 2012). In addition, studies measuring chl *a* fluorescence also indicated P deficiency influences the PSII photo-physiology (Eker-Develi et al., 2006; Sylvan et al., 2007; Robert et al., 2008).

The effect of nutrient limitation is not only nutrient specific, but also species specific. The different response among phytoplankton could be induced by different nutrient requirements and affinities, activity of nutrient assimilation enzymes (such as nitrate reductase or alkaline phosphatase) and the structure of photosynthesis apparatus (Tilman, 1977, 1982; Sterner and Elser, 2002). In natural environments, nutrient status is quite variable so mixed-species competition experiments in large degrees have been determined by the performance of single species (Sterner and Elser, 2002; Litchman et al., 2007). In our study, we chose two common coastal species, *Phaeodactylum tricornutum* and *Emiliania huxleyi*, which usually form blooms in nutrient enriched environments and nutrient scarce environments, respectively (Tyrrel and Taylor, 1996; Lobel et al., 2010). We compared their response to N and P starvation by means of studying the population growth, mixed-species competitions, photosynthetic apparatus and celluar consitients, further to provide evidence explaining their acclimation to nutrient depletion beyond the angle of the nutrient assimilation dynamics.

4.2 Material and methods

Experimental microalgal species *Phaeodactylum tricornutum* and *Emiliania huxleyi* were purchased from the Culture Collection of Algae at the University of Texas (UTEX 640) and the National Center for Marine Algae and Microbiota (CCMP 374) respectively. The two species were cultured with natural seawater from National Oceanic and Atmospheric Administration (NOAA) Marine Fisheries Galveston Laboratory (Galveston, TX) and enriched with f/4 trace metals, vitamins, and Si for the diatom (Guillard, 1975) and sterilized (30 mins, 121^{o}C). Before the experiments were started, the cultures were maintained in semi-continuous mode to maintain the exponential growth in f/4 media ameliorated with nitrogen (440 μM nirate) and phosphate (18 μM) (final concentrations). Cultures were grown with 100-150 μmol m^{-2} s^{-1} light, under a 12h: 12h light: dark cycle at 19±1 ^{o}C.

For single species experiments, five treatments were designed with different initial nitrogen (NO_3^-) and phosphate (PO_4^{3-}) concentrations in batch mode. The five treatments were: control (f/4 medium), N1 (f/4 P, f/8 N), N2 (f/4P, f/16 N), P1 (f/4N, f/8 P), and P2 (f/4N, f/16 P) which had the following N and P concentrations: control (440 μM, 18 μM), N1 (220 μM, 18 μM), N2 (110 μM, 18 μM), P1 (440 μM, 9 μM) and P2 (440 μM, 4.5 μM). All the treatments were performed in triplicates. The initial cell concentrations for *P. tricornutum* and *E. huxleyi* were 1×10^4 and 5×10^4 cells mL^{-1}, respectively, and the culturing period to stationary phase was around 15 days. During the culturing period, the cell concentration and chl *a* fluorescence were measured daily. Cell numbers were counted using a hemocytometer by counting four fields in each chamber.

Cellular organic carbon, nitrogen and phosphorus were measured at Day 0 (initial), 9 (exponential phase) and 15 (stationary phase). At the end of the experiment, samples were taken to measure pigment compositions and photosynthetic carbon fixation rates (photosynthesis-irradiance (P-I) curves). For mixed-species experiments, we only included three treatments: control, N2 and P2. *P. tricornutum* and *E. huxleyi* were cultured together with initial cell concentrations of 1×10^4 and 5×10^4 cells mL^{-1}, respectively. Cell concentrations were counted daily until the stationary phase.

Chl *a* fluorescence was measured using the Fluorescence Induction and Relaxation (FIRe) System (Satlantic Instruments S/N 2) (Zhao and Quigg, 2014). Cultures (3 mL) were collected at the same time each day (1pm) and stored in darkness for 30 mins before measurements. In our study, we use only information collected from the single turnover (ST) component of the transient according to Kolber et al. (1998) and Kromkamp and Forster (2003). This includes minimum and maximum fluorescence (F_o and F_m), the maximum quantum yield of PS II (F_v/F_m), the functional absorption cross-section for PSII (σ_{PSII}; $Å^2$ $quanta^{-1}$), the connectivity factor (p) and the minimum turnover time of electron transfer from reaction centers to the acceptor side (τ_{QA}; μs). Fluorescence from pure culture medium was subtracted from the F_o and F_m values of samples to correct for the influence of background fluorescence (Cullen and Davis, 2003).

Cultures (20 mL) were filtered onto GF/F glass fiber filters (Whatman) and stored at -80^{o}C for the pigments analysis. The reverse-phase High Performance of Liquid Chromatography (HPLC) method based on the procedures of Pinckney et al. (1996) was

used in our experiment. The sample treatment procedures, HPLC instrumentation and pigments peak calculations were the same as described in Zhao and Quigg (2014).

Phytoplankton photosynthesis versus irradiance (P-I) curves were measured using the small bottle method developed by Lewis and Smith (1983) with some modifications. ^{14}C labeled sodium bicarbonate (1 mCi mL^{-1} $H^{14}CO_3^-$; 10-20 uL) was added to 20 mL cultures. Aliquots (1 mL) of ^{14}C labeled water were incubated at a range of irradiances from 15 to 900 µmol m^{-2} s^{-1} (16 samples for each P-I curve). The incubation (60 mins) was conducted in a photosynthetron attached a water bath at 19°C. A Beckman LS 6500 liquid scintillation counter was used to count all the samples for 5 mins each. Photosynthetic parameters, such as P_{max}^B, α and $I_k$were calculated by fitting the P-I model of Platt et al. (1980) using equation 1.

Equation 1: $P^B = P_{max}^B\left(1 - e^{-\alpha E/P_{max}^B}\right)e^{-\beta E/P_{max}^B}$, where P_{max}^B is the model estimated maximum photosynthetic production per unit chl *a*, α is the initial slope of the P-I curve, and E is the irradiance during incubation, β represents photoinhibition; I_k is calculated from $P_{max}^B/$.

For measurement of celluar organic C, N and P contents, 30-60 mL culture samples were collected on pre-combusted (600ºC for 4 hrs) GF/F glass fiber filters, one for organic C and N, and one for P, folded and stored frozen at -20°C prior to analysis. The filters were dried for 24 hours, and then acidified by placing samples in a desiccator with 8N HCl for 24 hours, and subsequently drying samples for another 24 hours. The filters were packed into the tin capsules before running by a Perkin-Elmer 2400 CHNS analyzer. The organic P content were determined in samples by a dry-oxidation, acid

hydrolysis extraction followed by a colorimetric analysis of phosphate concentration of the extract as described in Solorzano and Sharp (1980).

The statistical analysis was applied using SPSS16.0 and the figures were generated using Sigmaplot 12.3. The means and standard errors in the figures and tables were calculated from the triplicates for each treatment. For the population growth, the relative growth rate (μ) was calculated using Equation 2. The growth curves were regressed using the Logistic growth model (Wang and Tang, 2008; Equation 3) in the single-species experiments and the Lotka-Volterra competition model (Uchida et al., 1991; Equation 4) in mixed culture mode. Lotka-Volterra competition model was developed from the Logistic model and applied when more than one species competing one kind of resource (Bomze, 1983). One-way analysis of variance (one-way ANOVA) was used to determine the significance among treatments, in which LSD test was used to group-paired significance after the test of variance homogeneity.

Equation 2: $\mu = \frac{\ln(N_t) - \ln(N_0)}{t}$, N_t is the cell density at time t (10^4 cells mL^{-1}); N_0 is the initial cell density (10^4 cells mL^{-1}); and t is the time (day^{-1}).

Equation 3: $N_t = \frac{K}{1+e^{a-rt}}$, where N_t is the cell density at time t (10^4 cells mL^{-1}), K is the carry capacity of the population (10^4 cells mL^{-1}), t is the time (day^{-1}), a is a constant equal to ln $(\frac{K-N_0}{N_0})$, N_0 is the initial cell density of the population (10^4 cells mL^{-1}).

Equation 4: $\frac{dN_1}{dt} = r_1 N_1(\frac{K_1 - N_1 - \alpha N_2}{K_1})$, $\frac{dN_2}{dt} = r_2 N_2(\frac{K_2 - N_2 - \beta N_1}{K_2})$, where N_1 and N_2 are the cell densities of species 1 and species 2, respectively (10^4 cells mL^{-1}), K is the carry capacity derived from the Logistic model (10^4 cells mL^{-1}), α and β are the cell proliferation rates of species 1 and species 2, respectively. In this equation, when $K_1 > K_2/\beta$, $K_1 < K_2/\beta$, species 1 out-competes species 2 and when $K_1 < K_2/\beta$, $K_2 > K_1/\alpha$, the species 2 out-competes species one; and when $K_1 < K_2/\beta$, $K_1 < K_2/\beta$, the two species will co-exist.

4.3 Results

Population growth

Fig. 4.1 shows the population growth curves of the two species in the five different nutrient treatments, while Fig. 4.2 shows the population growth curves in mixed species competition mode. Regressed by the Logistic models, the growth parameters in single- and mixed-species cultures are shown in Table 4.1 and 4.2. Under nutrient replete conditions (control f/4), the carrying capacity (*K*) and the maximal specific growth rate (*r*) values were higher in *E. huxleyi* than in *P. tricornutum*. *K* was dependent on the nutrient concentrations in the media for both species, showing a more obvious decline in P starved treatments than N starved treatments. In the N2 and P2 treatments, *K* decreased by 18.6% and 41.2% in *P. tricornutum*, respectively, and 48.3 % and 57.2% in *E. huxleyi*, respectively. *r* in all the nutrient starved treatments was always higher or similar to the control, indicating the maximal specific growth rates were not influenced by N or P starvation. The behavior of *r* is consistent with former studies when

populations were examined under environmental stress (Wang and Tang, 2006). T_p is the inflection point where the population growth rate switches from increasing to decreasing, and is considered as the starting point of environmental stress. In control groups, T_p occurred in both species at around 12 days, but it then appeared around 9 or 10 days in the N or P starved treatments. The specific growth rates (μ) did not vary in different treatments in the before T_p, with the values from 0.364-0.779 day^{-1} in *P. tricornutum* and 0.396-0.500 day^{-1} in *E. huxleyi* (Fig. 4.1; Table 4.1).

In the mixed-species competition experiment, the growth parameters were different from the single species culture experiment (Table 4.1 and 4.2). In the control group, the *K* value of *P. tricornutum* was not very different from that measured in the single-species cultures, but the *K* value of *E. huxleyi* decreased by 56.9% compared to the single-species culture. In the N depleted treatment (N2), *K* values decreased by 52.4% in *P. tricornutum* but increased by 5.1% in *E. huxleyi* compared to the corresponding single-species experiments, showing a weak competitive ability of *P. tricornutum* when N is depleted. The change of competitive ability in N2 was also indicated by the short time to reach T_p in *P. tricornutum* (8.36 days) and longer time to reach T_p in *E. huxleyi* (10.65 day). In the P starved treatment, *K* values decreased by 32.5% in *P. tricornutum* and 15.6% in *E. huxleyi* compared to the single-species cultures. Similar with the single-species culture, *r* values increased with the decrease of *K* values (Tables 4.1 – 4.2).

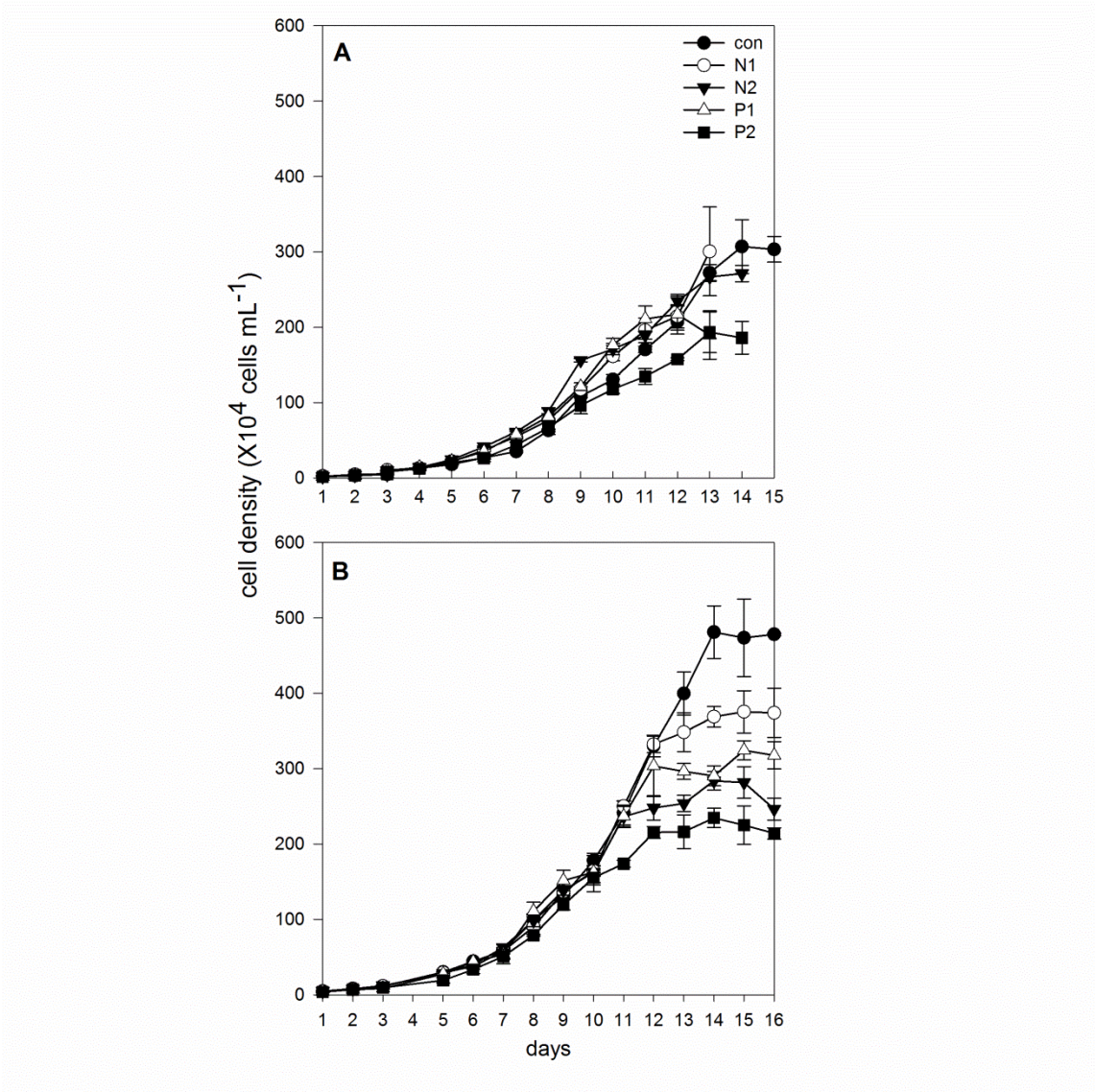

Figure 4.1 The growth curves of *P. tricornutum* (A) and *E. huxleyi* (B) in different nutrient status in single species culture. Data are given as means± standard error (S. E.).

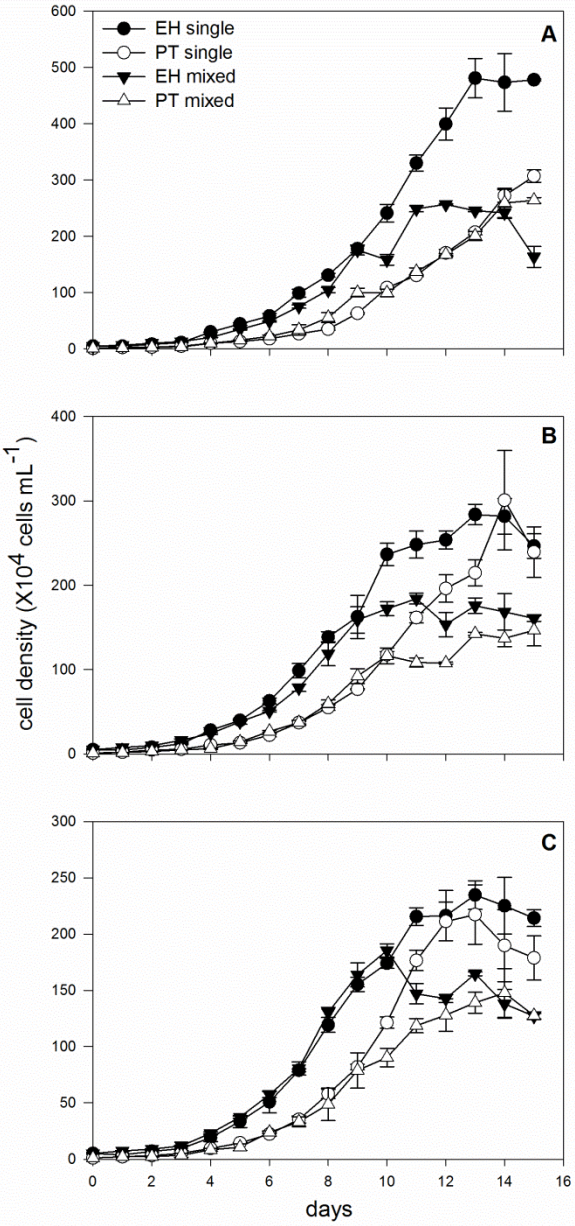

Figure 4.2 The growth curve of *P. tricornutum* and *E. huxleyi* in different nutrient status in mixed-species cultures. A: control group; B: N2 starved treatment; C: P2 starved treatment. Data are given as means± standard error (S. E.).

Treatments	The carrying capacity (K) ($\times 10^4$ cells mL^{-1})	The intrinsic growth rate (r/d^{-1})	R^2	T_p/day
P. tricornutum				
control	362	0.496	0.995	12.1
N1	291	0.569	0.989	9.6
N2	294	0.536	0.997	9.4
P1	260	0.637	0.998	9.0
P2	212	0.504	0.996	9.6
E. huxleyi				
control	538	0.534	0.994	11.2
N1	397	0.619	0.983	10.1
N2	278	0.633	0.988	8.9
P1	329	0.592	0.989	9.4
P2	231	0.649	0.995	8.9

Table 4.1 Calculated parameters derived from the Logistic equation regressed from population growth curves in different nutrient treatments in single-species culture experiments.

Treatments	The carrying capacity (K) ($\times 10^4$ cells mL^{-1})	The intrinsic growth rate (r/d^{-1})	R^2	T_p/day
P. tricornutum				
control	346	0.417	0.992	11.9
-N2	141	0.634	0.981	8.4
-P2	143	0.648	0.992	8.8
E. huxleyi				
control	233	0.763	0.934	7. 9
-N2	291	0.565	0.980	10.6
-P2	205	0.848	0.946	9.2

Table 4.2 Calculated parameters derived from the Logistic equation regressed from population growth curves in different nutrient treatments in the mixed-species culture experiments.

After modeling the data with the Lotka-Volterra two species competition model, the calculated parameters are given in Table 4.3, in which represents the competitive effect from *P. tricornutum* to *E. huxleyi*, and β represents the competitive effect from *E. huxleyi* to *P. tricornutum*. Although the two species co-existed in the culture under different nutrient conditions, their degree of competition to each other was different. in controls was 30.0 fold of β. In the N starved treatment (N2), was similar to β, indicating higher competitive ability of *E. huxleyi* relative to *P. tricornutum*. Although and β values were both smaller in the P starved treatment (P2) than in the N starved treatment (N2), β was higher than in controls while was lower than in controls, indicating increased competitive ability of *E. huxleyi* under P starvation.

Treatment		β	results
Control	0.899	0.030	co-exist
N starvation	0.434	0.477	co-exist
P starvation	0.196	0.110	co-exist

Table 4.3 Calculated parameters derived from the regression of Lotka-Volterra competition model in different nutrient treatments. indicated the competitive effect from *P. tricornutum* to *E. huxleyi*, while β indicated the competitive effect from *E. huxleyi* to *P. tricornutum*.

Cellular CNP

The C, N and P contents in cells were measured in exponential phase (Day 9) and in stationary phase (Day 15) (Table 4.4). The C: N: P ratios in normal conditions in both species were higher than the Redfield Ratio (C: N: P= 106: 16: 1), and the cellular organic C, N, P contents in *P. tricornutum* were 1.43, 0.95 and 0.87 fold higher than in *E. huxleyi*. For *P. tricornutum*, both N and P deficiency in cells started to show at Day 9 ($F=4.350$, $p=0.027$ for N, $F=7.678$, $p=0.004$ for P). For *E. huxleyi*, the cellular N or P deficiency did not show on Day 9 ($F=1.592$, $p=0.251$ for N; $F=0.649$, $p=0.641$ for P), but was very significantly measured on day 15 ($F=9.385$, $p=0.002$ for N; $F=17.770$, $p<0.01$).In Day 15, the loss of organic N was 87.8% in PT, N2, which was more obvious than in *E. huxleyi* (44.3%), and the C: N ratios declined to 77.65 in N2 treatment in *P. tricornutum*, and declined to 16.32 in *E. huxleyi*. The loss of organic P was 52% in *P. tricornutum*, which was not very different from the loss of *E. huxleyi* (and 40%). In Day 15, the cellular organic C contents were in N and P starved treatments were higher than the control groups, indicating the accumulation of organic C in cells. There were both C and N accumulation occurred in P starved treatment, which were statically significantly

in P1 and P2 in Day 15 in *P. tricornutum* (p=0.001 in P1 and p<0.01 in P2) and just in P2 in *E. huxleyi* (p<0.01).

	Organic C (pg cell^{-1})	Organic N (pg cell^{-1})	Organic P (pg cell^{-1})	C:N(mol/mol)	N:P(mol/mol)
P. tricornutum					
Day9-control	15.40(0.85)	1.89(0.13)	0.30(0.07)	9.5	14.0
Day9-N1	12.73(0.52)	1.25(0.09)	0.29(0.02)	11.9	9.5
Day9-N2	13.78(0.32)	1.18(0.19)	0.29(0.01)	13.6	9.0
Day9-P1	14.12(0.44)	1.79(0.10)	0.24(0.02)	9.2	16.5
Day9-P2	13.66(1.2)	1.70(0.17)	0.18(0.01)	9.4	20.9
Day15-control	10.52(0.43)	1.48(0.13)	0.25(0.01)	8.3	13.1
Day15-N1	14.82(0.90)	0.8(0.07)	0.23(0.01)	21.6	7.7
Day15-N2	11.98(0.45)	0.18(0.008)	0.24(0.01)	77.7	1.7
Day15-P1	17.03(1.00)	1.82(0.15)	0.16(0.008)	10.9	25.2
Day15-P2	18.09(0.31)	1.93(0.07)	0.12(0.01)	10.9	35.6
E. Huxleyi					
Day9-control	6.34(0.53)	0.97(0.09)	0.16(0.02)	7.6	13.4
Day9-N1	5.65(0.14)	0.87(0.01)	0.16(0.01)	7.6	12.0
Day9-N2	6.85(0.12)	0.9(0.05)	0.16(0.004)	8.9	12.5
Day9-P1	5.76(0.42)	0.89(0.04)	0.15(0.003)	8.0	13.1
Day9-P2	6.84(0.16)	0.99(0.11)	0.15(0.006)	8.0	14.6
Day15-control	6.17(0.0.50)	0.97(0.15)	0.15(0.008)	7.4	14.3
Day15-N1	6.55(0.24)	0.68(0.03)	0.16(0.009)	11.3	9.4
Day15-N2	7.51(0.004)	0.54(0.009)	0.18(0.02)	16.3	6.6
Day15-P1	6.80(0.26)	0.92(0.06)	0.10(0.009)	8.6	20.3
Day15-P2	10.12(0.77)	1.20(0.14)	0.09(0.01)	9.8	29.5

Table 4.4 The cellular organic carbon (C), nitrogen (N) and phosphorus (P) contents and ratios in different nutrient treatments during the exponential phase (Day9) and the stationary phase (Day15) in single-species experiments. * indicated there was a statically significant difference between this treatment and the corresponding control group.

The average total organic N and P was calculated by the organic N per cell (pg). For *P. tricornutum* , the average total organic N values in Day 9 in N1 and N2 were 68.5 μM and 74.5 μM, respectively, which were lower than the 220 μM (f/8) and 110 μM (f/16) at Day 15. The average total organic P at Day 9 in P1 and P2 was 12.91 μM and 7.84 μM, which were higher than 9 μM (f/8) and 4.5 μM (f/16) at Day 15. Due to the N or P deficiency, N: P (mol/mol) ranged from 9.00 to 20.91 in Day 9, and 1.66 to 35.61 in Day 15. For *E. huxleyi*, the average total organic N on Day 9 in N1 and N2 were 107 μM and 84.4 μM, respectively, and the average total organic P in Day 9 in P1 and P2 were 7.29 μM and 5.74 μM.

Pigments quotas

Chl *a* contents (per cell) in *P. tricornutum* were 9 fold higher than in *E. huxleyi* in controls in the late exponential phase (Fig. 4.3). Compared to the control, the cellular chl *a* concentrations significantly declined in N starved treatments (*P. tricornutum*: $p<0.01$ in N1 and N2; *E. huxleyi*: $p=0.02$ in N1, $p=0.001$ in N2), but accumulated in the P2 treatment in both species ($p=0.002$ and <0.01 in *P. tricornutum* and *E. huxleyi*, respectively) (Fig. 4.3). *P. tricornutum*s showed a more pronounced chl *a* decline than *E. huxleyi* under N starvation, with chl *a* concentrations declining by 71.7% and 58.1% in *P. tricornutum* and *E. huxleyi* in N2 treatments, respectively.

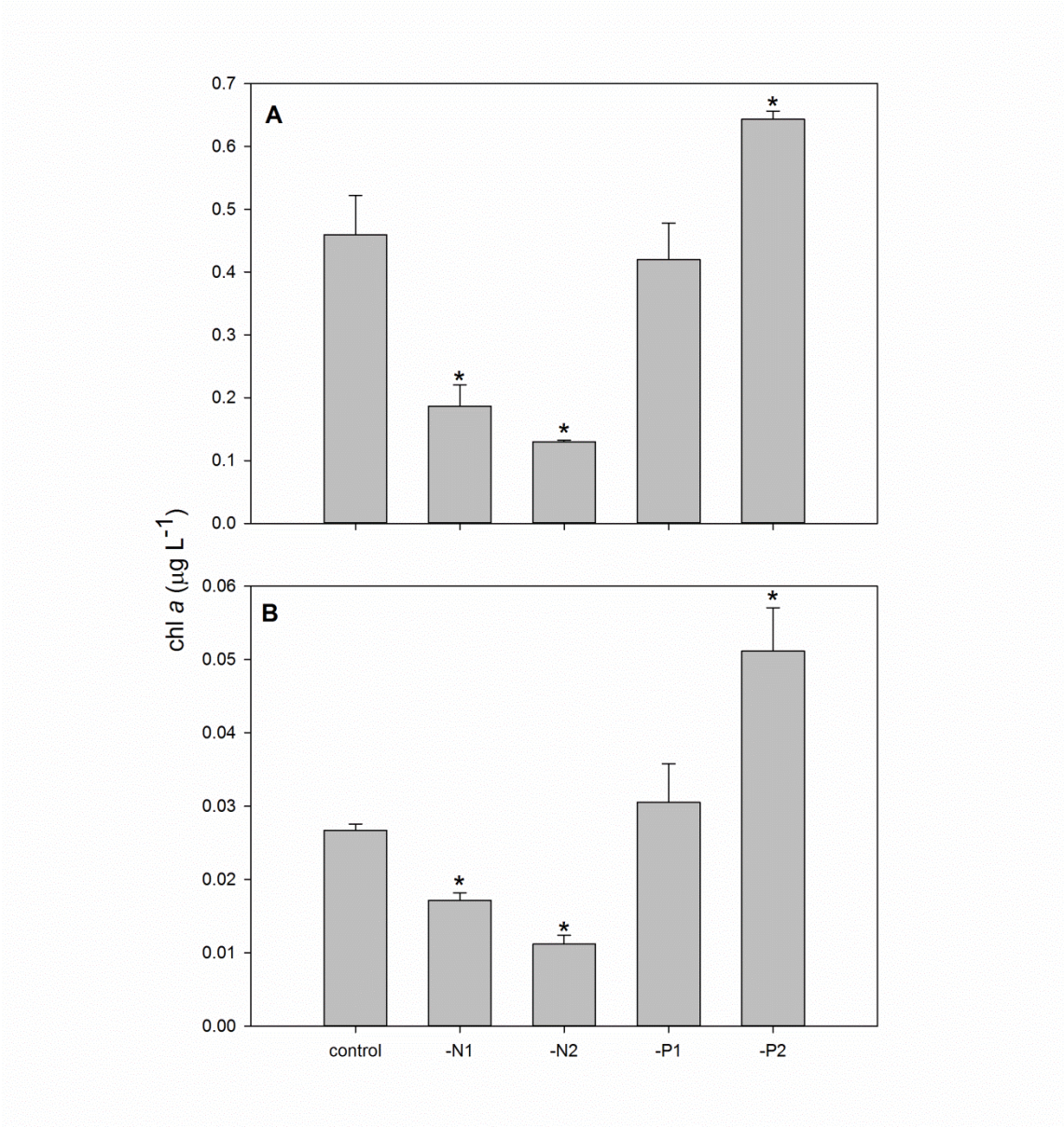

Figure 4.3 Variations of cellular chl *a* in different nutrient treatments at the late exponential phase (around day 13). A: *P. tricornutum*; B: *E. huxleyi*. Data are given as means± standard error (S. E.). * indicated there was a statically significant difference between this treatment and the corresponding control group.

In the late exponential phase, we also measured the concentrations of accessory light-harvesting pigments and normalized the changes to chl *a* (Fig. 4.4). Chl *c*, fucoxanthin (fuco, in *P. tricornutum*), 19'hex- fucoxanthin (hfuco in *E. huxleyi*) and β-carotene (bcaro, in both), and the photoprotective pigments in the xanthophyll cycle: diadinoxanthin (dd) and diatoxanthin (dt). In *P. tricornutum*, the ratios of chl *c* and fuco to chl *a* were independent of the different nutrient treatments ($p>0.05$), while bcaro/ chl *a* increased in N starved treatments ($p<0.01$ in both N1 and N2). The xanthophyll cycle pools ((dd+dt)/ chl *a*) in N starved treatments were significantly larger than the control and P starved treatments ($p<0.01$ in both N1 and N2). However, the transformation between dd to dt (dt/dd) only showed significantly increase in P2 treatment ($p=0.009$), although dt/dd values were 20.3%, 15.6% higher than the controls in N2 and P1, respectively. Compared to N starvation, P starvation did not influence the relative cellular pigment composition significantly in *P. tricornutum*.

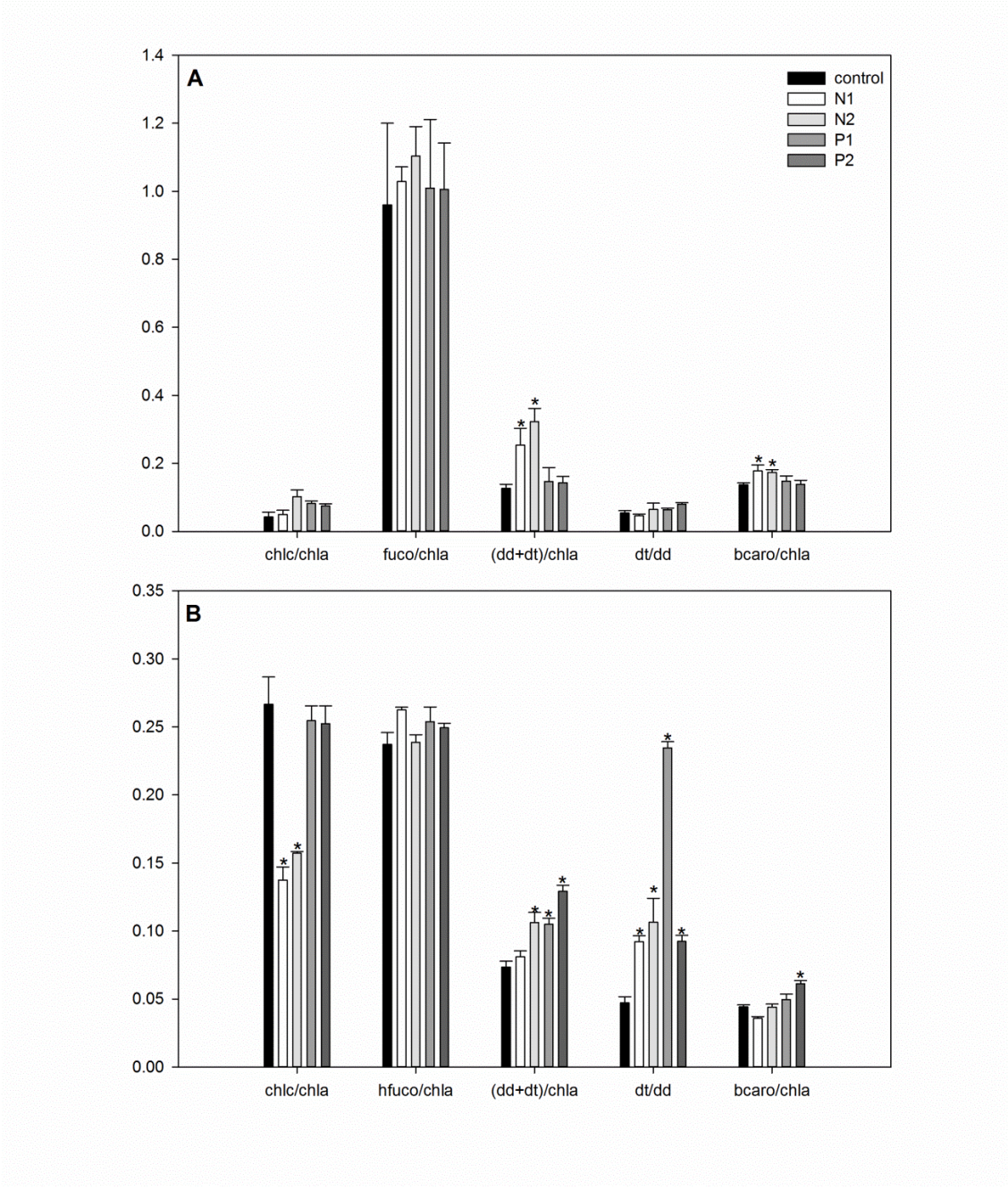

Figure 4.4 Variations of cellular pigments in different nutrient treatment in *P. tricornutum* (A) and *E. huxleyi* (B) in the late exponential phase. Data are given as means± standard error (S. E.). * indicated there was a statically significant difference between this treatment and the corresponding control group.

The response of *E. huxleyi* cellular pigment compositions in different treatments was more complicated than *P. tricornutum*, which was mainly indicated by the xanthophyll cycle pigments (Fig. 4.4). Only hfuco/ chl *a* was independent of the different treatments. (dd+dt) / chl *a* showed an increase in N2, P1 and P2 treatments ($p<0.01$), and dt/dd increased in all the N and P starved treatments ($p=0.044$, 0.002, $p<0.01$ and 0.047 in N1, N2 and P2, respectively). dt/dd increased 3.0 fold in P1 than the controls, showing the most pronounced increase than other treatments ($p<0.01$). Besides, chl *c*/ chl *a* showed a decrease in N1 and N2 treatments ($p<0.01$), while bcaro/chl *a* only showed significantly increase in P2 treatment ($p<0.01$).

Photosynthetic physiology

At the start of the experiment, F_v/F_m values were 0.57-0.61 and 0.45-0.48 and σ_{PSII} values were 318-305 and 388-370 ($Å^2$ $quanta^{-1}$) in *P. tricornutum* and *E. huxleyi*, respectively (Fig. 4.5). In the early exponential phase (around 9 days in *P. tricornutum* and 12 days in *E. huxleyi*), there was no difference in F_v/F_m and σ_{PSII} values among different treatments. As the depletion of the nutrients continued, changes in these values first started to show in N2 treatments with F_v/F_m (day 9, $p<0.01$) changing earlier than σ_{PSII} (day 10, $p<0.01$) in *P. tricornutum*. In day 15, F_v/F_m values in *P. tricornutum* in the four treatments were all smaller in the control treatments ($p<0.01$), declining to 0.53 and 0.49 in N1 and N2 treatments, respectively (control: 0.60). On the contrary, σ_{PSII} values increased to 308 and 328 ($Å^2$ $quanta^{-1}$) in N1 and N2 treatments, respectively (control: 288) (Fig. 4.5). The effect of nutrient starvation on F_v/F_m in *E. huxleyi* started to show

later than *P. tricornutum*, and the decline of F_v/F_m started in day 12 in N2 treatment ($p<0.01$). In day 15, F_v/F_m declined to 0.38 in N2 treatment (Fig. 4.5). Although the response of σ_{PSII} in *E. huxleyi* was later than in *P. tricornutum*, the σ_{PSII} values declined by 33.3% in *E. huxleyi*, a much greater change than in *P. tricornutum* (14.3%).

The connectivity factor (p) and the rate of electron transfer to the acceptor (τ_{QA}) at the start of the experiment (Day 1), exponential phase (Day 9) and stationary phase (Day 15) were shown in Fig. 4.6. The initial p and τ_{QA} values were on average 0.09 and 2560 (μs) in *P. tricornutum*, respectively, while these two values averaged 0.04 and 1260 (μs) in *E. huxleyi*. Similar with F_v/F_m and σ_{PSII}, N starvation had a more pronounced effect on these two parameters but the changes were limited to day 15 in both species. Under N starvation, p values declined 27.3% (p=0.004) in *P. tricornutum* and only declined by 13.0% (p=0.049) in *E. huxleyi*. There was no significant difference between N1 and N2 treatments with respect to p values. τ_{QA} values only showed a greater decline in N starved treatments in the stationary phase in both species. On the contrary to the decline of τ_{QA} in *P. tricornutum* under N starvation, the change was more obvious in *E. huxleyi*. In N2 treatments, τ_{QA} declined 31.6% and 61.3% in *P. tricornutum* and *E. huxleyi* respectively compared to the controls. P starvation did not influence p and τ_{QA} values in both species.

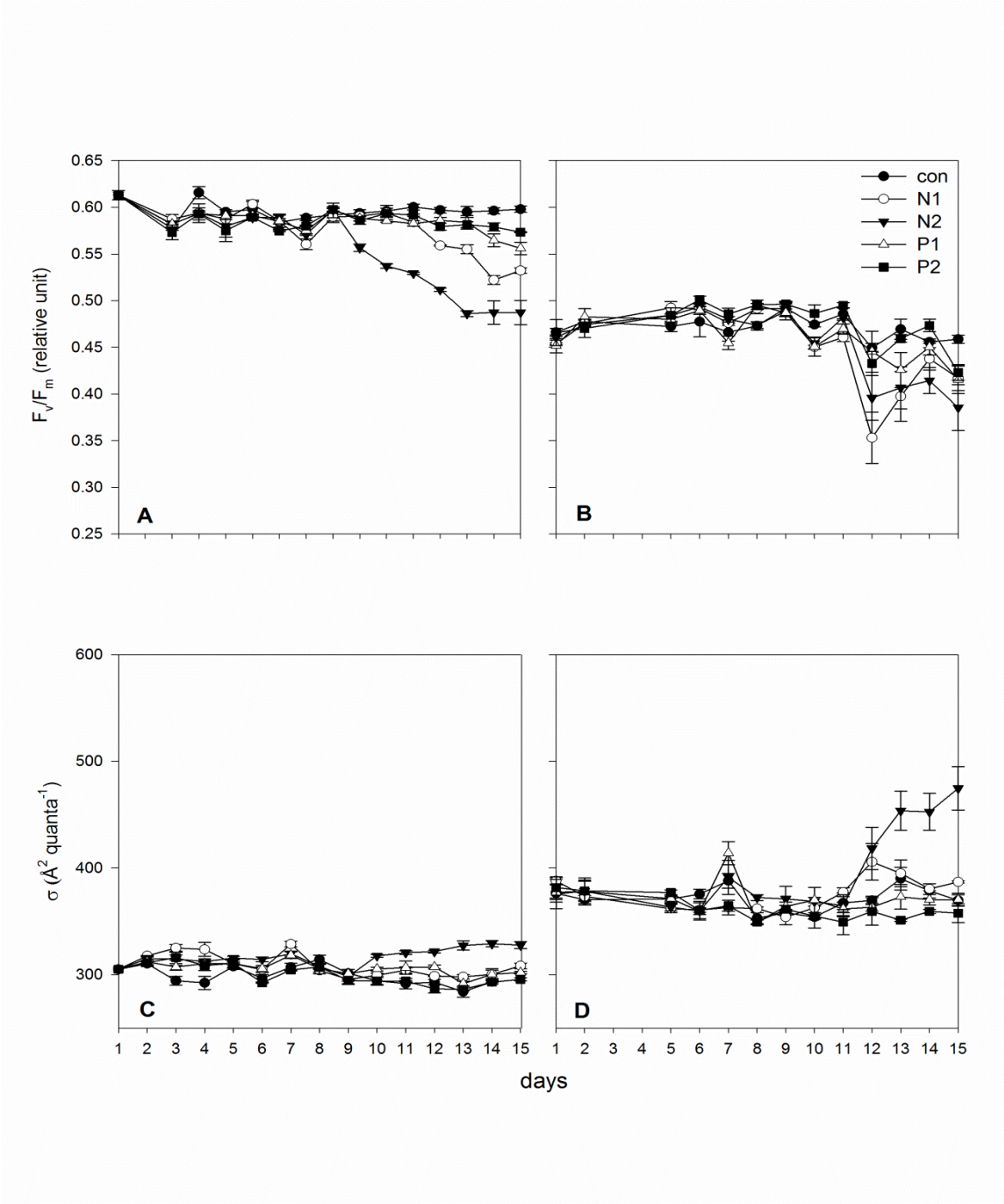

Figure 4.5 Variations in F_v/F_m and σ ($Å^2$ $quanta^{-1}$) in different nutrient treatment during the incubation in PT (A and C) and *E. huxleyi* (B and D). Data are given as means± standard error (S. E.).

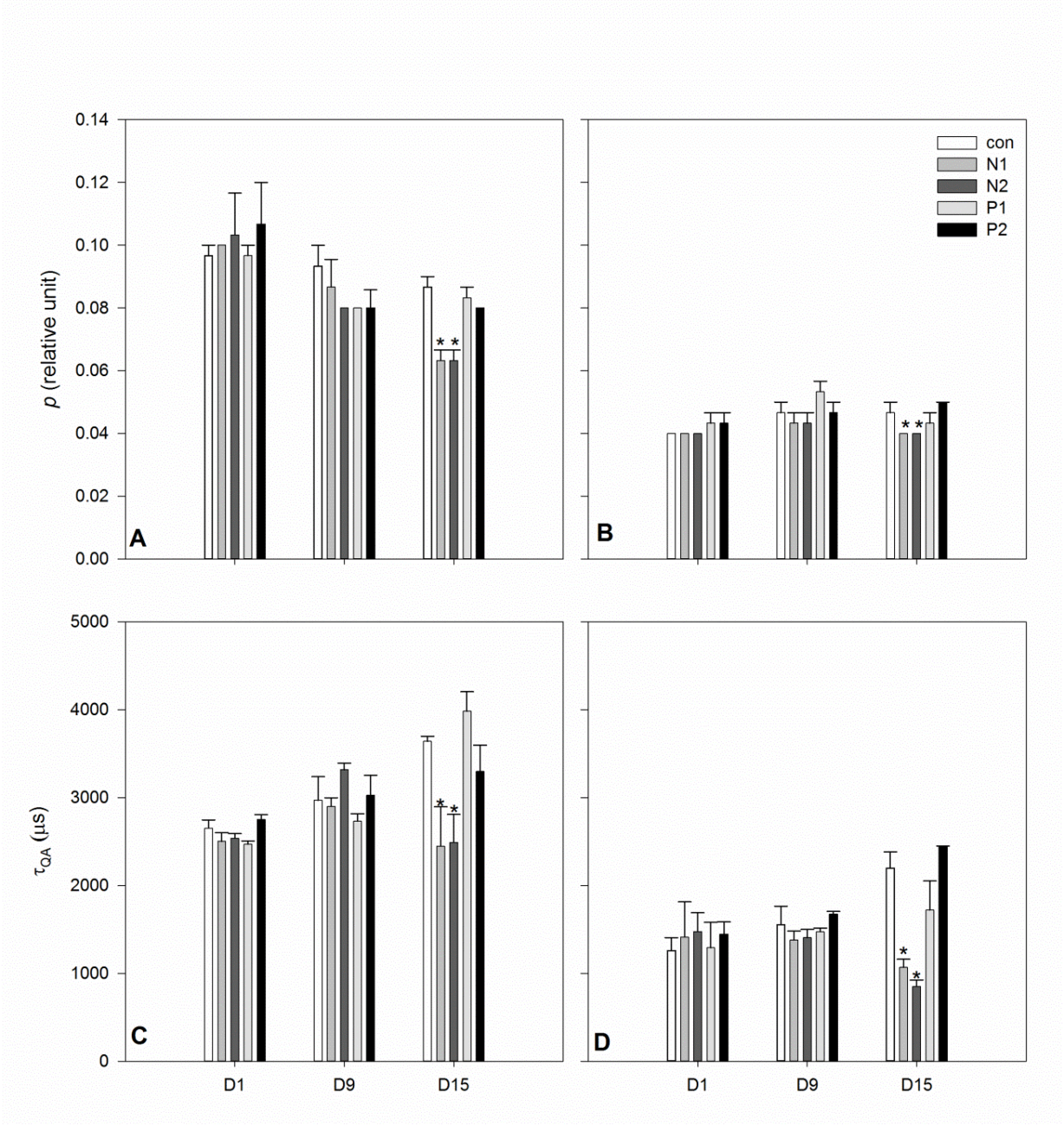

Figure 4.6 Variations of *p* and τ_{QA} (μs) in the initial (Day1), the exponential phase (Day9) and the stationary phase (Day 16) in different nutrient treatments. A and C represent *P. tricornutum* while B and D represent *E. huxleyi*. Data are given as means± standard error (S. E.). * indicated there was a statically significant difference between this treatment and the corresponding control group.

P^B_{max} is the maximum chl *a*-specific carbon fixation rate derived from the P-I curve regressions, which could be taken as the indictor of dark reactions efficiency in light-saturated conditions (Fig. 4.7). P^B_{max} was 2.8 fold greater in *E. huxleyi* than in *P. tricornutum* in controls. P^B_{max} values declined in both N and P starved treatments but were more influenced by N starvation in both species (p<0.05). *P. tricornutum* $P_{max}{}^B$ declined by 35.0% in N1 and 58.8% in N2, while for *E. huxleyi* declined 46.3% in N1 and 94.7% in N2 (Fig. 4.7).

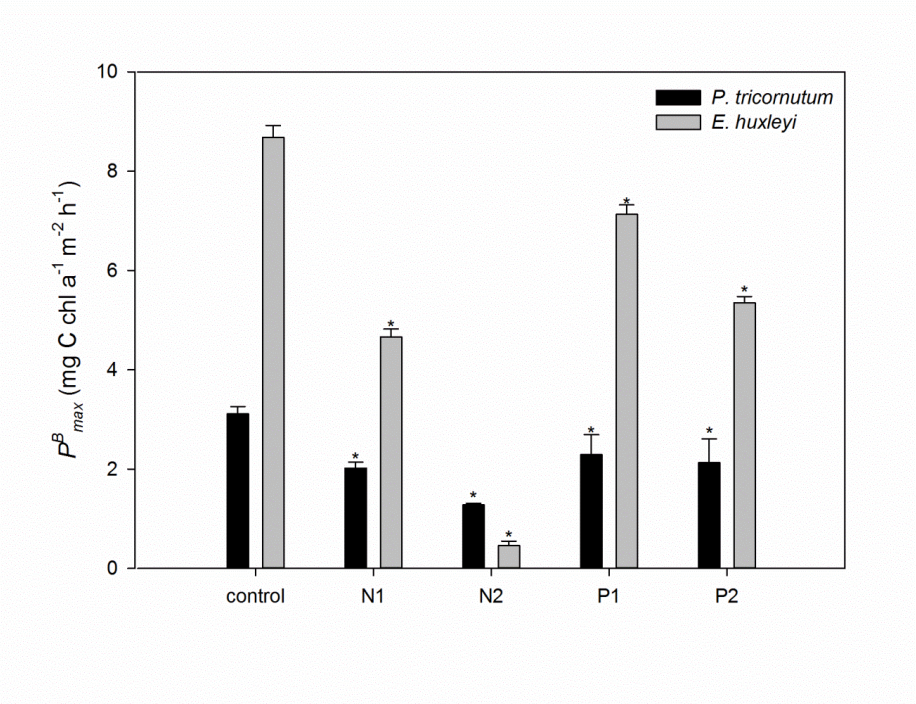

Figure 4.7 Variations of the maximum photosynthetic carbon fixation rate (P^B_{max}) in different nutrient treatments at the late exponential phase (around day 13). Data are given as means± standard error (S. E.). * indicated there was a statically significant difference between this treatment and the corresponding control group.

4.4 Discussion

Competition between *P. tricornutum* and *E. huxleyi*

In coastal ecosystems, coccolithophores (and other small sized phytoplankton, like cyanobacteria) blooms usually follow spring diatom blooms, when the N, P and Si start to become limiting after the consumption of riverine nutrients exported in spring (Sieracki et al., 1993; Cermeño et al., 2011). Accompanied by high light conditions, both N and P limitation have been reported as triggers for *E. huxleyi* blooms in natural environments (Lobel et al., 2010; Tyrrell and Taylor, 1996; Oguz and Merco, 2006). It has been demonstrated that *E. huxleyi* has the highest uptake affinity for inorganic P of any measured phytoplankton species, which was attributed to the high efficiency of the two alkaline phosphatase systems (Riegman et al., 2000). By contrast, *E. huxleyi* acted as poor N competitors in some lab experiments (mostly in continuous cultures) (Cermeño et al., 2011), but it is also known to form blooms in N limited waters (Riegman et al., 1992; Lessard et al., 2005; Lobel et al., 2010). Common to coastal areas and inland waters, the diatom *P. tricornutum* has been illustrated as a dominate species in nutrient enriched coastal waters and it has a high tolerance to iron limitation (Soria-Dengg and Horstmann, 1995; Allen et al., 2008). The nitrate competitive ability of diatoms is typically stronger than that of dinoflagellates and coccolithophores (Litchman et al., 2007), and it has been demonstrated that *P. tricornutum* is a good competitor for nutrients (D'Elia et al., 1979).

Former studies of nutrient competition were based on equilibrium conditions and non- equilibrium conditions (Tilman, 1982; Sommer, 1985; Sterner and Elser, 2002). In

equilibrium conditions, the nutrient ratios in the culture are constant and determine the outcome of mixed-species competition (Tilman, 1982; Egge and Aksnes, 1992). Non-equilibrium conditions refer to the ecosystem frequently experiencing dynamical nutrient supplies, which results in more complicated selective pressure and diverse mixed-species competition results (Sommer 1985, 1995). Cermeño et al. (2011) illustrated that the coccolithophore *Coccolithis braarudii* outcompeted the diatom *Thalassiosira pseudonana* in N limited chemostats (equilibrium) while *T. pseudonana* outcompeted *C. braarudii* after nitrate (N) pulse was added (non-equilibrium). Our results also indicated that different nutrient status in the culture changed their competitive abilities between the two species: in nutrient replete conditions when there is ample N, P and Si present, *P. tricornutum* obtained a higher competitive ability than *E. huxleyi*, but its competitive ability decreased under both N and P starved conditions. *E. huxleyi* showed competitive advantages in nutrient starved conditions compared to *P. tricornutum.* These findings are consistent with former studies that diatoms favored N enriched conditions while coccolithophores do not and the distributions of diatoms and coccolithophores in natural environments (Qian, et al., 2003; Lobel, et al., 2010; Jiang et al., 2014).

P versus N effects

In our study, we measured a series of parameters in single species experiments, mainly comparing population growth and photosynthetic apparatus, in order to compare the response of the two species and illustrate the competitive advantages for *E. huxleyi* in different nutrient starved conditions relative to *P. tricornutum*. In batch cultures, the

population growth in different nutrient treatments revealed the inhibitory effect of P starvation was more pronounced than N starvation on both species. The lack of P in the medium resulted in severe cellular P deficiency in cells (Table 4.4). Cellular C: N: P concentrations were used as proxies for cellular carbohydrates: proteins: RNA (Lourenco et al., 2007; Sterner and Elser, 2002; Finkel et al., 2009). N deficiency was often considered to be affected at translational levels while P deficiency was often considered as transcriptional levels (Latasa and Berdalet, 1994). The growth rate hypothesis (GRH) predicts that cellular P is closely linked to RNA content and determines the cell division and growth rates, and species with high P content usually have high maximal growth rates (Sterner and Elser, 2002; Shimizu and Urabe, 2008; Finkel et al., 2009; Flynn et al., 2010). The inhibition of cell divisions is also indicated by the accumulation of carbon, N and chl *a* in cells and the increased cell volume (data not shown) in P1 and P2 treatments. Such changes were consistent with former studies: Litchman et al. (2003) found P limitation increased cellular chlorophyll content in a freshwater microalga *Sphaerocytis*; Litasa and Berdalet (1994) observed the increased cell size of a marine dinoflagellate *Heterocapsa* sp. under both N and P limitation.

Different from P, N is closely linked to proteins in cells and is mainly responsible for the structural construction within cells, particularly the photosynthetic apparatus (Sterner and Elser, 2002; Quigg and Beardall, 2003; Falkowski and Raven, 2007), thus the lack of N has more of an impact on the photosynthetic apparatus in terms of chl *a*, accessory pigments, reaction centers and dark reaction key enzymes (RuBisCO). Our results indicated more modified photosynthetic apparatus in cells experiencing N

starvation than P starvation, which is consistent with former studies (Geider et al., 1993; Wykoff et al., 1998). The response of photosynthesis to N deficiency for both species mainly included: a. the decline of F_v/F_m, p and τ_{QA}, and the increase of σ_{PSII}; b. the decrease of chl *a* contents and accessory pigments to chl *a* ratios in cells; c. dd to dt transformation in xanthophyll cycle for photoprotection (limited in *E. huxleyi*); d. the decline of chl *a* specific carbon fixation rates (P^B_{max}). The four aspects combined together indicated the impact of N deficiency to light harvesting pigments, electron transfer (PET) chain and the Calvin cycle (the dark reaction). Similar results were also observed by Kolber et al. (1988), Geider et al. (1993), Greene et al. (1992), Silva et al. (2009), Parkhill et al. (2001), Young and Beardall (2003), Petrou et al. (2012) in a wide range of phytoplankton species and experimental designs.

σ_{PSII} is the functional absorption cross-section of antenna serving PSII reaction centers and the efficiency of the excitation transfer from the antenna (pigments) to reaction centers, so it is dependent on both the size of antennae and the number of reaction centers. N deficiency leads to a reduction in the cellular density of PSII reaction centers but an increase in the effective size of the antennae serving PSII, resulting in an increase of σ_{PSII} (Lobel et al., 2010). Meanwhile, the decreased number of reaction centers decreased the efficiency of energy transfer between reaction centers (p), and the electron transfer time from reaction centers to the acceptor side (τ_{QA}). The decline of P^B_{max} in nutrient starvation is demonstrated to correlate with the activity of the RuBisCO enzyme (Fisher et al., 1989; Geider et al., 1993). N and P starvation both decreased P^B_{max} but by different mechanisms. N starvation directly leads to the degradation of the

RubisCO enzyme structure, especially the small subunit (Geider et al., 1993). P starvation does not influence the RuBisCO enzyme content in cells, but suppressed the regeneration of adenosine triphosphate (ATP) and reduced nicotinamide adenine dinucleotide phosphate (NADPH), as well as the transcriptional mRNA, leading to a decreased activity of the RuBisCO enzyme (Liu et al., 2012).

The response of phytoplankton pigment compositions to N starvation was similar to high light photoacclimation (Geider et al., 1993; Wykoff et al., 1998), which was also indicated in our results. As the depletion of ambient N, cells start to consume intracellular inorganic and organic stores for the essential structural proteins to support cell divisions. This process usually involves the breakdown of light-harvesting complex proteins, in which chl *a* is firstly degraded (Falkowshi and Raven, 2007). The degradation of photosynthetic proteins increases the possibility of photoinhibitory damage (Geider et al., 1993). The increase of xanthophyll cycle pigment pools (both species) and the transformation from dd to dt (*E. huxleyi*) in cells undergoing N and P starvation indicated the photoprotective effect to dissipate extra absorbed energy by non-photochemical quenching. In N starvation, the bcaro: chl *a* ratios increased in *P. tricornutum* and decreased in *E. huxleyi*, which was also consistent with the variable changes of bcaro: chl *a* ratios in diatoms and coccolithophore under excess solar light (MacIntyre et al., 2002). The response of pigment composition to nutrient starvation was very different between the two species, and the photoprotective effects were more pronounced in *E. huxleyi* (the highest dt/dd ratio in P1 treatment).

Geider et al. (1993) conducted nutrient starvation experiments on *P. tricornutum* which lasted 4 days. They found the transformation from dd to dt, especially in under P starvation; this was not consistent with our results. Our experiment was designed over a longer term (15 days) than Geider's et al. (1993), thus the photosynthetic pigments may have been too degraded to perform the photoprotective role. The less damaged photosystems in *E. huxleyi* than *P. tricornutum* in our study was also indicated by the less and later decline of F_v/F_m values. There was also a significant decline of chl *c*/ chl *a* ratios in N starvation treatments for *E. huxleyi*, but not in *P. tricornutum*, indicating faster degradation of chl *c* in *E. huxleyi*. Therefore, the allocations of pigments were different between N and P starvation and varied between the two species.

Comparation between *P. tricornutum* and *E. huxleyi*

Comparing with the four parameters derived from FIRe, *P. tricornutum* and *E. huxleyi* has very different photosynthetic apparatus. The four parameters derived from FIRe representing four key sections in light reactions: the quantum yield efficiency of the photochemistry in PSII reaction centers (F_v/F_m), the energy transfer from the antenna (pigments) to reaction centers (σ_{PSII}), the connectivity factor between reaction centers (p) and the electron transportation rate to the from reaction centers to the electron-acceptor (τ_{QA}) (Kolber et al. 1998). The F_v/F_m values in normal conditions in *P. tricornutum* and *E. huxleyi* were consistent with former studies (Geider et al., 1993, Lobel et al., 2010). In *P. tricornutum*, The F_v/F_m values were higher than *E. huxleyi*, corresponding to lower σ_{PSII}, higher p and τ_{QA}. The difference indicated the reaction centers in *P. tricornutum*

were controlled by low efficiency to accept energy from antenna (low σ_{PSII}) compare to *E. huxleyi*. Although the electron transfer (PET) chain in *E. huxleyi* was not as efficient as *P. tricornutum* (low *p* and τ_{PSII}), the reaction centers had higher abilities to accept energy and process the charge separation (high σ_{PSII}) (Suggett et al. 2007). For dark reactions, small-sized phytoplankton possess higher chl *a* specific carbon fixation rates (P_{max}^{B}), consistent with our results. The cell size of *P. tricornutum* was bigger than *E. huxleyi* in our experiments.

Based on the calculation of the organic N and P in the two species in day 9, the consumption of ambient N and P was similar by day 9. However, *P. tricornutum* started to show decline of F_v/F_m values by day 9 but not for *E. huxleyi*. Combined with the less photoprotective effects (the transformation from dd to dt was not obvious), we know the photosynthetic apparatus of *P. tricornutum* was impaired compared to that in *E. huxleyi* at the same time by the depletion of nutrients, especially N. Under N starvation, *E. huxleyi* showed higher capacity to sustain photosynthetic function than *P. tricornutum* (*E. huxleyi*: 12 days, *P. tricornutum*: 9 days), and the increase of σ_{PSII} was much higher (33.3%) in *E. huxleyi* than in *P. tricornutum* (14.4%), while the change of *p* and τ_{QA} were similar between the two species. This result indicated the more functional absorption cross sections (σ_{PSII}) were very pivotal for *E. huxleyi* to resist N starvation. Lobel et al. (2010) compared the photosynthetic apparatus performance between *E. huxleyi* and two marine diatoms under N and P depleted conditions, whose results also emphasized the importance of σ_{PSII} in *E. huxleyi* to adapt N limited conditions. Under N depletion, they found the lowest susceptibility to PSII reaction centers damage

(photoinactivation, σ_i) and the highest increase of σ_{PSII} (functional reaction centers): σ_i (inactive reaction centers) ratios from nutrient replete to depletion, all of which was used to explain the longest time to sustain the photosynthetic function for *E. huxleyi*. The pigment compositions were not measured in their study, while we also found *E. huxleyi* processed higher efficiency to dissipate extra solar energy to protect the reaction centers (high dt/dd) under nutrient starvation, which provided us evidence for the less damaged PSII reaction centers in *E. huxleyi*.

In summary, the competition experiment between *E. huxleyi* and *P. tricornutum* in nutrient replete, N starved and P starved conditions indicated *E. huxleyi* was a stronger competitor under nutrient starvation. Although the population growth of *E. huxleyi* was more suppressed by nutrient starvation, the photosynthetic apparatus showed higher resistance to the nutrient starvation (especially N starvation) in terms later and less decline of F_v/F_m values in *E. huxleyi* than *P. tricornutum* and less decline of cellular chl a contents, which might be caused by the higher functional absorption cross section (σ_{PSII}) and more effective photoprotective effect in *E. huxleyi*. On the contrary, P_{max}^{B} representing the rate of dark reaction, decreased more significantly in *E. huxleyi*. Our results indicated *E. huxleyi* and *P. tricornutum* had different way to allocate the elements and energy under nutrient starvation, and *E. huxleyi* had a more economic way to adapt the nutrient depleted environment.

CHAPTER V

THE RECOVERY KINETICS OF *PHAEODACTYLUM TRICORNUTUM* AND *EMILIANIA HUXLEYI* FROM N STARVATION IN A 24 HOUR CYCLE

5.1 Introduction

Phytoplankton in freshwater and marine ecosystems often experience nutrient limitations. Nutrient pulses are introduced to aquatic systems by freshwater inflows, upwelling, Ekman transport, or with passage of an eddy, leading to the fast acquisition of nutrients and the recovery of physiological functions in stressed cells, eg., nutrient pulses in the NGOM lead to diatoms blooms which are ultimately thought to increase of vertical transportation of organic matters and the potential of hypoxia occurrence (Miller, 2003; Moore et al., 2013; Zhao and Quigg, 2014).

The uptake of nutrients could be regressed by kinetics models (e.g., V_{max} determined from the Monod equation, Q_{max} determined from the Droop equation), which are species-specific and dependent on the cell volume and nutrient uptake sites on the cell surface (Litchman et al., 2007, 2010). Except for fast nutrient assimilation, the impaired physiological functions in nutrient deficient cells are restored by the re-supplement of nutrients even on short time scales of minutes to hours to days. The rapid response of nutrient starved cells to nutrient re-supplement has been applied to field studies as an important diagnostic tool for understanding nutrient limitation, especially in coastal areas (Sylvan et al., 2006, 2007; Quigg et al., 2011; Moore et al., 2008). Nutrient enrichment bioassays are typically from 24 hours - 2 weeks (Turner and

Rabalais, 2013; Lugus et al., 2004) and response of biomass, chl *a* fluorescence and community structure shifts has been demonstrated as reliable parameters to detect N or P limitation (Sylvan et al., 2007; Quigg et al., 2011; Zhao and Quigg, 2014). Generally speaking, the recovery of phytoplankton cells including the increase of growth rates, the recovery of photochemical functions could be measured within 24 hours of nutrient re-supply (Slyvan et al., 2007; Quigg et al., 2011).

Most of the impaired cellular functions caused by nutrient deficiency can be restored within short time scales, and time lags among different parameters are often observed. For example, Healey (1979) illustrated the recovery of dark respiration and ATP synthesis after P deficiency was faster than the recovery of photosynthesis after N deficiency in *Scenedesmus quadricauda*. Plumley and Schmidt (1989) indicated the recovery of N limited *Chlamydomonas reinhardtii* involved the accumulation of light harvesting complex (LHC) and membrane proteins, pigments and DNA synthesis, while the cell division recovered later than protein and pigment accumulation. Greene et al. (1992) showed that chl *a* fluorescence physiology and LHC recovered and were restored to nearly normal conditions after 18 hours iron re-supplement for iron starved *Dunaliella tertiolecta* and *Phaeodactylum tricornutum* cells. Geider et al. (1993) studied the response of photosynthetic apparatus of *P. tricornutum* over the course of N, P and iron starvation and recovery, and the found the chl *a* fluorescence physiology, pigments and proteins all recovered to normal conditions after 24 hours. Dong et al. (2013) measured proteomic changes after the additions of nitrate to N starved *Nannochloropsis oceanic* IMET1 cells; they found the functional proteins were amended completely within 4 days.

The amount of assimilated inorganic N used for protein synthesis can be as high as 30%, higher than that used for nucleic acids and chlorophylls (Quigg and Beardall, 2003; Lourenco et al., 2004). The outcome of N deficiency includes the breakdown of enzyme systems, the inhibition of photosynthesis and carbon fixation, the accumulation of lipids in cells and the induction of peroxide stress (Rhee, 1978; Greene et al., 1992; Flynn et al., 2010; Dong et al., 2013). The effect of N deficiency on light reactions includes the degradation of chlorophyll (chl) molecules and the impairment of photosynthetic reaction centers (eg. LHC, D1 proteins), while the impact on the dark reactions mainly involves a reduction in the concentrations and/or activities of the ribulose 1, 5-biphosphate carboxylase (RuBisCO) enzyme (Plumley and Schmidt, 1995; Latasa and Berdalet, 1994; Berges et al., 1996). The alteration of cellular structures and functions by N starvation can also induce oxidative stress in terms of the increase of the reactive oxygen species (ROS), the induction of antioxidants and the peroxidation of cell membrane (the induction of MDA) (Thompson, 1996; Zhang et al., 2013).

Although the effect of N limitation and starvation on phytoplankton has been well studied in long time scales, there are only a few studies focused on the short-term (first 24 hours) recovery kinetics of phytoplankton physiology from N deficiency. Young and Beardall (2003) examined the kinetics of photosynthetic functions in *D. tertiolecta* under N (as nitrate) starvation and recovery phases, and they indicated different recovery time scales of different parameters resulted in the competitive advantage of *D. tertiolecta* after N re-supplement. Whether this scheme also occurs in

other phytoplankton groups or the recovery kinetics is species-specific still needs investigation.

In this study, we chose one diatom (*Phaeodactylum tricornutum*) and one coccolithophore (*Emiliania huxleyi*) to examine the recovery kinetics over 24 hours in N (as nitrate) starved cells. Cellular responses were followed after N re-supplement with fresh media including N in order to study the fast repair and recovery of photosynthesis on fine time scales. The recovery of N starved cells was indicated by comparing with the N replete cells in same time scales. In natural environment, diatoms and coccolithophores often show different competitive abilities when nutrient pulses are introduced (Litchman et al., 2007; Moore et al., 2013; Zhao and Quigg, 2014). The comparison of their different strategies to recover from nutrient starvation will provide us evidence to explain their competitive differences. We hypothesize that *Emiliana huxleyi* is more competitive in terms of recovery kinetics than *Phaeodactylum tricornutum* given the findings in Chapter IV.

5.2 Material and methods

Experimental microalgal species *Phaeodactylum tricornutum* and *Emiliana huxleyi* were purchased from the Culture Collection of Algae at the University of Texas (UTEX 640) and the National Center for Marine Algae and Microbiota (CCMP 374) respectively. The two species were cultured with natural seawater from National Oceanic and Atmospheric Administration (NOAA) Marine Fisheries Galveston Laboratory enriched with f/4 nutrients, trace elements and vitamins (Guillard, 1975) and

sterilized (30 minutes, 121^{o}C) before using. Si was added to the media for *P. tricornutum* but not *E. huxleyi*. Before the experiment, the cultures were sustained in semi-continuous mode to maintain them in exponential growth (See Chapter IV). These cultures were used for the control treatments. The irradiance in the culture chamber was 100-150 µmol/m^{2}/s light, under a light: dark cycle of 12h: 12h and 19±1^{o}C.

N (nitrate) starved cells were prepared by the dilution of N-replete culture with N-free media prepared by omitting only nitrate from the media. Cells in the exponential phase in N-replete (f/4, 440 µM NO_3^-) medium were diluted with N-free media in a ratio of 1:1 to accelerate the consumption of N in the culture. As the growing of cells, same dilutions were conducted three times to keep the medium fresh and avoid carbon limitation. The cells were monitored by the Fluorescence Induction and Relaxation (FIRe) System (Satlantic Instruments S/N 2). The maximum quantum yield of PS II (F_v/F_m) was measured at the same time each day after incubating the cultures were kept in the dark for 30 mins at room temperature (more details below). Based on the previous experimental results (Chapter IV), we started the recovery experiments when the F_v/F_m values declined from ~0.60 to ~0.40 for *P. tricornutum* and from ~0.50 to ~0.40 for *E. huxleyi*. This was followed for around 10 days. These are referred to as the N-starved cells. N replete cells were set up as controls were treated similar with N starved cells except using N-replete (f/4) medium for the dilutions.

For the recovery experiments, cultures with N starved cells and N replete cells (control) were diluted in to 1 L of medium as triplicates, and the final concentrations of nitrate in each bottle were adjusted 440 µM NO_3^-, which was that found in f/4 media. A

number of parameters were measured over 24 hours, including cell counts, pigments (chl *a*, chl *c* and carotenoids), proteins, cell organic carbon (C) and N, chl *a* fluorescence, malondialdehyde (MDA) and superoxide anion ($O_2^{\bullet-}$) levels. In each experiment, t=0 hour to t=10 was measured during the light period, t=10 hour to t=21 hour during the dark (night) period, and t=21 hour to t=23 hour was in light period again. Cell numbers were counted using a hemocytometer by counting four fields in each chamber.

The relative growth rate was calculated using Equation 1 below.

Equation 1: $\mu = \frac{\ln(N_t) - \ln(N_0)}{t}$, N_t is the cell density at time t (10^4 cells mL^{-1}); N_0 is the cell density at initial (10^4 cells mL^{-1}); t is the time (day^{-1}).

Cultures (10 mL) were filtered on GF/F glass fiber filters (Whatman) for pigment analysis. Pigments were extracted with 90% cold acetone overnight in the dark at -20°C for spectrophotometric chl (*a* and *c*) and total carotenoids determination (Parsons et al., 1984; Davies, 1976). For the organic C and N, 30-60 mL culture samples were collected on pre-combusted (600ºC for 4 hours) GF/F glass fiber filters (Whatman), folded and stored frozen on -20°C prior to analysis. The filters were dried for 24 hours, and then acidified by placing samples in a desiccator with 8N HCl for 24 hours, and subsequently drying samples for another 24 hours at 60°C. The filters were packed into the tin capsules before running with a Perkin-Elmer 2400 CHNS analyzer.

Proteins and stress markers

Cultures (50-80 mL) were centrifuged (4000 g, 15 min) and the supernatant was discarded. The harvested cell pellets were washed and re-suspended in 200 µM PBS

buffer solution (pH=7.9). Samples were then grinded and centrifuged again (10000 g, 15 min), and the supernatant was kept for the measurements of total soluble protein, superoxide anion ($O_2^{\bullet-}$) levels and malondialdehyde (MDA) levels. Total soluble protein content was measured using a Pierce ® BCA Protein Assay Kit (Thermo Scientific, USA) based on the method of Bradford, with bovine serum albumin (BSA) as the standard.

The measurement of superoxide anion ($O_2^{\bullet-}$) concentrations were determined by the oxidation of hydroxyl-ammonium chloride to NO_2^- which is produced by the reaction of superoxide anion and hydroxyl-ammonium (Wang and Luo, 1990; Yin et al., 2010). The reaction system (final concentrations) included 100 μL supernatant, 100 μL PBS buffer solution (50 μM, pH=7.9), 200 μL hydroxyl ammonium chloride (1 mM) in 5 mL centrifuge tubes, and then incubated for 1 hour at 25°C (in the dark). After the incubation, 0.5 mL p-aminobenzene sulfonic (17 mM) and 0.5 mL -naphthylamine (7 mM) were added into the centrifuge tubes and mixed by hand. The absorption at 530 nm was measured in a UV/VIS spectrophotometer after 20 mins to allow the chromogenic reactions to develop at room temperature. The NO_2^- concentration was calculated from the standard curve of $NaNO_2^-$ prepared with all reaction components except the cells.

The measurement of MDA was modified from Peever and Higgins (1989)'s method. The reaction system included 200-500 μL supernatant and 1.5 mL 20% trichloroacetic acid (TCA) + 0.5% thiobarbituric acid (TBA) in 5 mL plastic centrifuge tubes. The centrifuge tubes were incubated in 100^oC for 15 mins and cooled down in an ice-bath immediately. The absorption of each sample was measured in a UV/VIS

spectrophotometer at 532 nm, and the MDA content (mg L^{-1}) was calculated by (OD_{532}/0.156)*(total reaction system volume/supernatant volume) (Peever and Higgins, 1989).

Fluorescence Induction and Relaxation (FIRe)

Chl *a* fluorescence physiology was measured using the FIRe as described in Zhao and Quigg (2014). We used only information collected from the single turnover (ST) component of the transient according to Kolber et al. (1998) and Kromkamp and Forster (2003), including the minimum and maximum fluorescence (F_o and F_m), the maximum quantum yield of PS II (F_v/F_m) and the functional absorption cross-section for PSII (σ_{PSII}; $Å^2$ $quanta^{-1}$). Fluorescence from pure culture medium was subtracted from the F_o and F_m values of samples to correct for the influence of background fluorescence (Cullen and Davis, 2003). The external light source was used to measure the fluorescence parameters and quotients at different PAR values. In our experiments, the external actinic light varied between 0-200 μmol m^{-2} s^{-1} (10 steps) was applied for 20 sec each with a 10 sec dark period, before increasing the light intensity. The photochemical quenching (qP) and non-photochemical quenching (NPQ) values were calculated by equation 2 and 3 (Quigg et al., 2012)

Equation 2: $qP = (F_m'-F_t)/(F_m'-F_o')$, F_m' is the maximum fluorescence yield in the light; F_t is actual fluorescence level at a given time excited by the actinic light; $F_o'$is the minimum fluorescence yield in the light.

Equation 3: $NPQ = (F_m-F_m')/F_m'$.

5.3 Results

Cell growth

The initial cell concentrations in the control and N-recovery treatments were not same due to separate pre-treatments (Fig. 5.1). We compared the relative growth rates (μ) between the two treatments to measure the N-recovery rates. For both species and both treatments, the population did not grow during for the first 10 hours (light period) with cell divisions occurring during the dark period (after the first 10 hours) (Fig. 5.1). Between 10 and 14 hour, the cell counts in the control groups for both species started to increase while the cell counts showed obvious increase after 14 hours in N recovery groups (Fig. 5.1). In the 24-hour recovery phase, the relative growth rates in *P. tricornutum* were 0.30 (±0.04) /day and 0.33 (±0.06) / day in the control and N recovery treatments, respectively, and relative growth rates in *E. huxleyi* were 0.26 (±0.04) / day and 0.22(±0.05) / day, respectively.

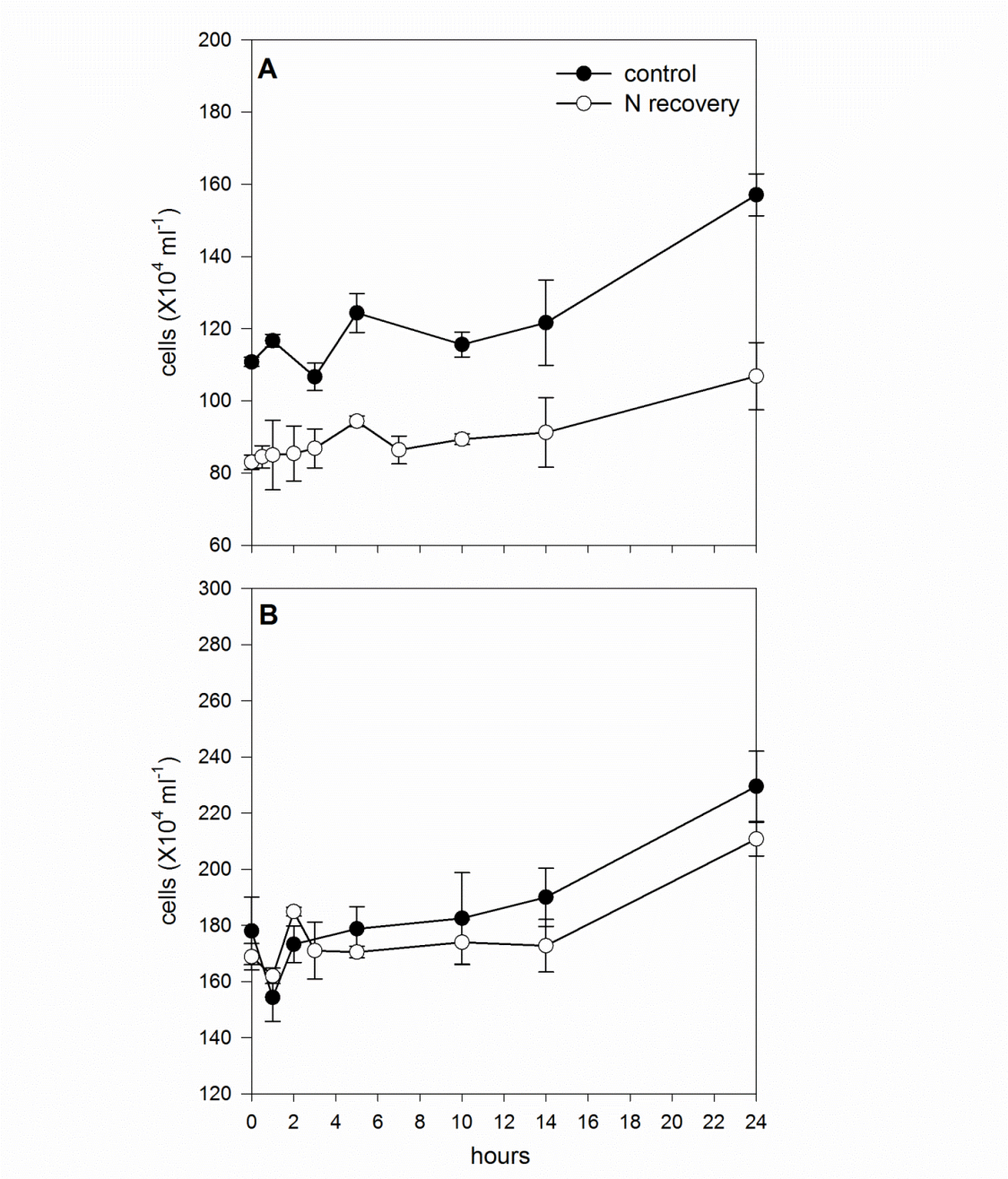

Figure 5.1 The population growth measured by the change in cell density of the two species (A: *P. tricornutum*, B: *E. huxleyi*) in the 24 hour recovery from N starvation. Data points shown are means± standard error (S. E.)

Chl *a* fluorescence

N starvation significantly influenced the chl *a* fluorescence physiology in both species, which was indicated by the decline of F_v/F_m and qP values and the increase of σ_{PSII} and NPQ values prior to the start of the experiment at t=0 hour (Fig. 5.2-5.3). In *P. tricornutum*, F_v/F_m and qP values in the N-recovery treatments at t=0 hour were 29.5 % and 27.3% lower than the control, while σ_{PSII} values were 11.9 % higher than the control, indicating the photosynthetic apparatus in the N-starved cells was in a different physiological status to that in the controls (Fig. 5.2A-D). During the recovery phase, F_v/F_m values showed a quick increase from 0-5 hours, and then followed a relative slow recovery between 6 and 14 hours, and another quick increase after 14 hours (Fig. 5.2A). The F_v/F_m values recovered to control values (~0.60) at the 24 hour time (Fig. 5.2A). The recovery pattern of σ_{PSII} values was consistent (but opposite in direction) with F_v/F_m values (R^2=0.52, p=0.02) (Fig. 5.2B) with quick decline before 5 hours and after 14 hours (in the light period). qP values overall recovered faster than F_v/F_m values and σ_{PSII} values, at around 14 hours after the start of the recovery phase (Fig. 5.2C). NPQ declined faster within 5 fours from 5.6 to 1.4 times higher than the control after the re-supplement of N, while it showed a slow decline from 0.27 to 0.20 after that until 24 hour (Fig. 5.2D). The chl *a* fluorescence parameters in the control groups were relatively constant for *P. tricornutum* over the 24 hours with F_v/F_m values and σ_{PSII} values varying from 0.61 to 0.57 and 309.5 to 330.3 respectively (Fig. 5.2A and 5.2B). Similarly qP and NPQ were not highly variable with ranges from 0.10 to 0.13 and 0.10 to 0.13 respectively (Fig. 5.2C and 5.2D).

Compared to the control *E. huxleyi* cultures (N replete), F_v/F_m values declined by 14.9 % under N starvation and σ_{PSII} values only increased by 3.53% at t=0 hour (Fig. 5.3A-B) (while these changes were more significant in *P. tricornutum*). After the re-supplement of N to starved *E. huxleyi*, F_v/F_m kept declining in the first hour, but started to increase after 3 hours (Fig. 5.3A), before reaching values similar to the N-replete controls (~0.45) after 7 hours (Fig. 5.3A). The recovery of F_v/F_m was faster in *E. huxleyi* than *P. tricornutum* (Fig. 5.2A and 5.3A respectively). The average size of σ_{PSII} in the N-recovery treatments was 419.3 $Å^2$ $quanta^{-1}$ ±6.74 (Fig. 5.3B); this is not very different from that in the control treatments (415.5 $Å^2$ $quanta^{-1}$ ±14.2) for *E. huxleyi*. After a decline at first from 0-5 hours in the N-recovery treatments, qP values started to recover from values of 0.13 to 0.22, and reached values similar to those measured in the controls at 24 hours (Fig. 5.3C). NPQ was not induced by N starvation in *E. huxleyi* before the recovery experiment (Fig. 5.3D). During the recovery experiment, there was no difference between the control groups and the N-recovery treatments in NPQ values. NPQ in *E. huxleyi* behaved very different from that in *P. tricornutum*.

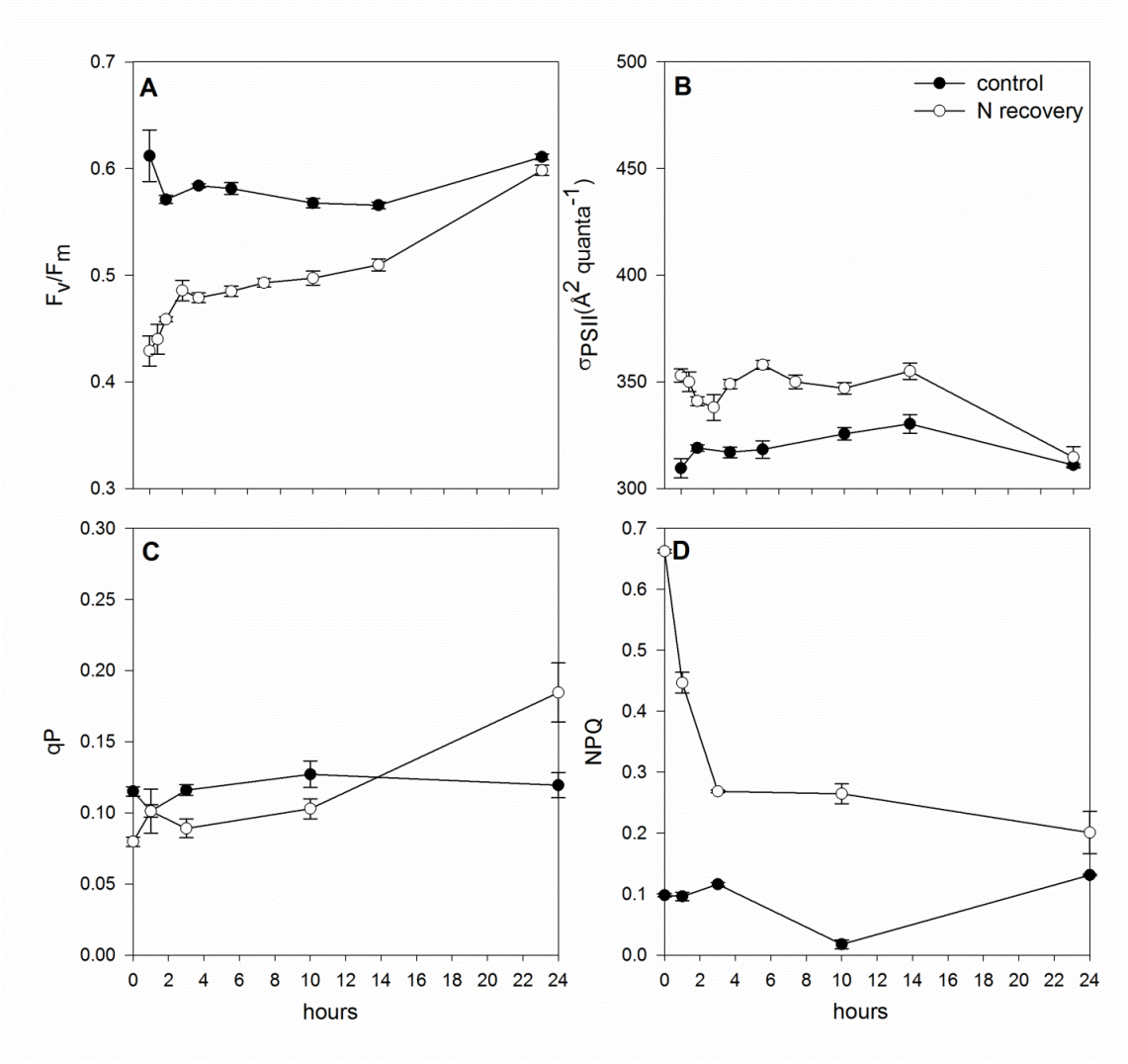

Figure 5.2 The chl *a* fluorescence parameters of *P. tricornutum* in the 24 hour recovery phase. A. The recovery of the maximum quantum yield (F_v/F_m). B. The recovery of the functional absorption cross-section (σ_{PSII}). C. The recovery of photochemical quenching (qP). D. The recovery of non-photochemical quenching (NPQ). Data points shown are means± standard error (S.E.).

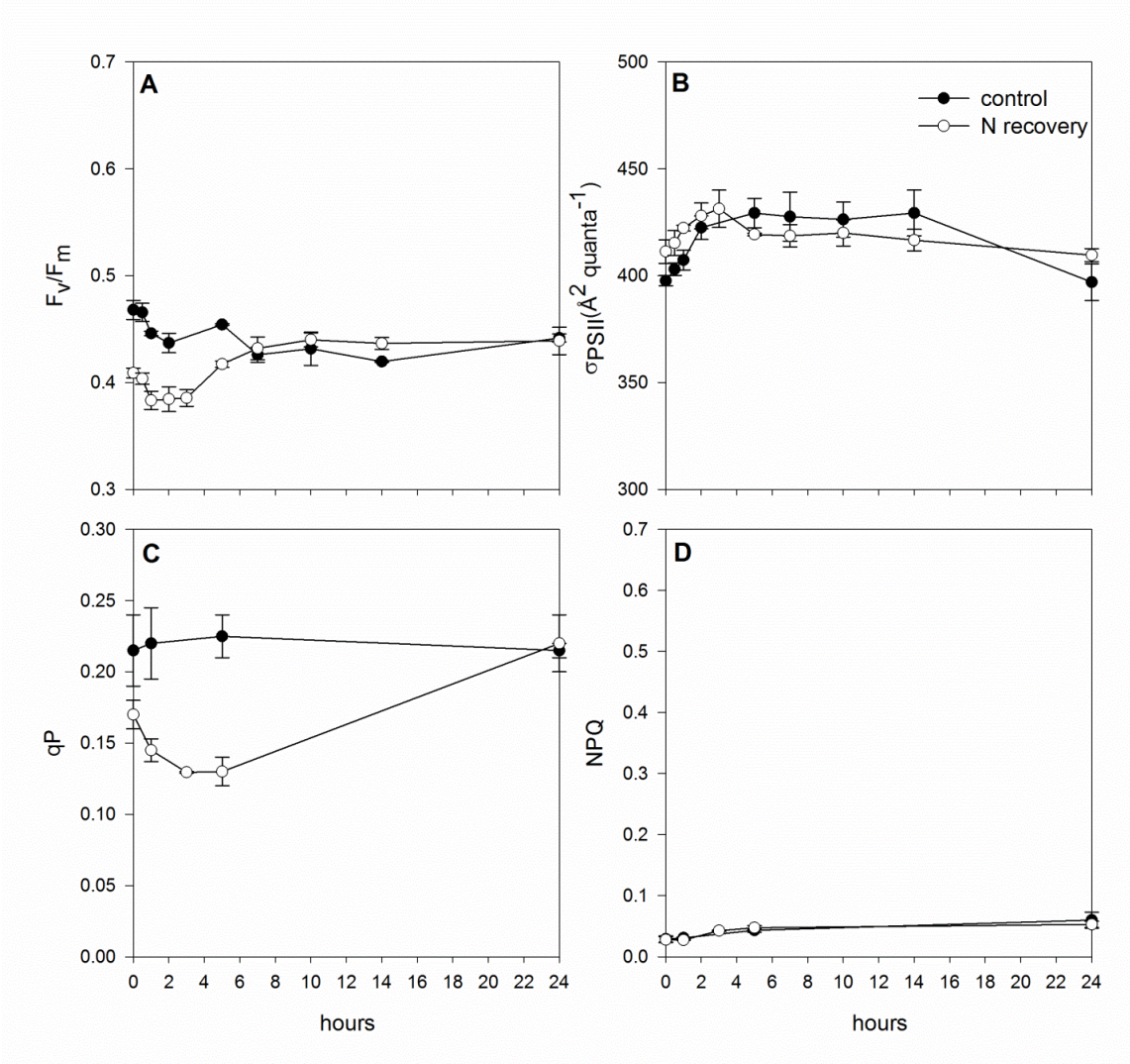

Figure 5.3 The chl *a* fluorescence parameters of *E.huxleyi* in the 24 hour recovery phase. A. The recovery of the maximum quantum yield (F_v/F_m). B. The recovery of the functional absorption cross-section (σ_{PSII}). C. The recovery of photochemical quenching (qP). D. The recovery of non-photochemical quenching (NPQ). Data points shown are means± standard error (S. E.).

Cell organic C and N

Before starting the 24 hour recovery experiments, the cellular organic N content indicated obvious N deficiency in *P. tricornutum* and *E. huxleyi*. In the N-recovery treatment cells, there were 36.6 % and 76.6 % less organic N at t=0 hour in *P. tricornutum* and *E. huxleyi*, respectively, compared to the controls which were maintained in nutrient replete media (Table 5.1 and 5.2). In *P. tricornutum*, organic N started to accumulate in cells after 3 hours of the re-supplement of N, while the decline of C: N ratios started within the first 1 hour due to the decline of organic C contents relative to N. N uptake rates were calculated using the cellular organic N contents and cell numbers. In the N recovery treatment, *P. tricornutum* assimilated N with a rate 50% of the value in the controls between 1 and 3 hours, and the rate increased to 2.3 and 4.4 fold higher than in the controls between 3 and 5 hours and between 5 and 10 hours, respectively. The N uptake rate in recovery treatments reached maximal values between 5 and 10 hours (11.22 - 21 pg N h^{-1}) (Table 5.1) with the rate slowing down at t=24 hour (0.31 pg N h^{-1}) as the N concentration in the N recovery cells (1.89 pg N $cell^{-1}$ ±0.008) became similar to that in the control cells (1.78 pg N $cell^{-1}$ ±0.05) (Table 5.1). The total N uptake in *P. tricornutum* in the N-recovery treatment cultures (145 pg N day^{-1}) was 1.3 fold higher than that of the controls (115 pg N day^{-1}) over the course of 24 hour experiment (Table 5.1).

Control	**0h**	**1h**	**3h**	**5h**	**10h**	**24h**
C (pg cell^{-1})	10.44±0.18	10.83±0.78	NA	11.35±0.12	11.68±0.24	11.23±0.43
N (pg cell^{-1})	1.73±0.01	1.76±0.12	NA	1.78±0.02	1.83±0.006	1.78±0.05
C:N (mol:mol)	7.04±0.15	7.18±0.08	NA	7.44±0.02	7.45±0.11	7.34±0.08
N uptake rate (pg h^{-1})	4.82					
N uptake rate (pg day^{-1})	115.68					
N-recovery	**0h**	**1h**	**3h**	**5h**	**10h**	**24h**
C (pg cell^{-1})	11.34±0.27	10.50±0.01	10.85±0.02	10.66±0.04	12.74±0.5	9.65±0.07
N (pg cell^{-1})	0.80±0.05	0.78±0.02	0.81±0.02	1.08±0.0004	2.21±0.09	1.89±0.008
C:N (mol: mol)	16.53±0.05	15.71±0.61	15.62±0.17	11.52±0.033	6.73±0.083	5.96±0.033
N uptake rate (pg h^{-1})	NA	NA	2.16	11.22	21.00	0.31
N uptake rate (pg day^{-1})	144.59					

Table 5.1 The cellular organic C and N contents, C: N ratios and the calculated N uptake rates from cellular organic N in *P. tricornutum*. NA indicated the cellular organic N did not increase in the certain time periods or was not measured in the time point. Data shown are means± standard error (S. E.)

In *E. huxleyi*, the N uptake rate in the N-recovery treatment was 1.51 pg h^{-1} in 1 hour, 1.8 fold of the average N uptake rate in the controls, indicating *E. huxleyi* had a faster recovery of N uptake than *P. tricornutum* (Table 5.1-5.2). The cellular organic N contents recovered to concentrations measured in the N-replete conditions within 5 hours, while the C: N ratio declined until 10 hours, which resulted in the increase of cellular C in the first 5 hours (Table 5.2). Cells in the N-recovery treatment took up 28.97 pg N day^{-1}, which was 2.1 fold higher than the of the control group (13.85 pg N day^{-1}) (Table 5.2).

Control	**0h**	**1h**	**5h**	**10h**	**14h**	**24h**
C (pg cell^{-1})	4.13±0.13	4.15±0.19	4.25±0.10	4.96±0.23	4.22±0.18	3.40±0.24
N (pg cell^{-1})	0.64±0.009	0.63±0.03	0.64±0.02	0.73±0.04	0.60±0.009	0.49±0.09
C:N (mol:mol)	7.53±0.22	7.47±0.06	7.74±0.12	8.00±0.31	8.25±0.32	8.13±0.23
N uptake rate (pg h^{-1})	0.85					
N uptake rate (pg day^{-1})	13.85					
Recovery	**0h**	**1h**	**5h**	**10h**	**14h**	**24h**
C (pg cell^{-1})	4.15±0.06	4.41±0.05	4.43±0.04	4.19±0.02	4.39±0.02	3.65±0.009
N (pg cell^{-1})	0.49±0.001	0.52±0.002	0.60±0.002	0.62±0.002	0.63±0.004	0.53±0.001
C:N (mol: mol)	9.95±0.29	9.89±0.10	8.61±0.49	7.88±0.39	8.11±0.55	8.06±0.51
N uptake rate (pg h^{-1})	NA	1.51	4.51	1.12	0.24	0.29
N uptake rate (pg day^{-1})	28.97					

Table 5.2 The cellular organic C and N contents, C: N ratios and the calculated N uptake rates from cellular organic N in *E. huxleyi*. NA indicated the cellular organic N did not increase in the certain time periods. Data shown are means± standard error (S. E.).

Soluble proteins

P. tricornutum lost 34.3% cell soluble proteins after N-starvation (see t=0 hour; Fig. 5.4A). Proteins are the major compounds using the cellular organic N, and the recoveries of protein contents were similar with the changes in organic N in our experiments. For cell protein contents in *P. tricornutum*, the changes which occurred within the first 5 hours were not obvious, and the fast recovery started after 5 hours (Fig. 5.4A), similar to the increase of organic N (Table 5.1). The recovery of proteins was accomplished within 10 hours for *P. tricornutum* (Fig. 5.4A). After the dark period, cellular organic C, N and proteins all declined as the active cell divisions during the dark period in both control and N-recovery treatments (Table 5.1; Fig. 5.4A). There was linear relationship between cell proteins and organic N contents (R^2=0.87, p=0.002) (Fig. 5.5A). Cellular protein contents were linearly correlated with organic N contents in *E. huxleyi* as well (R^2=0.85, p=0.003), but the protein contents recovered to the same

values as in the control group within 5 hours (Fig. 5.4C; Fig. 5.5B). The dilution of cellular organic C, N and proteins after the dark period also occurred in *E. huxleyi* (Table 5.2, Fig. 5.4C).

Pigment composition

Chl *a*, chl *c* and total carotenoids declined under N-starvation in both species, and recovered to different degrees after N re-supplement (Figs. 5.4, 5.6-5.7). The loss of chl *a*, chl *c* and carotenoids contents in *P. tricornutum* during starvation was 62.2 %, 32.3 % and 57.3 %, respectively (Fig. 5.4 and 5.6). During the N-recovery for *P. tricornutum*, chl *a* concentrations in cells remained at around 0.17±0.01 pg cell^{-1}; some 2.9 times lower than in the control cells (0.50±0.06 pg cell^{-1}). Chl *c* and total carotenoids did not increased in *P. tricornutum* during the 24 hours of the N-recovery experiment, consistent with the chl *a* changes but not the changes of proteins and cellular N (Fig. 5.4B, Fig. 5.6A-B). Chl *c* and total carotenoids were present in lower concentrations in the N-recovery treatments compared to the controls for *P. tricornutum* (Fig. 5.6A-5.6B). The total carotenoid contents declined by 35.7% of the values measured at t=0 hour at the end (t=24 hour) in the N-recovery treatments, resulting to the increase of chl *a*/carotenoids ratios (Fig. 5.6B and 5.6D). The chl *a*/carotenoid ratio at t=24 hour was higher in N-recovery treatments than in controls (Fig. 5.6D). Chl *a*/chl *c* ratios did not change during the 24 hours N-recovery experiment in both the controls and treatment cells of *P. tricornutum* (Fig. 5.6C).

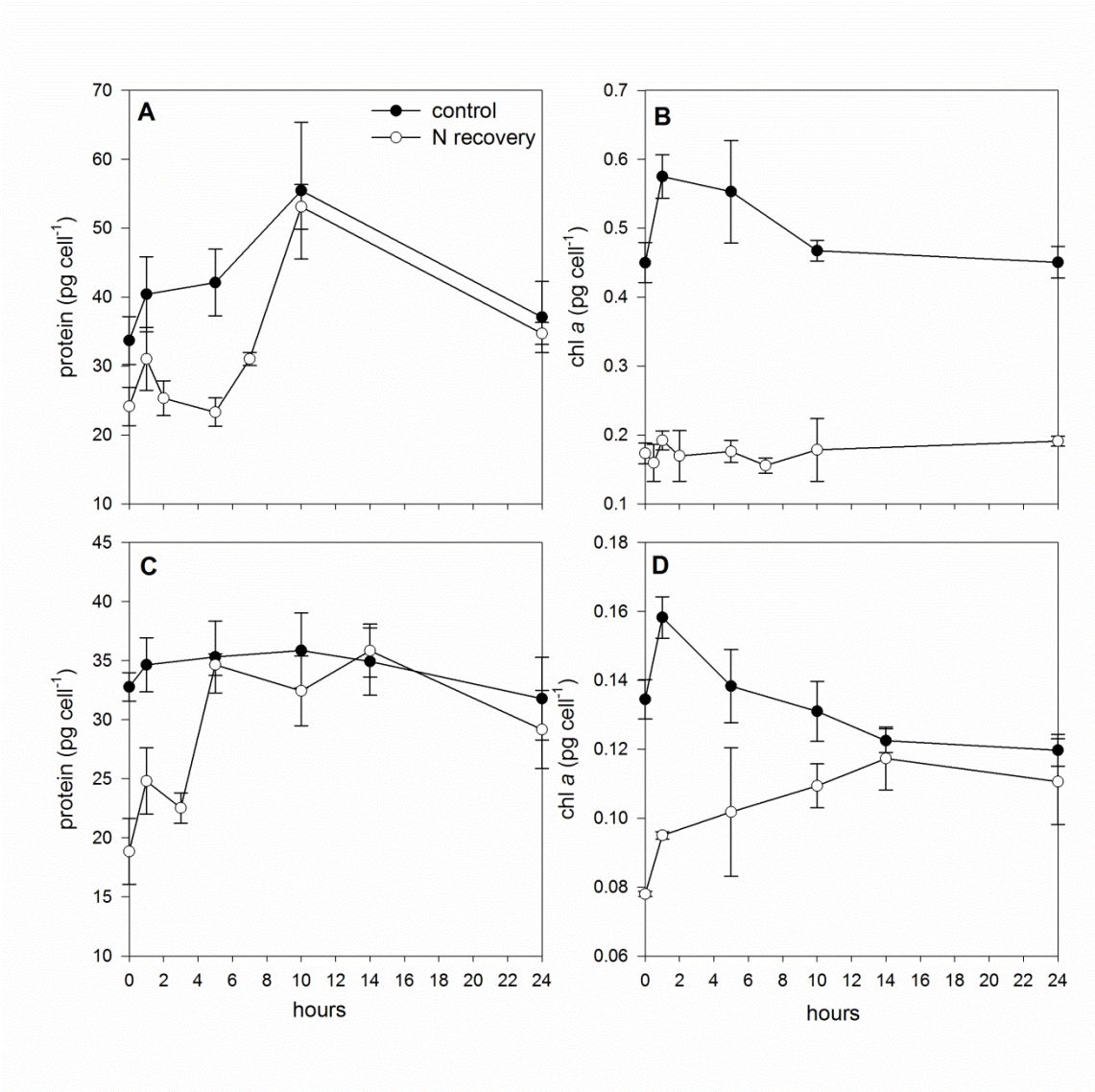

Figure 5.4 The changes of cellular proteins and chl *a* in *P. tricornutum* and *E. huxleyi* in the 24 hour recovery phase. A and B: *P. tricornutum*, C and D: *E. huxleyi*. Data points shown are means± standard error (S. E.).

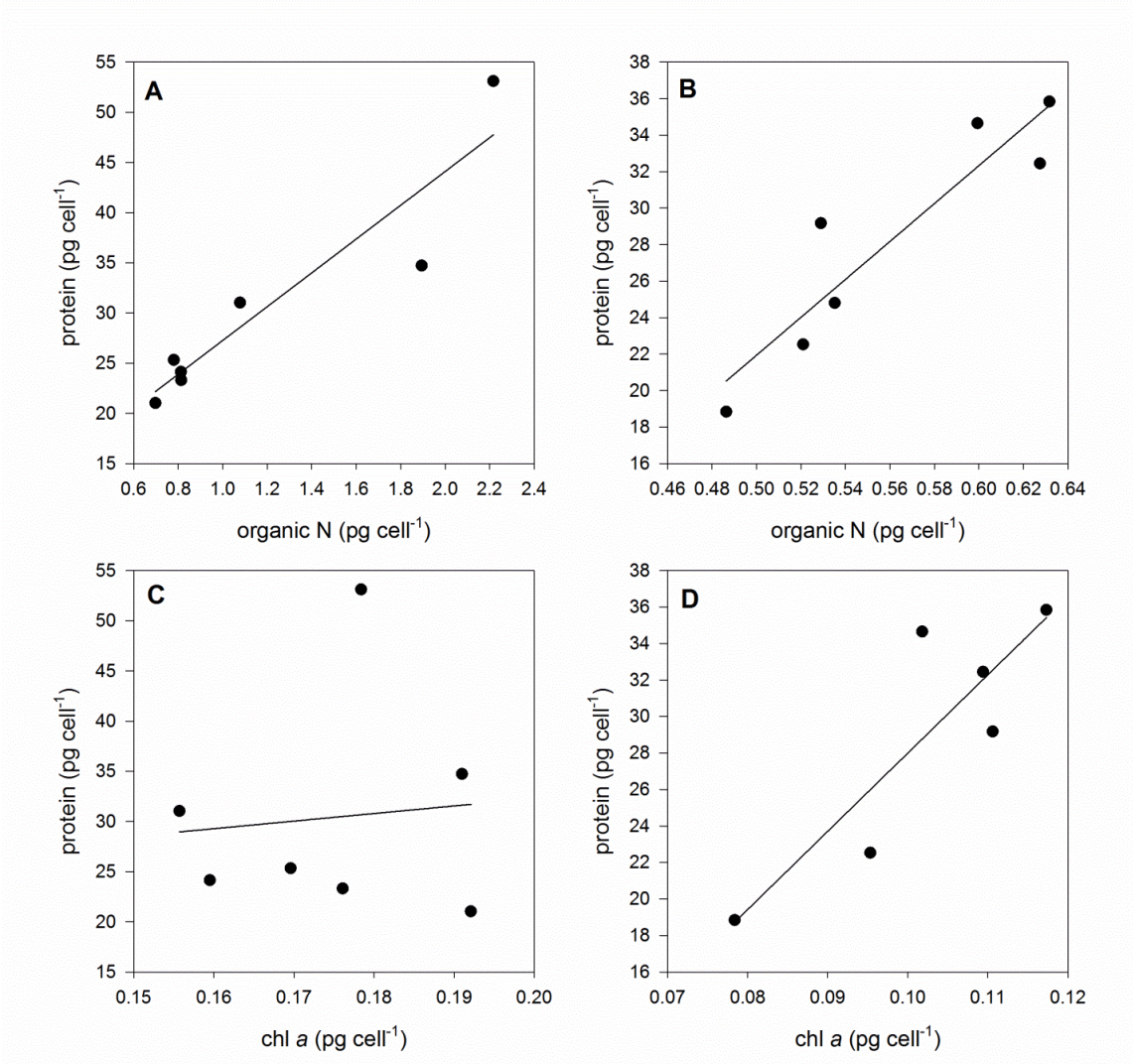

Figure 5.5 The correlation between cellular organic N and protein contents, cellular chl a and protein contents in the 24 hour recovery from N starvation. A and C: *P. tricornutum,* B and D: *E. huxleyi*. A: R^2=0.87, p=0.002; B: R^2=0.85, p=0.003; C: R^2=0.01, p>0.05; D: R^2=0.75, p=0.03.

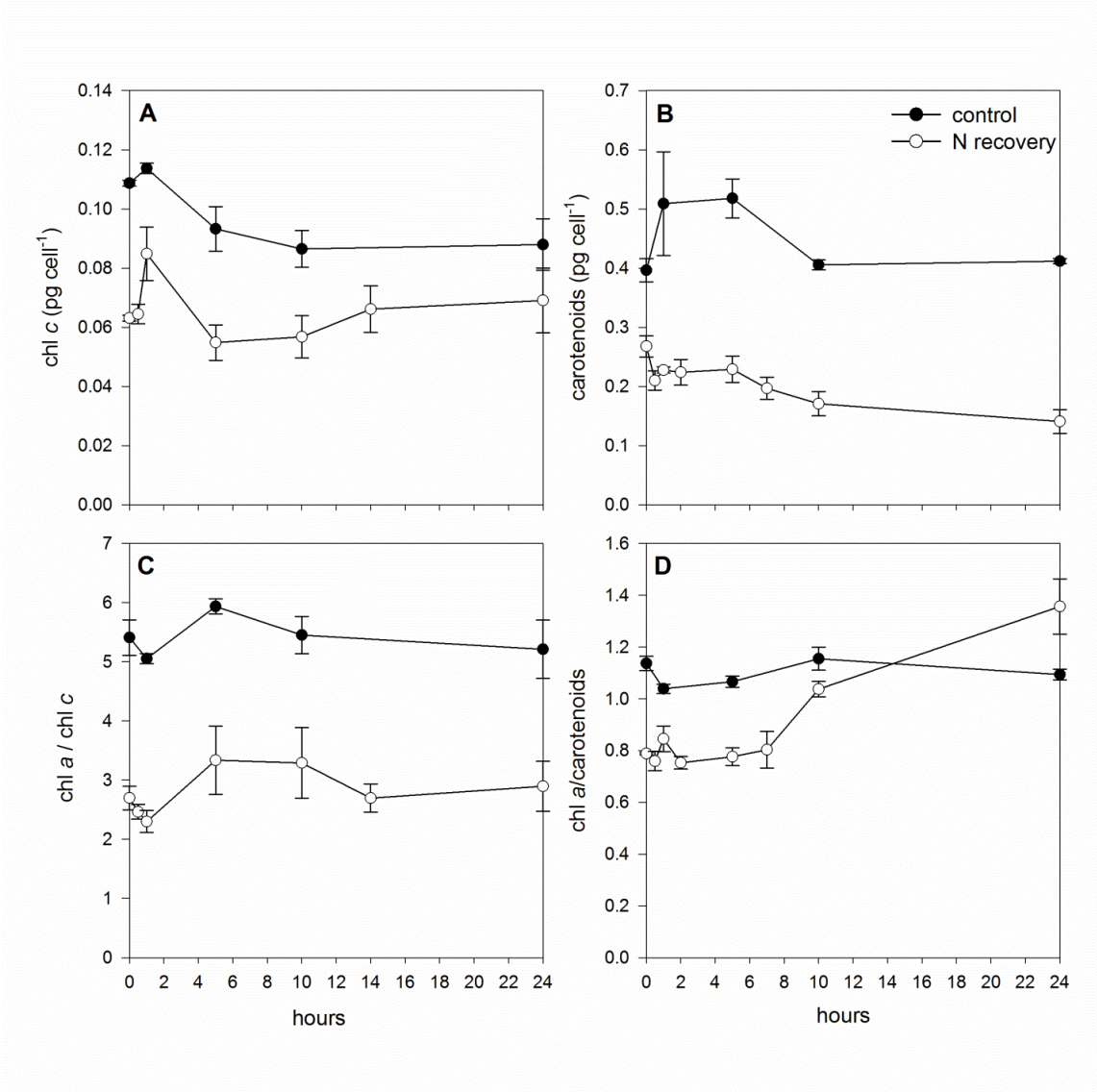

Figure 5.6 The cellular chl *c* and total carotenoids contents and their ratios to chl *a* of *P. tricornutumin* in the 24 hour recovery phase. Data points shown are means± standard error (S. E.).

The loss of chl *a*, chl *c* and carotenoids contents in *E. huxleyi* after N starvation was 44.4 %, 29.5 % and 27.2 %, respectively (Fig. 5.4 and 5.7). Different from *P.*

tricornutum, cellular chl *a* contents under N starvation increased after N re-supplement as well as proteins, and recovered to the same values as in the control group at around t=14 hour (Fig. 5.4C and D). There was linear relationship between proteins and chl *a* contents in *E. huxleyi* (R^2=0.75, p=0.03; Fig. 5.5D).

Chl *c* values in the N-recovery treatments increased to the same concentrations as those in the controls at t=10 hour (0.057 pg chl c $cell^{-1}$), much faster than the recovery of chl *a* in *E. huxleyi* (Fig. 5.7A). The total carotenoids contents changed in parallel in the controls and the N-recovery cultures of *E. huxleyi* (Fig. 5.7). Chl *a*/carotenoids ratios increased during the 24 hours in the controls and the N-recovery treatments in parallel to one another (Fig. 5.7D).

Stress markers - $O_2^{\bullet-}$ and MDA levels

The $O_2^{\bullet-}$ and MDA levels in cells represent the peroxidation of membranes and the reactive oxygen species (ROS) levels, respectively, both of which are markers of cellular stress. Fig. 5.8 showed the relative amount of $O_2^{\bullet-}$ and MDA per cell in the N-recovery treatments compared to the control groups for *P. tricornutum* and *E. huxleyi*. MDA and $O_2^{\bullet-}$ were induced by N-starvation in both *P. tricornutum* and *E. huxleyi*, indicating an increase of oxidization pressure and the damage of membrane systems in cells. Under N-starvation, $O_2^{\bullet-}$ increased 43.5 % and 31.8 % in *P. tricornutum* and *E. huxleyi*, respectively, and MDA increased 52.3 % and 21.0 % in *P. tricornutum* and *E. huxleyi*, respectively in the N-recovery and control cultures.

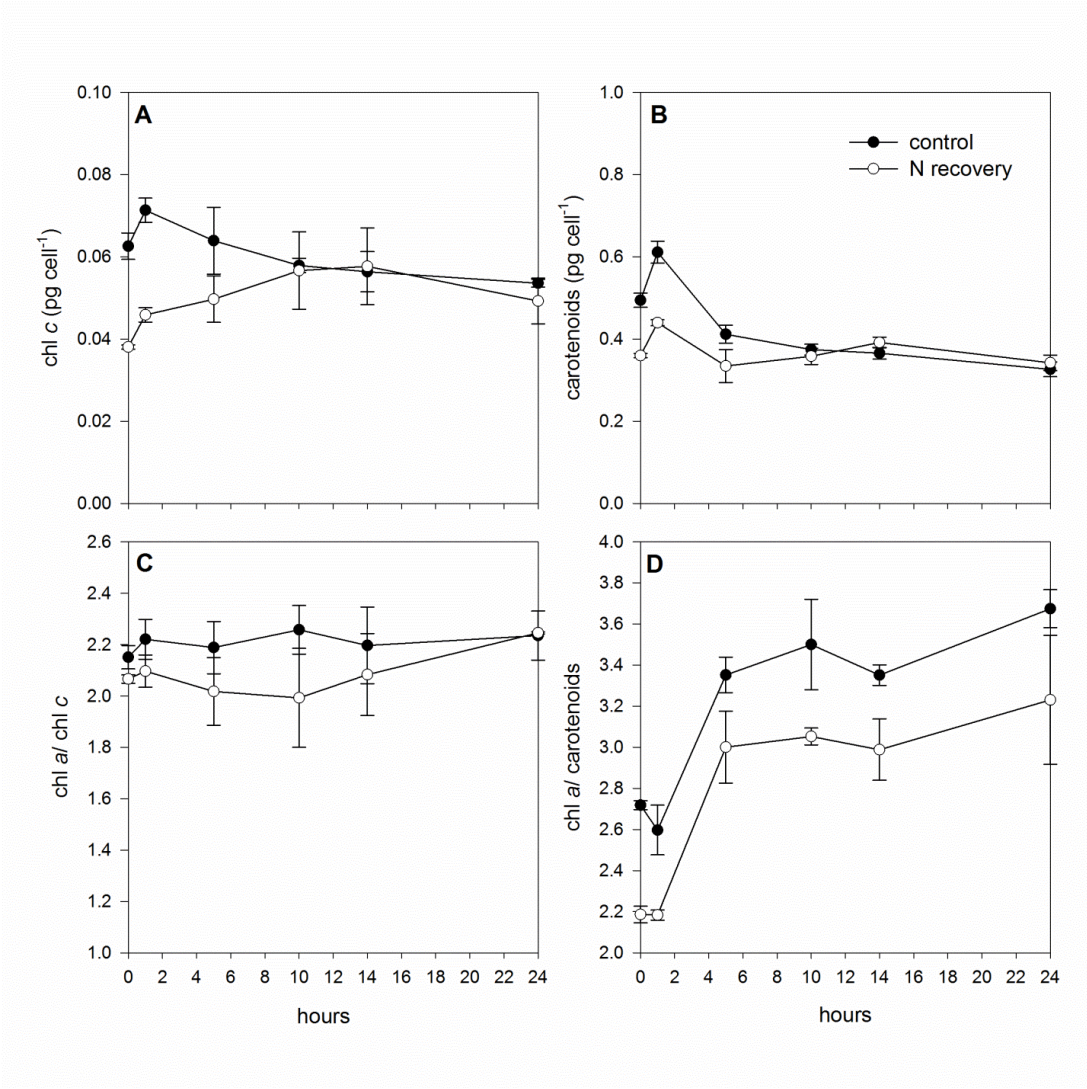

Figure 5.7 The cellular chl *c* and total carotenoids contents and their ratios to chl *a* of *E. huxleyi* in the 24 hour recovery phase. Data points shown are means± standard error (S. E.).

$O_2^{\bullet-}$ was scavenged back to very low levels within 5 to 10 hours in the N-recovery phase both in *P. tricornutum* and *E. huxleyi* (Fig. 5.8A and C respectively).

MDA contents started to decline within 1 hour in the N-recovery experiments for *P. tricornutum* but in *E. huxleyi*, the decline started a little later but still within 1-3 hours (Fig. 5.8B and D respectively).

5.4 Discussion

After the pre-treatment of *P. tricornutum* and *E. huxleyi* by N starvation, cells of both species showed N deficiency, which was indicated by the lower cellular organic N contents and the increased C: N ratios, as seen before in other species (e.g., Leonardos and Geider, 2004). The response of photo-physiology and cellular constituents in both species showed some similarities, including the decline of F_v/F_m, qP values, the increase of σ_{PSII} values; the loss of cellular proteins and chl *a*, corresponding to the loss of organic N; the reallocation of chl *a* and accessory light harvesting pigments (chl *c* and carotenoids); and the induction of $O_2^{\bullet-}$ and MDA. The reponses of the two species under N-starvation were consistent with former studies and our experimental data involving the long-term starvation of the two species (Rhee, 1978; LaRoche et al., 1993; Geider et al., 1993, 1998; Parkhill et al., 2001; Young and Beardall, 2003; data in Chapter IV). The outcome of N-starvation mainly involves the turnover of proteins which are involved in the construction of pigments, light reaction centers, enzymes of dark reactions (e.g., RuBisCO), leading to the inhibition of photosynthesis as expressed by the decline of F_v/F_m and qP values in our results. The dramatic increase of NPQ in *P. tricornutum* under N-starvation resulted from the light stress induced by the loss of light reaction centers, corresponding to the increase of (diadinoxanthin (dd) and diatoxanthin (dt)) pool

and the transformation from dd to dt in xanthophylls cycle (Geider et al., 1993; Latasa and Berdalet, 1994; Chapter IV). In *P. tricornutum*, although carotenoids were degraded as well as chl *a*, the chl *a*/carotenoids ratios declined under N-starvation, indicating the possibility of increased proportions xanthophyll cycle pigments and the synthesis of antioxidants (e.g., β-carotene) (Fig. 5.6). In *E. huxleyi*, NPQ was not induced by N-starvation pretreatment, which might be explained by the high efficiency of reaction centers (high σ_{PSII}) and high repair rates of photo-inactivation (Lobel et al., 2010). The chl *a*/carotenoids ratios were also lower in *E. huxleyi* starved cells than in the control groups, corresponding to the induction of $O_2^{\bullet-}$ and MDA under N starvation.

The addition of N to starved cells resulted in both species showing recovery of cellular and photosynthetic functions within 24 hours in terms of cell divisions, chl *a* fluorescence physiology, organic N, proteins and pigments, and stress markers ($O_2^{\bullet-}$ and MDA). The fast recovery of photosynthetic functions was consistent with former studies which have measured different cellular responses (Healey, 1979; Greene et al., 1992; Geider et al., 1993; Young and Beardall, 2003; Merzlyak et al., 2007; Dong et al., 2013).

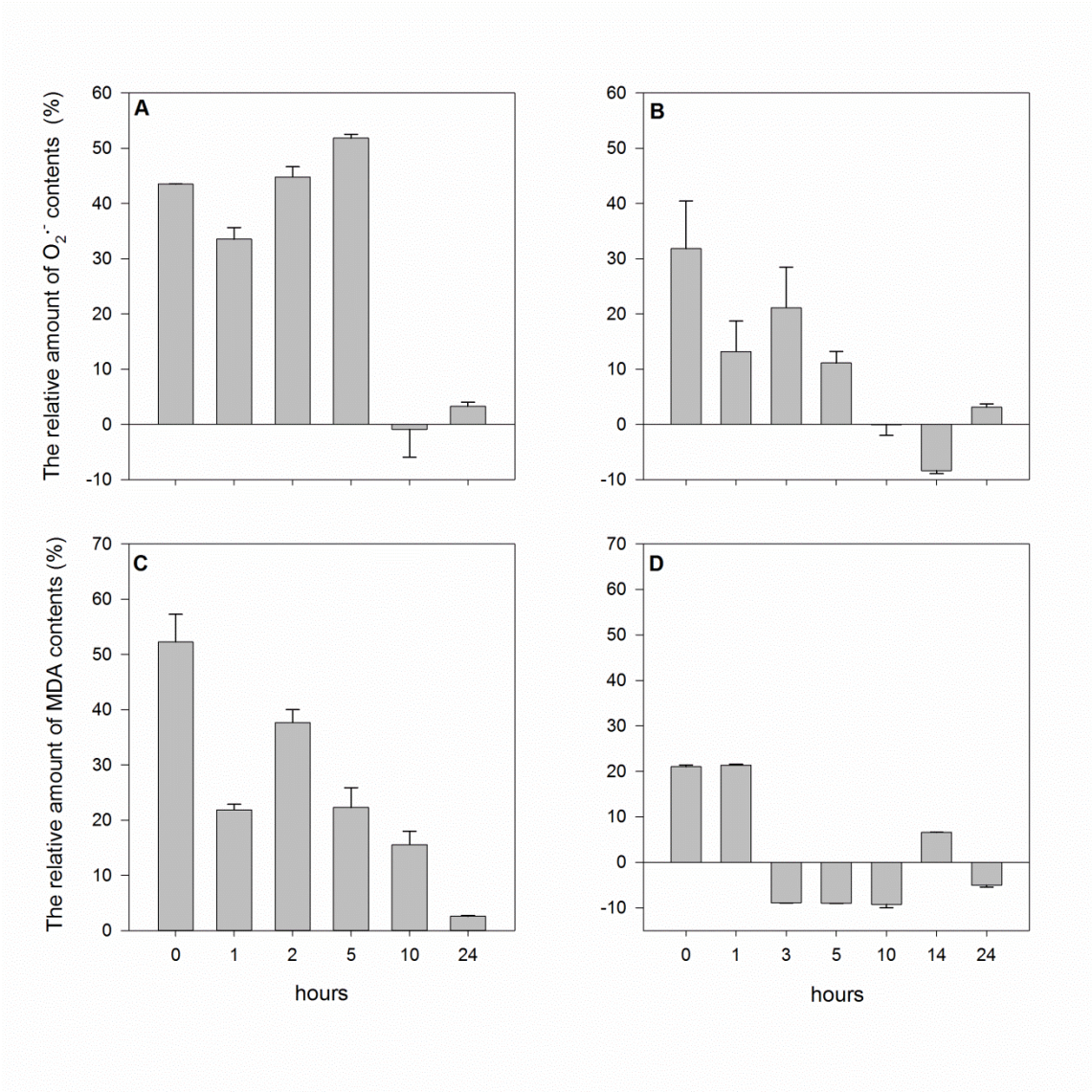

Figure 5.8 The relative amount of $O_2^{\bullet -}$ and MDA contents in the N recovery treatments comparing to the control groups in the N recovery phase. A and C: *P. tricornutum,* B and D: *E. huxleyi*. Data points shown are means± standard error (S. E.).

The relative growth rates were similar between the control and N-recovery treatments in both species. Although the pigments (chl *a*, chl *c* and carotenoids) contents did not recover to normal conditions during the 24 hours in *P. tricornutum*, the relative growth rates in N-recovery treatments were still as high as in the controls, indicating the independence of cell divisions on cellular pigments for this species. For *E. huxleyi*, proteins and pigments were recovered between 10-14 hours, such that this species was well prepared for the cell divisions before dark period. There is usually a time lag before cell division after N addition to starved cells in order to prepare the necessary proteins and DNA, which was from 7-10 hours in former studies (Healy, 1979; Plumley and Schmidt, 1989; Young and Beardall, 2003).

F_v/F_m and σ_{PSII} represent the maximum quantum yield and the transportation of electrons from pigments antenna to PSII reaction centers. The recovery of F_v/F_m in *P. tricornutum* could be divided into two phases; the first one was between 1-5 hours and the second one between 14-24 hours, which is consistent with former similar studies (Greene et al., 1992; Young and Beardall, 2003). The increase of F_v/F_m values in our study were mainly attributed to the increase of the maximal fluorescence emission, F_m, corresponding to the relative consistent chl *a*/F_o ratios and an increase of chl *a*/F_m ratios (data not show). The increase of chl *a*/F_m ratios was the repair process of the PSII reaction centers, which was correlated to the recovery of protein synthesis and was independent of the recovery of cellular chl *a* contents. The time lag of chl *a* synthesis after protein synthesis in our results (especially in *P. tricornutum*) was also found in other studies (Greene et al., 1992; Young and Beardall, 2003). Greene et al. (1992)

studied the recovery of *D. tertiolecta* after iron starvation, in which they found there was rapid synthesis of the cytochrome b6/f complex increased the electron transfer rates within 3-5h, and the accumulation of D1 protein occurred between 10 and 15 hour to increase the quantum yield, while the last step of repair process was the increase of chl contents after 18 hours. Correspondingly, NPQ declined fast in the first five hours in *P. tricornutum*, indicating the recovery of energy transfer efficiencies in the light reaction centers. NPQ acting as a protective function to dissipate heat was induced by irradiance absorbed by light reaction centers but cannot be transferred as electrons effectively, which involved the accumulations and transformations of the xanthophyll cycle pigments.

The light reaction centers of *E. huxleyi* were less impacted before the start of the N recovery experiments, which was indicated by the lack of changes of NPQ under N-starvation and the shorter time for F_v/F_m recovery to values in the control treatments. However, the F_v/F_m values kept declining after the 1 hour of N re-supplement and started to increase after 3 hours. Although the light reaction centers were not as altered as those in *P. tricornutum*, the recovery of photochemical functions in *E. huxleyi* started later than in *P. tricornutum*.

The changes in σ_{PSII} were consistent with those of F_v/F_m values in the N-recovery phase for *P. tricornutum* and *E. huxleyi*. σ_{PSII} represents the efficiency of electron from light harvesting complex to the reaction centers. The increase in σ_{PSII} under N-starvation is due to the decreased number of light harvesting reaction centers but increase of pigment antenna size per reaction center (Lobel et al., 2010). As the repair of light

reaction centers took place, σ_{PSII} values declined to values observed in the control treatments. Our results in *P. tricornutum* indicated the recovery of σ_{PSII} could be independent of cell chl *a* contents as well as F_v/F_m. In *E. huxleyi*, the recovery of F_v/F_m and σ_{PSII} values started synchronous with cellular organic N and chl *a*, different from *P. tricornutum*.

Although the cellular organic N started to accumulate between 3-5 hours, the increase of cellular protein started after 5 hours in *P. tricornutum* (Table 5.1, Fig. 5.5). This time lag between N accumulation and protein synthesis was consistent with former studies, indicating the build of the amino acid pool which requires a certain amount of time (Greene et al., 1992) associated with both protein turnover and reallocation of resources and energy (Quigg and Beardall, 2003). Cytosolic proteins are known to be restored faster than chloroplastic proteins in *P. tricornutum*, which in the present study was indicated by the lower stimulation of pigments synthesis at the start of the N-recovery experiments. Dong et al. (2013) measured the changes of proteome during N-starvation and recovery in *Nannochloropsis oceanica* IMET1 and found degraded proteins relating to nitrogen assimilation, antioxidants and photosynthesis and carbon fixation. In the recovery phase (within 24 h), the 60S acidic ribosomal proteins increased 1.5-6.6 fold, while the light-harvesting complex proteins and chloroplast proteins only increased 1.6 fold and 1.5-2.0 fold, respectively. In *E. huxleyi*, the recovery of proteins, pigments and cellular organic N started almost synchronously, indicating a different recovery mechanism from *P. tricornutum*. The synchronous recovery of proteins and chl

a was consistent with the findings of Young and Beardall (2003) in the recovery experiment for *D. tertiolecta*.

In the recovery phase, the cellular contents of chl *a*, chl *c* and total carotenoids did not change significantly but their relative proportions in the total pigment pool did change in *P. tricornutum*, thus the reallocation of pigments occurred to facilitate the recovery of physiological functions in cells. The chl *a*/carotenoids increased under N starvation could be attributed to two reasons: (i) the induction of photoprotective pigments in the xanthophyll cycle for the degraded and damaged light reaction centers or (ii) the induction of anti-oxidant systems for scavenging ROS produced by N-stress (Demming-Addms et al., 1996; Zhang et al., 2013; Dong et al., 2013). In our results, the induction of MDA, $O_2^{\bullet-}$ and NPQ in *P. tricornutum* under N-starvation indicated the two possibilities. As the recovery of photochemical functions and the scavenging of ROS, the chl *a*/carotenoids increased to levels observed in the controls after 10 hours. The recovery of pigments in *E. huxleyi* was very different from *P. tricornutum* with chl *a*, chl *c* and carotenoids recovered to the same levels with the control treatments. The chl *a*/carotenoids in the recovery phase also increased, but the ratio increased in the control treatments to which caused by the declined carotenoids contents in controls. It is unclear what the underlying mechanism is in *E. huxleyi*; future studies may consider this phenomenon.

The recovery time kinetics of different nutrient uptake parameters is shown in Table 5.3. In our experiments, cell divisions occurred during dark period accompanied with the dilutions of pigments and proteins. Before the cell divisions started (10-14 hour),

the photochemical functions, cell protein contents and chl *a* contents were all recovered to levels similar to those in the controls in *E. huxleyi*, but not in *P. tricornutum*, despite the relative growth rates in N-recovery treatments were similar with the control groups in both species. In *P. tricornutum*, the recovery of photochemical functions (fast increase of F_v/F_m from 1-5 hours) was faster than the reestablishment of chl and proteins (after 24 hours and 5 hours). Therefore, *P. tricornutum* cells in the recovery phase prioritized restoring the photosynthetic functions and cell divisions over the re-building of chl and proteins, and this mechanism was consistent with several former studies involving recovery experiments after nutrient starvations (Healey, 1979; Young and Beardall, 2003). The recovery of *E. huxleyi* after N starvation was a different strategy, with cell chl and proteins accumulation started synchronously or earlier than the recovery of photochemical functions, indicating the dependence of the photosynthetic efficiency on chl and proteins, which was different from *P. tricornutum*. The decline of MDA and $O_2^{\bullet-}$ started early (within 1-3 hours) in both species. For protein synthesis, it has been illustrated that only a few proteins showed recovery within 24 hours to ensure the preferential restoration of metabolisms necessary for the metabolic shift from N-starvation to N- recovery (Dong et al. 2013), thus it is possible that the two species have different strategies to adjust to the increased energy requirement of N assimilation. Compared with the recovery strategy of *E. huxleyi*, *P. tricornutum* showed competitive advantages due to the preferential to restoration of the photochemical functions and cell division.

Recovery time (h)	*P. tricornutum*	*E. huxleyi*
Cell division	10-24	10-24
F_v/F_m, σ_{PSII}	0-24	1-7
Cell N	3-10	1-10
C:N	1-10	1-10
Cell protein	5-10	1-5
Cell chl *a*	>24	1-14
Chl *a*/carotenoids	7-24	NA

Table 5.3 The recovered timeline in the photosynthetic functions and cellular constituents in *P. tricornutum* and *E. huxleyi* in the 24 hour recovery phase. NA indicated the parameter did not recover to the normal levels after 24 hours.

Phytoplankton in coastal areas often experience N-deficiency, with the possibility that N-pulses could be introduced to the photic zone by means of freshwater inflows, upwelling, Ekman transport, or with passage of an eddy, etc. The introduction of N-pulses to N-limited environments has been reported to influence the local phytoplankton community structure due to different nutrient competitive abilities and growth rates (Lugus et al., 2004; Litchman et al., 2007; Zhao and Quigg, 2014). Zhao and Quigg (2014) conducted nutrient enrichment bioassays in N deficient waters in the Northern Gulf of Mexico (NGOM), where they found the increased proportions of diatoms and decreased proportions of coccolithophores in some bioassays, which were explained by the faster nutrient uptake rates (V_{maxN}) and growth rates (μ) of diatoms relative to the coccolithophores as was also reported in Litchman et al. (2007, 2010). In our present study, *P. tricornutum* and *E. huxleyi* had similar growth rates, but the N uptake rate for *P. tricornutum* was much higher than *E. huxleyi* in response to the N-

pulse (Table 5.1-5.2). Additionally, *P. tricornutum* showed advantages to restore the impaired photochemical functions and cell divisions.

In conclusion, N starvation caused the impairment of photosynthetic functions, the turnover of cellular constituents and the induction of MDA and $O_2^{\bullet-}$. With the re-supplement of N, most of the measured photosynthetic and cellular functions recovered within 24 hours with values similar to those in the corresponding control treatments, but the two species showed different preferences in which functions were reestablished in the recovery phase, which might be the result of different allocation of assimilated N and energy. *P. tricornutum* showed the priority to recover photosynthetic functions and cell divisions, while *E. huxleyi* did not show this pattern. This difference between the two species indicated the competitive advantages of *P. tricornutum* by N-pulse stimulation, consistent with the community shift to diatoms in N enrichment bioassays in N limited waters.

CHAPTER VI

MAJOR CONCLUSIONS

Our results demonstrated the regulation of light and nutrients on phytoplankton photosynthesis, primary productivity and community structure in the NGOM, by means of focusing on diel cycles and nutrient enrichment bioassays in April and August, 2012 (Chapter II and III). This is the first time to study the influence of mixing and depth on diel changes of photosynthetic physiology (Chapter II) and the community structure shift in nutrient enrichment bioassays (Chapter III) in the NGOM. Based on the results of Chapter III in which diatoms were more competitive than coccolithiophores in the nutrient enrichment bioassays, we choose two species from the two groups to compare their competitions and single species response in different nutrient conditions, including N and P starvation (Chapter IV) and N re-supplement after N starvation (Chapter V). Mainly from the point of photosynthetic physiology, the coccolithiophore (*Emiliana huxleyi*) showed competitive advantages in nutrient (N or P) starved conditions while the diatom (*Phaeodactylum tricornutum*) was more competitive under the N re-supplement after N starvation. Understanding the species-specific difference of physiological response could help us better understanding the adaption to their natural inhabitants and their different performance during nutrient competitions.

Diel changes of phytoplankton have been well examined in the lab but have not been widely demonstrated in different ecosystems in field studies (Coxson and Mackey, 1990; Isada et al., 2009; Bruyant et al., 2005; Quigg et al., 2012). Phytoplankton photosynthesis and carbon fixation rates in the NGOM showed obvious diel rhythms,

and the depth dependent rhythms were impacted by the effect of mixing and stratification. Photoacclimation was observed by the fast response of chl *a* fluorescence quenching and long-term response of photoprotective pigment accumulation.

Phytoplankton cells responded to the nutrient additions within 24-48 hours, in terms of the changes in photosynthesis and community structure (Chapters II and III). The recovery of photosynthetic parameters was consistent with earlier studies in the NGOM (e.g., Sylvan et al., 2007; Quigg et al., 2011) and other coastal areas with fluctuating nutrient conditions (e.g. Quigg et al., 2013a), but was different from studies in ecosystems without frequent nutrient variations (e.g. North Atlantic, Moore et al., 2006; Gulf of Aqaba, Suggett et al., 2009a). Phytoplankton community shifts also happened within short time frames (48 hours), which were consistent with the results of long-term bioassays with the community shift from small-sized cyanobacteria and prymnesiophytes to large-sized diatoms and prasinophytes (Lugus et al., 2004). The community shift caused by nutrient pulses could change the structure of food web and carbon cycles (Dortch and Whitledge, 1992; Eldridge and Roelke, 2010).

Based on the findings for phytoplankton dynamics regulated by light and nutrient, we know that phytoplankton cells in the NGOM were not under "steady-state", and prepared for the instant response and acclimation to fluctuated environmental forcing also known as unbalanced growth (Grover, 1990, 1991; Sommer, 1995; Parkhill et al., 2001), which could be attributed to the complex hydrographical characteristics in the NGOM. Anthropogenic activities in the latest century increased the amounts of nutrients introduced to the NGOM from the Mississippi River system and changed the nutrient

ratios to a large degree (Bianchi et al., 2010). As a result of that, the flourished phytoplankton blooms in spring indirectly result in the second largest hypoxic area in the worldwide. In the models designed for the prediction and evolution for bottom hypoxia in the NGOM, phytoplankton biomass and productivity are considered as important components (Hetland and DiMarco, 2008; Fennel et al., 2011, 2013; Laurent et al., 2012). Understanding the regulation of diel cycles and nutrient pulses could help us to improve models involving the calculation of primary biomass and productivity, as well as the vertical carbon transportation and bottom oxygen consuming (Dortch and Whitledge, 1992; Eldridge and Roelke, 2010).

In Chapter III, we found diatoms had higher competitive abilities than prymnesiophytes (coccolithophore) after nitrate (N) additions in N limited waters, while in literature prymnesiophytes performed better in nutrient limited waters than diatoms (Sterner and Elser, 2002; Qian et al., 2004; Litchman et al., 2007, 2010; Lobel et al., 2010), indicating the different performance of the two phytoplankton groups under a range of nutrient conditions. In the laboratory study presented in Chapter 4 and 5, we found *E.huxleyi* was more adaptive to N and phosphate (P) starvation than *P. tricornutum* in terms of higher competitive ability (indicated by the competition model regressions) under N or P starvation, more efficient photoprotective response and the less impaired photosynthetic functions (less reduced photosynthetic parameters, more active xanthophylls cycle involved pigments) (Chapter IV). On the contrary, *P. tricornutum* showed the priority to recover photosynthesis and cell divisions than recover cell constitutes after N re-supplement to N starved cells, which was not shown

by *E. huxleyi* (Chapter V). From the point of photosynthesis, the performance of the two species was consistent with the actual situations in the field, indicating their different competitive advantages in different nutrient conditions were not just the result of unique nutrient requirements and assimilated abilities.

This thesis provided more empirical data for the phytoplankton dynamics in the NGOM, filled some former studies' gaps including the diel changes of photosynthesis and community structure shift under nutrient pulses. The work performed in Chapter IV and 5 for the first time combined the species competition with the measurements of photosynthetic physiology, as well as the recovery of physiological functions and cellular constituents from nutrient starvations. Our studies and bioassays were limited in three stations in or nearby the Mississippi River plume (green water), while it would be meaningful to compare the difference with river mouth area (brown water) and the oligotrophic area (blue water) in the future. We only examined the effect of nutrient fluctuations on the two species (competition and single species response) without the consideration of light fluctuations, CO_2 concentrations and other factors in the complicated coastal ecosystems, which also need to be investigated in the future.

REFERENCES

Adolf J.E., Yeager C.L., Miller, W.D., Mallonee, M.E., Harding Jr., L.W., 2006. Environmental forcing of phytoplankton floral composition, biomass, and primary productivity in Chesapeake Bay, USA. Estuarine. Coastal Shelf Sci. 67, 108122.

Aksnes, D.L., and Egge, J.K., 1991. A theoretical model for nutrient uptake in phytoplankton. Mar. Ecol. Prog. Ser. 70, 6572.

Allen, A.E., LaRoche, J., Maheswari, J., Lommer, M., Schauer, N., Lopez, P.J., Finazzi, G., Fernie, A.R., Bowler, C., 2008. Whole-cell response of the pinnate diatom *Phaeodactylum tricornutum* to iron starvation. PNAS. 2008, 1043810443

Becker, V., Cardisi, L.S., Huszar, V.L.M., 2009. Diel variation of phytoplankton functional groups in a subtropical reservoir in southern Brazil during an autumnal stratification period. Aquat. Ecol. 43, 285293.

Behrenfeld, M.J., Randerson, J.T., McClain, C.R., Feldman, G.C., Los, S.O., Tucker, C.J., Falkowski, P.G., Field, C.B., Frouin, R., Esaias, W.E., Kolber, D.D., Pollack, N.H., 2001. Biospheric primary production during an ENSO transition. Science 291, 25942597.

Berges, J.A., Charlebois, D.O., Mauzerall, D.C., Falkowski, P.G.1996., Differential effects of nitrogen limitation on photosynthetic efficiency of photosystems I and II in microalgae. Plant Physiol. 110, 689696.

Bianchi T.S., DiMarco S.F., Cowan Jr. Hetland R.D., Chapman P., Day J.W., Allison M.A., 2010. The science of hypoxia on the Northern Gulf of Mexico: A review, Sci. Total Environ. 208, 14711484

Bomze, I.M., 1983. Lotka-Volterra equation and replicator dynamics: a two-dimensional classification. Biol. Cybern. 48, 201211.

Brooks, A., 1986. Effects of phosphorus nutrition on ribulose-1.5-bisphosphate carboxylase activation, photosynthetic quantum yield and amounts of some Calvin-cycle metabolites in spinach leaves. Aust. J. Plant Physol. 13, 221237.

Brunet, C., Casotti, R., Vantrepotte, V., 2008. Phytoplankton diel and vertical variability in photobiological responses at a coastal station in the Mediterranean Sea. J. Plankton. Res. 6, 645654.

Bruyant, F., Babin, M., Genty, B., Prasil, O., Behrenfeld, M.J., Claustre, H., Bricaud, A., Garczarek, L., Holtzendorff, J., Koblizek, M., Partensky., F., 2005. Diel variations in the photosynthesis parameters of Prochlorococcus strain PCC 9511:

combined effects of light and cell cycle. Limnol. Oceanogr. 50, 850863.

Cermeño, P., Lee, J., Wyman, K., Schofield, O., Falkowski P.G., 2011. Competitive dynamics in two species of marine phytoplankton under non-equilibrium conditions. Mar. Ecol. Prog. Ser. 429, 1928.

Chekalyuk, A., Barnard, A., Quigg, A., Hafez, M., Zhao, Y., 2014. The Aquatic Laser Fluorescence Analyzer: Field evaluation in the Northern Gulf of Mexico. Opt. express 22, 2164121656.

Cho, K.W., Reid, R.O., Nowlin, W.D., 1998. Objectively mapped stream function fields on the Texas-Louisiana shelf based on 32 months of moored current meter data. J. Geophys. Res.-Oceans 103, 1037710390.

Claustre, H., Kerhervé, P., Marty, J.C., Prieur, L., 1994. Phytoplankton photoadaptation related to some frontal physical processes. J. Mar. Syst. 5, 251265.

Cochrane, J.D., Kelly, F.G.,1986. Low-frequency circulation on the Texas-Louisiana shelf. J. Geophys. Res. 91, 1064510559.

Coxson, D.S., Mackey, R.L., 1990. Diel periodicity of photosynthetic response in the subalpine moss Pohlia wahlenbergii. The Bryologist 93, 417422.

Cullen, J.J., Yang, X., MacIntyre, H.L., 1992. Nutrient limitation of marine Photosynthesis, in: Falkowski, P.G., Woodhead, A.D. (Eds.), Primary Productivity and Biogeochemical Cycles in the Sea. Plenum Press, New York, pp. 6988.

Cullen, J.J., Davis, R.F., 2003. The blank can make a big difference in oceanographic measurements. Limnol. Oceanogr. Bulletin 12, 2935.

Dagg, M.J., Breed, G.A., 2003. Biological effects of Mississippi River nitrogen on the Northern Gulf of Mexico-a review and synthesis. J. Mar. Syst.43, 133152.

Dagg, M.J., Ammerman, J.W., Amon, R.M.W., Gardner, W.S., Green, R.E., Lohrenz, S. E., 2007. A review of water column processes influencing hypoxia in the Northern Gulf of Mexico. Estuaries Coasts 30, 735752.

Dale, V.H., Kling, C.L., Meyer, J.L., Sanders, J., Stallworth, H., Armitage, T., Wangsness, D., Bianchi, T.S., Blumbery, A., Boynton, W., 2010. Hypoxia in the Northern Gulf of Mexico, first ed. Springer, Berlin.

Danger, M., Daufresne, T., Lucus, F., Pissard, S. and Lacroix, G., 2008. Does Liebig's law of the minimum scale up from species to communities? Oikos 117,

17411751.

Darley, W.M., 1982. Algal biology: A physiological approach (Basic Microbiology), first ed. Blackwell Scientific, London.

Davies, B.H., 1976. Carotenoids, in Goodwin, T.W. (Ed.) Chemistry and Biochemistry of Plant Pigments. Academic Press, London, pp. 38166.

D'Elia, C.F., Guillard, R.R.L., Nelson, D.M., 1979. Growth and competition of the marine diatoms *Phaeodactylum tricornutum* and *Thalassiosira pseudonana*. I. Nutrient effects. Mar. Bio. 50, 305312.

Demers, S., Roy, S., Gagnon, R., Vignault, C., 1991. Rapid light-induced changes in cell fluorescence and in xantophyll-cycle pigments of *Alexandrium excavatum* (Dinophyceae) and *Thalassiosira pseudonana* (Bacillariophyceae): a photo-protection mechanism. Mar. Ecol. Prog. Ser. 76, 185193.

Demmig-Adams, B., Adams III,W.W., 1992. Photoprotection and other response of plants to high light stress. Annu. Rev. Plant Physiol. Plant Mol. Biol. 43, 599 626.

Diaz, R.J., 2001. Overview of hypoxia around the world. J. Envrion. Qual. 30, 275281.

Diaz, R.J., Rosenberg, R., 2008. Spreading dead zones and consequences for marine ecosystems, Science 321, 926929.

DiMarco, S.F., Chapman, P., Walker, N, Hetland, R.D., 2010. Does local topography control hypoxia on the eastern Texas-Louisiana shelf? J. Mar. Sys. 80, 2535.

Doblin, M.A., Petrou, K.L., Shelly, K., Westwood, K., Enden, R., Wright, S., Griffiths, B., Ralph, P.J., 2011. Diel variation of chlorophyll-*a* fluorescence, phytoplankton pigments and productivity in the Sub-Antarctic and Polar Front Zones south of Tasmania, Australia. Deep- Sea Res. II 58, 21892199.

Dong, H., Williams, E., Wang, D., Xie, Z., Hsia, R., Jenck, A., Halden, R., Li, J., Chen, F., Place, A.R., 2013. Responses of Nannochloropsis oceanic IMET1 to long-term nitrogen starvation and recovery. Plant Physiol. 162, 11101126.

Dortch, Q., Whitledge, T.E., 1992. Does nitrogen or silicon limit phytoplankton production in the Mississippi River plume and nearby regions? Cont. Shelf Res. 12, 12931309.

Edwards, K.F., Klausmeier, C.A., and Litchman, E., 2011. Evidence for a threeway trade-off between nitrogen and phosphorus competitive abilities and cell size in phytoplankton. Ecology 92, 20852095.

Edwards, K.F., Litchman, E., and Klausmeier, C.A., 2013. Functional traits explain phytoplankton community structure and seasonal dynamics in a marine ecosystem. Ecol. Lett. 16, 5663.

Eker-Develi, E., Kideys, A.E., Tugrul, S., 2006. Effect of nutrients on culture dynamics of marine phytoplankton. Aquat. Sci. 68, 2939.

Eldridge, P.M., Roelke, D.L., 2010. Origins and scales of hypoxia on the Louisiana shelf: importance of seasonal plankton biomass and river nutrients discharge. Ecol. Model. 221, 10281042.

Erga, S.R., Skjoldal, H.R., 1990. Diel variations in photosynthetic activity of summer phytoplankton in Lindåspollene, western Norway. Mar. Ecol. Prog. Ser. 66, 73 85.

Falkowski, P.G., LaRoche, J., 1991. Acclimation to spectral irradiance algae. J. Phycol. 27, 814.

Falkowski, P.G., Raven, J., 2007. Aquatic photosynthesis, second ed. Princeton Univeristy, New Jersey.

Fennel, K., Hetland, R., Feng, Y., DiMarco, S., 2011. A coupled physical-biological model of the Northern Gulf of Mexico shelf: model description, validation and analysis of phytoplankton variability. Biogeosciences Discussions 8,121156.

Fennel, K., Hu, J., Laurent, A., Marta-Almeida, M. and Hetland, R., 2013. Sensitivity of hypoxia predictions for the northern Gulf of Mexico to sediment oxygen consumption and model nesting. J. Geophys. Res.-Oceans. 118, 113.

Finkel, Z.V., Beardall, J., Flynn, K.J., Quigg, A., Rees, A.V., Raven, J.A., 2009. Phytoplankton in a chaning world: cell size and elemental stoichiometry. J. Plankton Res. 0, 119.

Fisher, T., Shurtz-Swirski, R., Gepstein, S., Dubinsky, Z., 1989. Changes in the levels of ribulose-l, 5-bisphosphate carboxylase/oxygenase (Rubisco) in *Tetraedron minimum* (chlorophyta) during light and shade adaptation. Plant Cell Physiol. 30, 221.

Fisher, T.R., Peele, E.R., Ammerman J.W., and Harding Jr., L.W., 1992. Nutrient limitation of phytoplankton in Chesapeake Bay. Mar. Ecol. Prog. Ser. 82, 5163.

Flynn, K.J., Raven, J.A., Rees, T.A.V., Finkel, Z. Quigg, A., Beardall, J., 2010. Is the growth rate hypothesis applicable to microalgae. J. Phycol. 46, 112.

Gauthier, D., Turpin, D., 1997. Interactions between inorganic phosphate (Pi) assimilation, photosynthesis and respiration in the Pi-limited green alga *Selenastrum minutum*. Plant Cell Environ. 20,1224.

Glibert, P.M., Kana, T.M., Anderson, D.M., 1988. Photosynthetic response of *Gonyaulax tamarensis* during growth in a natural bloom and in batch culture. Mar. Ecol. Prog. Ser. 42, 303309.

Geider, R.J., Platt, T., Raven, J.A., 1986. Size dependence of growth and photosynthesis in diatoms: a synthesis. Mar. Ecol. Prog. Ser. 30, 93104.

Geider, R.J., La Roche, J., Greene, R.M., Olaizola, M., 1993. Response of the photosynthetic apparatus of Phaeodactylum tricornutum (Bacillariophyceae) to nitrate, phosphate, or iron starvation. J. Phycol. 29, 755766.

Geider, R.J., MacIntyre, H.L., Graziano, L.M., McKay, R.M.L., 1998. Responses of the photosynthetic apparatus of *Dunaliella tertiolecta* (Chlorophyceae) to nitrogen and phosphorus limitation. Eur. J. Phycol. 33, 31532.

Greene, R.M., Geider, R.J., Kolber, Z., Falkowski, P.G., 1992. Iron-indeuced changes in light harvesting and photochemical energy conversion process in eukaryotic marine algae. Plant Physiol. 100, 565575.

Grover, J.P., 1990. Resource competition in a variable environment: phytoplankton growing according to the variable-internal-stores model. Am. Nat. 138, 811835.

Grover, J. P., 1991. Non-steady state dynamics of algal population growth: experiments with two chlorophytes. J. Phycol. 27, 7079.

Grover, J. P., Chrzanowshi, T. H., 2006. Seasonal dynamics of phytoplankton in two warm temperate reservoirs: association of taxonomic composition with temperature. J. Plankton Res. 28, 117.

Guillard, R.R.L.,1975. Culture of phytoplankton for feeding marine invertebrates, in: Smith, W.L., Chanley, M.H. (Eds.), Culture of Marine Animals. Plenum Press, New York, pp. 2660.

Habib, O.A., Tippett, R., Murphy, K.J., 1997. Seasonal changes in phytoplankton community structure in relation to physic-chemical factors in Loch Lomond, Scotland. Hydrobiologia. 350, 6379.

Harding, L.W., Meeson, B.W., Prézelin, B.B., Sweeney, B.M., 1981. Diel periodicity of photosynthesis in marine phytoplankton. Mar. Biol. 61, 95105.

Harding, L.W., Prézelin, B.B., Sweeney, B.M., Cox, J.L., 1982. Primary production as influenced by diel periodicity of phytoplankton photosynthesis. Mar. Biol. 67, 179186.

Healey, F.P., 1979. Short-term response of nutrient-deficient algae to nutrient addition. J. Phycol. 15, 289299.

Hecky, R.E., Kilham, P., 1988. Nutrient limitation of phytoplankton in freshwater and marine environments: A review of recent evidence on the effects of enrichment, Linmol. Oceanogr. 33, 796822.

Hetland, R.D., DiMarco, S.F., 2008. How does the character of oxygen demand control the structure of hypoxia on the Texas-Louisiana continental shelf. J. Mar. Syst. 70, 4962.

Howarth, R. W., Marino, R., 2006. Nitrogen as the limiting nutrient for eutrophication in coastal marine ecosystems: evolving views over three decades. Limnol. Oceanogr. 51, 364376.

Huston M.A., Wolerton, S., 2009. The global distribution of net primary production: resolving the paradox. Ecol. Monograph. 79, 343377.

Isada, T., Kuwata, A., Saito, H., Ono, T., Ishii, M., Yoshikaka-Inoue, H., Suzuki, K., 2009. Photosynthetic features and primary productivity of phytoplankton in the Oyashio and Kuroshio-Oyashio transition regions of the northwest Pacific. J. Plankton Res. 31, 10091025.

Jiang, M., Borkman, D.G., Scott Libby, P., Townsend, D.W., Zhou, M., 2014. Nutrient input and the competition between Phaeocystis pouchetii and diatoms in Massachusetts Bay spring bloom. J. Mar. Sys. 134, 2944.

John, D.E., López-Díaz, J.M., Cabrera, A., Santiago, N.A., Corredor, J.E., Bronk, D.A., Paul, J.H., 2012. A day in the life in the dynamics marine environment: how nutrients shape diel patterns of phytoplankton photosynthesis and carbon fixation gene expression in the Mississippi and Orinoco River plumes. Hydrobiologia 679, 155173.

Kana, T.M., Watts, J.L., Gilbert, P.M., 1985. Diel periodicity in the photosynthetic capacity of coastal and offshore phytoplankton assemblages. Mar. Ecol. Prog. Ser. 25, 131139.

Kirk, J.T.O., 1983. Light and Photosynthesis in Aquatic Ecosystems, third ed. Cambridge University Press, Cambridge.

Kolber, Z., Zehr, J., Falkowski, P., 1988. Effects of growth irradiance and nitrogen limitation on photosynthesis energy conversion in photosystem II. Plant Physiol. 88, 923929.

Kolber, Z.S., Prášil, O., Falkowski, P.G., 1998. Measurments of variable chlorophyll fluorescence using fast repetition rate techniques: defining methodology and experimental protocols. Biochim. Biophys. Acta. 1367, 88106.

Kromkamp, J.C., Forster, R.M., 2003. The use of variable fluorescence measurements in aquatic ecosystems: differences between multiple and single turnover measuring protocols and suggested terminology. Eur. J. Phycol. 38, 103112.

Kuipers, B. R., Witte, H. J., 1999. Grazing impact of microzooplankton on different size classes of algae in the Northern Sea in early spring and mid-summer. Mar. Ecol. Prog. Ser. 180, 93104.

Lambert, C. D., Bianchi, T. S., Santschi, P. H., 1999. Cross-shelf changes in phytoplankton community composition in the Gulf of Mexico (Texas shelf/slope): the use of plant pigments as biomarkers. Cont. Shelf Res. 19, 121.

Latasa, M., Berdalet, E., 1994. Effect of nitrogen or phosphorus starvation on pigment composition of cultured *Heterocapasa* sp. J. Plankton Res. 16, 8394.

Lavaud, J., Rousseau, B., Etienne, A.L., 2004. General features of photoptotection by energy dissipation in planktonic diatoms (Bacillariophyceae). J. Phycol. 40, 130 137.

Laurent, A., Fennel, K., Hu, J., Hetland, R., 2012. Simulating the effects of phosphorus limitation in the Mississippi and Atchafalaya River plumes. Biogeosciences 9, 47074723.

LaRoche, J., Geider, R.J., Graziano, L.M., Murray, H., Lewis, K. 1993. Induction of specific proteins in eukaryotic algae grown under iron-, phosphorus-, or nitrogen-deficient conditions. J. Phycol. 29, 767777.

Laza-Martinez, A., Seoane, S., Zapata, M., and Orive, E., 2007. Phytoplankton pigment patterns in a temperate estuary: from unialgal cultures to natural assemblages. J. Plankton Res. 29, 913929.

Lehrter, J.C., Murrell, M.C., Kurtz, J.C., 2009. Interactions between freshwater input,

light, and phytoplankton dynamics on the Louisiana continental shelf. Cont. Shelf Res. 29, 18611872.

Leonardos, N., Geider, R.J., 2004. Effects of nitrate: phosphate supply ratio and irradiance on the C: N: P stoichiometry of *Chaetoceros muelleri*. Eur. J. Phycol. 39, 173180.

Lessard, E.J., Merico, A, Tyrrell, T., 2005. Nitrate: phosphate ratios and *Emiliania Huxleyi* blooms. Limnol. Oceanogr. 50, 10201024.

Levy, O., Dubinsky, Z., Schneider, K., Achituv, Y., Zakai, D., Gorbunov, M.Y., 2004. Diurnal hysteresis in coral photosynthesis. Mar. Ecol. Pro. Ser. 268, 105117.

Lewitus A. J., White D.L. Tymowski R. G., Geesey M. E., Hymel S. N., Noble P.A., 2005. Adapting the CHEMTAX method for assessing phytoplankton taxonomic composition in southeastern U.S. estuaries. Estuaries 29, 160172.

Litaker, R.W., Warner, V.E,, Rhyne, C., Duke, C.S., Kenney, B.E., Ramus, J., Tester, P.A., 2002. Effect of diel and interday variations in light on the cell division pattern and in situ growth rates of the bloom-forming dinoflagellate *Heterocapsa triquetra*. Mar. Ecol. Prog. Ser. 232, 6374.

Litchman, E., Steiner, D., Bossard, P., 2003. Photosynthetic and growth responses of three freshwater algae to phosphorus limitation and daylength. Freshwater Biol. 48, 21412148.

Litchman, E., Klausmeier, C.A., Schofield, O.M., Falkowski, P.G., 2007. The role of functional traits and trade-offs in structuring phytoplankton communities: scaling from cellular to ecosystem level. Ecol. Lett. 10, 11701181.

Litchman, E. and Klausmeier, C.A., 2008. Trait-based community ecology of phytoplankton. Annu. Rev. Ecol. Evol. Syst. 39, 615639.

Litchman, E., Pinto, P.T., Klausmeier, A., Thomas, M.K., Yoshiyama, K., 2010. Linking traits to species diversity and community structure in phytoplankton. Hydrobiologia 653, 1528.

Liu, Y., Song, X., Cao, X., Yu, Z., 2012. Response of photosynthetic characters of *Skeletonema costatum* to different nutrient conditions. J. Plankton Res. 0, 112.

Lobel, M., Cockshutt, A.M., Campbell, D.A., Finkel, Z.V., 2010. Physiological basis for high resistance to photoinhibition under nitrogen depletion in *Emiliania huxleyi*. Linmol. Oceanogr. 55, 21502160.

Lohrenz, S.E., Fahnenstiel, G.L., Redalje, D.G., 1994. Spatial and temporal variations of photosynthetic parameters in relation to envrionmental conditions in coastal water of the Nothern Gulf of Mexico. Estuaries 17, 779795.

Lohrenz, S.E., Fahnenstiel, G.L., Redalje, D.G., Lang, G.A., Chen., X., Dagg, M.J., 1997. Variations in primary production of northern Gulf of Mexico continental shelf waters linked to nutrient inputs from the Mississippi River. Mar. Ecol. Prog. Ser. 155, 4554.

Lohrenz, S. E., Fahnenstiel, G. L., Redalje, D. G., Lang, G. A., Dagg, M. J., Whitledge, T. E., Dortch, Q., 1999. Nutrients, irradiance and mixing as factors regulating primary production in coastal water impacted by the Mississippi River plume. Cont. Shelf Res.19, 11131141.

Long, S.P., Humphries, S., Falkowski, P.G., 1994. Photoinhibition of photosynthesis in nature. Annu. Rev. Plant Physial. Mol. Biol. 45, 633662.

Lourenco, S.O., Barbarino, E., Lavín, P.L., Marquez, U., Aidar, E., 2007. Distribution of intracellular nitrogen in marine microalgae: calculation of new nitrogen-to-protein conversion factors. Eur. J. Phycol. 39, 1732.

Lugus, A., Suomela, J., Weithoff, G., Heikkilä, K., Helminen, H., Sipura, J., 2004. Species-specific differences in phytoplankton responses to N and P enrichments and the N: P ratio in the Archipelago Sea, northern Baltic Sea. J. Plankton Res. 26, 291305.

MacIntyre, H.L., Kana, T.M., Anning, T., Geider, R.J., 2002. Photoacclimation of photosynthesis irradiance response curves and photosynthetic pigments in microalgae and cyanobacteria. J. Phycol. 38, 1738.

Mackey, M.D., Mackey, D.J., Higgins, H.W., Wright, S.W., 1996. Chemtax- a program for estimating class abundances from chemical markers: application to HPLC measurements of phytoplankton. Mar. Ecol. Prog. Ser. 144, 265283.

McAllister, C.D., 1963. Measurements of diurnal variation in productivity at ocean station "P". Limnol. Oceanogr. 8, 289292.

Mahaffey, C., Bjorkman, K.M., Karl, D.M., 2012. Phytoplankton response to deep seawater nutrient addition in the North Pacific Subtropical Gyre. Mar. Ecol. Prog. Ser. 460, 1334.

Martin, J.H., Fitzwater, S.E., 1988. Iron-deficiency limits phytoplankton growth in the Northeast Pacific Subarctic. Nature 331, 341343.

Merzlyak, M.N., Chivkunova, O.B., Corelova, O.A., Reshetnikova, I.V., Solovchenko, A.E., 2007. Effect of nitrogen starvation on optical properties, pigments, and arachidonic acid content of the unicellular green alga *Parietochloris incisa* (Trebouxiophyceae, Chlorophyta). J. Phycol. 43, 833843.

Miller, C.B., 2003. Biological Oceanography, first ed. Blackwell, Massachusetts.

Moore, C.M., Suggett, D.J., Hickman, A.E., Kim, Y., Tweddle, F., Sharples, J., Geider, R.J., Holligan, P.M., 2006. Phytoplankton photoacclimation and photoadaption in reponse to environmental gradients in a shelf sea. Limnol. Oceanogr. 51, 936949.

Moore, C.M., Mills, M.M., Langlois, R., Milne, A., Achterberg, E.P., Geider, R.J., LaRoche, J., 2008. Relative influence of nitrogen and phosphorus availability on phytoplankton physiology and productivity in the oligotrophic sub-tropical North Atlantic Ocean. Limnol. Oceanogr. 53, 291305.

Moore, C.M., Mills, M.M., Arrigo, K.R., Berman-Frank, I., Bopp, L., Boyd, P.W., Galbraith, E.D., Geider, R.J., Guieu, S.L., Jaccard, T.D., Jickells, T.D., La Roche, J., Lenton, T.M., Mahowald, N.M., Marañón, E., Marinov, I., Moore, J.K., Nakatsuka, T., Oschlies, A., Saito, M.A.m Thingstad, T.F., Tsuda, A., Ulloa, O., 2013. Processes and patterns of oceanic nutrient limitation. Nat. Geosci. 6, 701710.

Nowlin, W.D., Jochens, A.E., DiMarco, S.F., Reid, R.O., Howard, M.K., 2005. Low-frequency circulation over the Texas-Louisiana Continental Shelf, in: Sturges, W., Lugo-Fernandez, A. (Eds.), Circulation in the Gulf of Mexico: Observations and Models. American Geophysical Union Geophysical Monograph GM161, pp. 219240.

Oguz, T., Merico, A., 2006. Factors controlling the summer *Emiliania Huxleyi* bloom in the black sea: a modeling study. J. Mar. Sys. 59, 173188.

Ohi, N., Saito, H., Taguchi, S., 2005. Diel patterns in chlorophyll a specific absortion coefficient and absorption efficiency factor of picoplankton. Journal of Oceanography 61, 379388.

Paerl, H.W., 2009. Controlling eutrophication along the freshwater-marine continuum: dual nutrient (N and P) reduction are essential, Estuaries Coasts 32, 593601.

Parkhill, J. P., Maillet, G., Cullen, J. J., 2001. Fluorescence-based maximal quantum yield for PSII as a diagnostic of nutrient stress. J. Phycol. 37, 519529.

Parsons, T.R., Maita, Y., Lalli, C.M., 1984. A Manual of Chemical and Biological

Methods for Seawater Analysis, first ed. Pergamon, Oxford.

Peever, T.L., Higgins, V.J., 1989. Electrolyte leakage, lipoxygenase, and lipid peroxidation induced in tomato leaf tissue by specific and non specific elicitors from *Cladosporium fluvum*. Plant Physiol. 90, 867875.

Petrou, K., Kranz, S., Doblin, M.A., Ralph, P., 2012. Photophysiological responses of Fragilariopsis cylindrus (Bacillariophyceae) to nitrogen depletion at two temperatures. J. Phycol. 48, 127136.

Pinckney, J. L., Millie, D.F., Howe, K.E., Paerl, H.W., Hurley, J.P., 1996. Flow scintillation counting of ^{14}C-labeled microalgal photosynthetic pigments. J. Plankton Res. 18, 1867-1880.

Platt, T., Gallegos, C.L., Harrison, W.G., 1980. Photoinhibition of photosynthesis in natural assemblages of marine phytoplankton. J. Mar. Res. 38, 687701.

Plumley, F.G., Schmidt, G.W., 1989. Nitrogen-dependent regulation of photosynthetic gene expression. Proc. Natl. Acad. Sci. 86, 26782682.

Plumley, F.G., Schmidt, G.W., 1995. Light-harvesting chlorophyll a/b complexes: interdependent pigment synthesis and protein assembly. Plant. Cell 7, 689704.

Prézelin, B., 1992. Diel periodicity in phytoplankton productivity. Hydrobiologia 238, 1 35.

Qian, Y.R., Jochens, A.E., Kennicutt II, M.C., Biggs, D.C., 2003. Spatial and temporal variability of phytoplankton biomass and community structure over the continental margin of the northeast Gulf of Mexico based on pigment analysis. Cont. Shelf Res. 23, 117.

Quigg, A., Beardall, J., 2003. Protein turnover in relation to maintenance metabolism at low protein flux in two marine microalgae. Plant Cell Environ. 26, 693703.

Quigg, A., Sylvan, J.B., Gustafson, A.B. Fisher, T.R., Oliver, R.L., Tozzi, S., Ammerman, J.W., 2011. Going west: Nutrient limitation of primary production in the Northern Gulf of Mexico and the importance of the Atchafalaya River. Aquat. Geochem. 17, 519544.

Quigg, A., Kotabová, E., Jarešová, J., Kaňa, R., šetlík, J., šedivá, B., Komárek, O., Prášil, O., 2012. Photosynthesis in *Chromera velia* represents a simple system with high efficiency. PLOS ONE 7(10), e47036.

Quigg, A., Nunnally, C.C., McInnes, A.S., Gay, S., Rowe, G.T., Dellapenna, T.M., Davis, B., 2013a. Hydrographic and biological controls in two subarctic fjords: and environmental case study of how climate change could impact phytoplankton communities. Mar. Eco. Pro. Ser. 480, 2137.

Quigg, A., Al-Anasi, M., Nour Al Din, N., Wei, C.L., Nunnally, C.C., Al-Ansari, I. S., Rowe, G., Soliman, Y., Al-Maslamani, I., Mahmoud, I., Youseff, N., Abdel Moati, M.A., 2013b. Phytoplankton along the coastal shelf of an oligotrophic hypersaline environment in a semi-enclosed marginal sea: Qatar (Arabian Gulf). Cont. Shelf Res. 60, 116.

Raateoja, M., Seppälä, J., Ylöstalo, P., 2004. Fast repetition rate fluorometry is not applicable to studies of filamentous cyanobacteria from the Baltic Sea. Limnol. Oceanogr. 49, 10061012.

Rabalais, N.N., Turner, R.E., Dortch, Q., Justic, D., Bierman Jr., V.J., Wiseman Jr., W. J., 2002. Nutrient-enhanced productivity in the Northern Gulf of Mexico: past, present and future. Hydrobiologia 475/476, 3963.

Rabalais, N.N., Turner, R.E., Sen Gupta, B.K., Boesch, D.F., Chapman, P., Murrell, M.C., 2007. "Hypoxia in the northern Gulf of Mexico: Does the science support the plan to reduce, mitigate, and control hypoxia?" Estuaries Coasts 30, 753772.

Rabalais, N.N., Turner, R.E., Sen Gupta, B.K., Boesch, D.F., Chaoman, P., Schaeffer, B.A., Kurtz, J.C., Hein, M.K., 2012. Phytoplankton community composition in nearshore coastal waters of Louisiana. Mar. Pollut. Bull. 64, 17051712.

Redfield, A.C., Ketchum, B.H., Richards, F.A., 1963. The influence of organisms on the composition of sea-water, in Hill, M.N. (Ed.) The Sea. Interscience Publication, New York, pp. 2677.

Reynold R.C., 2006. Ecology of Phytoplankton, first ed. Cambridge University, Cambridge.

Rhee, G.Y., 1978. Effects of N: P atomic ratios and nitrate limitation on algal growth, cell composition, and nitrate uptake. Linmol. Oceanogr. 23, 1025.

Riegman, R., Stolte, W., Noordeloos, A.A.M., Slezak, D., 2000. Nutrient uptake and alkaline phosphatase (EC 3:1:3:1) activity of *Emiliania hyxleyi* (Prymnesiophyceae) during growth under N and P limitation in continuous

Robert, S., Shelly, K., Beardall, J., 2008. Interactions among phosphate uptake,

photosynthesis, and chlorophyll fluorescence in nutrient-limited cultures of the chlorophyte microalga *Dunaliella tertiolecta*. J. Phycol. 44, 662669.

Roelke, D.L., Li, H.P., Hayden, N.J., Miller, C.J., Davis, S.E., Quigg, A., Buyukates, Y., 2013. Co-occurring and opposing freshwater inflow effects on phytoplankton biomass, productivity and community composition of Galveston Bay, USA. Mar. Ecol. Prog. Ser. 477, 6176.

Schaeffer, B.A., Kurtz, J.C., Hein, M.K., 2012. Phytoplankton community composition in nearshore coastal waters of Louisiana. Mar. Pollut. Bull. 64, 1705-1712.

Schlüter, L., Møhlenberg, F., Havskum, H., Larsen, S., 2000. The use of phytoplankton pigments for identifying and quantifying phytoplankton groups in coastal areas: testing the influence of light and nutrients on pigments/chlorophyll a ratios. Mar. Ecol. Prog. Ser. 192, 4963.

Shimizu, Y., Urabe, J., 2008. Regulation of phosphorus stoichiometry and growth rate of consumers: theoretical and experimental analyses with Daphnia. Oecologia 155, 2131.

Sieracki, M.E., Verity, P.G., Stoecker, D.L., 1993. Plankton community response to sequential silicate and nitrate depletion during the 1989 North Atlantic spring bloom. Deep-Sea Res. II 40, 213225.

Silva, A.F., Lourenco, S.O., Chaloub, R.M., 2009. Effects of nitrogen starvation on the photosynthetic physiology of a tropical marine microalga Rhodomonas sp. (Cryptophyceae). Aquat. Bot. 91, 291297.

Smith, S.M., Hitchcock, G.J., 1994. Nutrient enrichments and phytoplankton growth in the surface waters of the Louisiana Bight. Estuaries 17, 740753.

Solorzano, L., Sharp, J.H., 1980. Determination of total dissolved phosphorus and particulate phosphorus in natural waters, Linmol. Oceanogr. 25, 754757.

Sommer, U., 1985. Comparison between steady state and non-steady state competition: experiments with natural phytoplankton. Limnol. Oceanogr. 30, 335346.

Sommer, U., 1995. An experimental test of the intermediate disturbance hypothesis using cultures of marine phytoplankton. Limnol. Oceanogr. 40, 12711277.

Sournia, A., 1976. Circadian periodicities in natural populations of marine phytoplankton. Adv. Mar. Biol. 12, 325389.

Soria-Dengg, S., Horstmann, U., 1995. Ferrioxamines B and E as iron sources for the

marine diatom *Phaeodactylum tricornutum*. Mar. Ecol. Prog. Ser. 127, 269277.

Sterner, R.W., Elser, J.J., 2002. Ecological stoichiometry: the biology of elements from molecules to the biosphere, first ed. Princeton University, New Jersy.

Strom, S.L., Strom, M.W., 1996. Microplankton growth, grazing, and community structure in the Northern Gulf of Mexico. Mar. Ecol. Prog. Ser. 130, 229240.

Strzepek, R.F., Harrison, P.J., 2004. Photosynthetic architecture differs in coastal and oceanic diatoms. Nature 431, 689692.

Suggett, D.J., Floc'H, E., Harris, G.N., Leonardos, N., Geider, R.J., 2007. Different strategies of photoacclimation by two strains of *Emiliania hyxleyi* (Haptophyta). J. Phycol. 43, 12091222.

Suggett, D.J., Stambler, N., Prášil, O., Kolber, Z., Quigg, A., Vázquez-Dominguez, E., Zohary, T., Berman, T., Iluz, D., Lawson,T., Meeder, E., 2009a. Nitrogen and phosphorus limitation of oceanic microbial growth during spring in the Gulf of Aqaba. Aquat. Microb. Ecol. 56, 227239.

Suggett, D.J., Moore, C.M., Hickman, A.E., Geider, R.J., 2009b. Interpretation of fast reprtition rate (FRR) fluorescence: signatures of phytoplankton community structure versus physiological state. Mar. Ecol. Prog. Ser. 376, 119.

Sylvan, J.B., Dorch, Q., Nelson, D.M., Brown, A.F., Morrison, W., Ammerman, J.W., 2006. Phosphorus limits phytoplankton growth on the Louisiana shelf during the period of hypoxia formation. Environ. Sci. Technol. 43, 75487553.

Sylvan, J.B., Quigg, A., Tozzi, S., Ammerman, J.W., 2007. Eutrophication induced phosphorus limitation in the Mississippi River plume: Evidence from fast repetition rate fluorometry. Limnol. Oceanogr. 52, 26792685.

Sylvan, J.B., Quigg, A., Tozzi, S., and Ammerman, J.W., 2011. Mapping phytoplankton community physiology on a river impacted continental shelf: testing a multifaceted approach. Estuaries Coasts 34, 12201233.

Suzuki, L., Johnson, C.H., 2001. Alage know the time of day: circadian and photoperiodic programs. J. Phycol. 37, 933942.

Thomas, W.H., Simmons, E.G., 1960. Phytoplankton production in the Mississippi Delta, in: Shepard F. (Ed.), Recent Sediments, Northwest Gulf of Mexico. American Association of Petrologists, Texas, Oklahoma, pp. 103116.

Thompson Jr., G.A., 1996. Lipids and membrane function in green algae. Biochimica et

Biophysica Acta. 1302, 1745.

Thornton, D.C.O., 2012. Primary production in the ocean, in: Najafpour, M.M. (Ed.) Advances in Photosynthesis – Fundamental Aspects. Edited by M. M. Intech, Rijeka, Croatia, pp 563588.

Tilman, D., 1977. Resource competition between phytoplankton algae: an experimental and theoretical approach. Ecology 58, 338348.

Tilman, D., 1982. Resource competition and community structure, first ed. Princeton University, New Jersey.

Tilman, D., Kilham, S. S., Kilman, P., 1982. Phytoplankton community ecology: the role of limiting nutrients. Annu. Rev. Ecol. Syst. 12, 349372.

Tomas, C.R., 1997. Identifying Marine Phytoplankton, 1st ed. Academic, Massachusetts.

Turner, R.E., Rabalais, N.N., 1991.Changes in Mississippi River water quality this century. Bioscience 41, 140147.

Turner, R.E., Rabalais, N.N., Justic, D., 2006. Predicting summer hypoxia in the Northern Gulf of Mexico: riverine N, P and Si loading. Mar. Pollut. Bull. 52, 139148.

Turner, R.E., Rabalais, N.N., Alexander, R.B., McIsaac, G., Howarth, R.W., 2007. Characterization of nutrient, organic carbon, and sediment loads and concentrations from the Mississippi River into the northern Gulf of Mexico. Estuar Coasts. 30, 773790.

Turner, R.E., Rabalais, N.N., 2013. Nitrogen and phosphorus phytoplankton growth limitation in the Northern Gulf of Mexico. Aquat. Microb. Ecol. 68, 158169.

Tyrrell, T., Taylor, A., 1996. A modelling study of *Emiliania Huxleyi* in the ne Atlantic. J. Mar. Sys. 9, 83112.

Uchida, T., Toda, S., Matsuyama, Y., Yamaguchi, M., Kotani, Y., Honjo, T., 1999. Interactions between the red tide dinoflagellates *Heterocapsa circularisquama* and *Gymnodinium mikinotoi* in laboratory culture. J. Exp. Mar. Biol. Ecol. 241, 285299.

Vaulot, D., Marie, D., 1999. Diel variability of photosynthetic picoplankton in the equatorial Pacific. J. Geophys. Res.-Oceans 104, 32973310.

Walker, N.D., 2005. Wind and eddy-related shelf/slope crculation processes and coastal Upwelling, in: Sturges, W., Lugo-Fernandez, A. (Eds.), Circulation in the Gulf of Mexico: Observations and Models. American Geophysical Union Geophysical Monograph GM161, pp. 295314.

Walker, N.D., Leben, R.R., Balasubramanian, S., 2005. Hurricane-forced upwelling and chlorophyll a enhancement within cold-core cyclones in the Gulf of Mexico. Geophys. Res. Lett. 32, L18160.

Wang, A.G., Luo, G.H., 1990. Quantitative relation of hydroxylamine and superoxide anion radicals in plants. Chin. Plant Physiol. Commun. 6, 5557.

Wang, Y., Tang, X., 2008. Interactions between *Prorocentrum donghaiense* Lu and *Scrippsiella trochoidea* (Stein) Loeblich III under laboratory culture. Harmful Algae 7, 6575.

Wawrik, B., Paul, J.H., Campbell, L., Griggin, D., Houchin, L., Fuentes-Ortega, A., Muller-Karger, F., 2003. Vertical structure of the phytoplankton community associated with a coastal plume in the Gulf of Mexico. Mar. Ecol. Prog. Ser. 251, 87101.

Wykoff, D.D., Davies, J.P., Melis, A., Grossman, A.R., 1998. The regulation of photosynthetic electron transport during nutrient deprivation in *Chlamydomonas reinhardtii*. Plant Physiol. 117, 129139.

Yin, Y., Wang, X., Yang, L., Sun, Y., Guo, H., 2010. Bioaccumulation and ROS generation in Coontail *Ceratophyllum demersum* L. exposed to phenanthrene. Ecotoxicology. 19, 11021110.

Young, E.B., Beardall, J., 2003. Photosynthetic function in *Dunaliella tertiolecta* (Chlorophyta) during a nitrogen starvation and recovery cycle. J. Phycol. 39, 897905.

Zhao, Y., Quigg, A., 2014. Nutrient limitation in Northern Gulf of Mexico (NGOM): phytoplankton communities and photosynthesis respond to nutrient pulse. PLOS ONE 9(2), e88732.

Zhang, Y., Chen, H., He, C., Wang, Q., 2013. Nitrogen starvation induced oxidative stress in an oil-producing green alga *Chlorella sorokiniana* C3. PlOS ONE. 8, e69225.